

The Owner on Behalf of Turkish Society of Nuclear Medicine

Prof. Dr. Zehra Özcan

Ege University Faculty of Medicine, Department of Nuclear Medicine, İzmir, Turkey

Publishing Manager

Prof. Dr. Hatice Durak

Dokuz Eylül University Faculty of Medicine, Department of Nuclear Medicine, İzmir, Turkey

Editor in Chief

Prof. Dr. Hatice Durak

Dokuz Eylül University Faculty of Medicine, Department of Nuclear Medicine, İzmir, Turkey

E-mail: durak.hatice@gmail.com

Associate Editors

Murat Fani Bozkurt

Hacettepe University Faculty of Medicine, Department of Nuclear Medicine, Ankara, Turkey

E-mail: fanibozkurt@gmail.com

Firat Güngör

Emsey Hospital, Clinic of Nuclear Medicine, İstanbul, Turkey

E-mail: firat.gungor@emseyhospital.com

Özhan Özdoğan

Dokuz Eylül University Faculty of Medicine, Department of Nuclear Medicine, İzmir, Turkey

E-mail: ozhan.ozdogan@deu.edu.tr

Statistics Editor

Gül Ergör

Dokuz Eylül University Faculty of Medicine, Department of Public Health, İzmir, Turkey

Editorial Board

Emel Ada

Dokuz Eylül University Faculty of Medicine, Department of Radiology, İzmir, Turkey

E-mail: emel.ada@deu.edu.tr

Işık Adalet

İstanbul University İstanbul Faculty of Medicine, Department of Nuclear Medicine, İstanbul, Turkey

Claudine Als

Clinique Zitha, Department of Nuclear Medicine, Luxembourg

Vera Artiko

University of Belgrade Faculty of Medicine, Clinical Center of Serbia, Center for Nuclear Medicine, Belgrade, Serbia

Neşe Atabey

Dokuz Eylül University Faculty of Medicine, Department of Medical Biology, İzmir, Turkey

Tamer Atasever

Medipol Hospital, Clinic of Nuclear Medicine, İstanbul, Turkey

Marika Bajc

University Hospital Lund, Clinic of Clinical Sciences, Lund, Sweden

Kemal Baysal

Dokuz Eylül University Faculty of Medicine, Department of Biochemistry, İzmir, Turkey

Lorenzo Biassoni

Great Ormond Street Hospital for Children NHS Foundation Trust, Department of Radiology, London, United Kingdom

Hans Jürgen Biersack

University of Bonn, Department of Nuclear Medicine, Bonn, Germany

Elvan Sayit Bilgin

Celal Bayar University Faculty of Medicine, Department of Nuclear Medicine, Manisa, Turkey

Doğan Bor

Ankara University Faculty of Engineering, Department of Physics Engineering, Ankara, Turkey

Patrick Bourguet

Cancer Center Eugène Marquis and University of Rennes, Service de Médecine Nucléaire, Rennes, France

Zeynep Burak

Ege University Faculty of Medicine, Department of Nuclear Medicine, İzmir, Turkey

Arturo Chiti

Humanitas University, Department of Nuclear Medicine, Milan, Italy

Josep Martin Comin

Bellvitge-Idibell University Hospital, Department of Nuclear Medicine, Barcelona, Spain

Alberto Cuocolo

University Federico II, Department of Advanced Biomedical Sciences, Napoli, Italy

Angelika Bischof Delaloye

University of Lausanne, Department of Radiology, Lausanne, Switzerland

Mustafa Demir

İstanbul University Cerrahpaşa Faculty of Medicine, Department of Nuclear Medicine, İstanbul, Turkey

Peter Joseph Ell

University College Hospital, Institute of Nuclear Medicine, London, United Kingdom

Taner Erselcan

Cumhuriyet University Faculty of Medicine, Department of Nuclear Medicine, Sivas, Turkey

Türkan Ertay

Dokuz Eylül University Faculty of Medicine, Department of Nuclear Medicine, İzmir, Turkey

Jure Fettich

University Medical Centre Ljubljana, Department for Nuclear Medicine, Ljubljana, Slovenia

Christiane Franzius

Centre of Nuclear Medicine and PET/CT, Bremen, Germany

Lars Friberg

Bispebjerg University Hospital, Clinic of Clinical Physiology and Nuclear Medicine, Copenhagen, Denmark

Maria Lyra Georgosopoulou

University of Athens, 1st Department of Radiology, Aretaieion Hospital, Radiation Physics Unit, Athens, Greece

Gevorg Gevorgyan

The National Academy of Sciences of Armenia, H. Buniatian Institute of Biochemistry, Yerevan, Armenia

Liselotte Højgaard

University of Copenhagen, Department of Clinical Physiology, Nuclear Medicine and PET, Rigshospitalet, Copenhagen, Denmark

Erkan İbiş

Ankara University Faculty of Medicine, Department of Nuclear Medicine, Ankara, Turkey

Ora Israel

Rambam Health Care Campus, and B&R Rappaport Faculty of Medicine, Department of Nuclear Medicine, Technion-Israel Institute of Technology, Haifa, Israel

Özlem Kapucu

Gazi University Faculty of Medicine, Department of Nuclear Medicine, Ankara, Turkey

Nevzat Karabulut

Pamukkale University Faculty of Medicine, Department of Radiology, Denizli, Turkey

Gamze Çapa Kaya

Dokuz Eylül University Faculty of Medicine, Department of Nuclear Medicine, İzmir, Turkey

Suna Kırac

Yakın Doğu University Faculty of Medicine, Department of Nuclear Medicine, Nicosia, Cyprus

Irena Dimitrova Kostadinova

Alexandrovka University Hospital, Clinic of Nuclear Medicine, Sofia, Bulgaria

Georgios S Limouris

Athens University Medical Faculty, Nuclear Medicine Division, Radiology Department I, "Aretaieion" Hospital, Athens, Greece

Ayşe Mudun

İstanbul University İstanbul Faculty of Medicine, Department of Nuclear Medicine, İstanbul, Turkey

Vladimir Obradovic

University of Belgrade Faculty of Medicine, Clinical Center of Serbia, Center of Nuclear Medicine, Belgrade, Serbia

Zehra Özcan

Ege University Faculty of Medicine, Department of Nuclear Medicine, İzmir, Turkey

Serdar Özçelik

İzmir Institute of Technology, Faculty of Science, Department of Physic, İzmir, Turkey

Mehmet Ali Özgüven

Koru Hospital, Clinic of Nuclear Medicine, Ankara, Turkey

Francesca Pons

Hospital Clinic of Barcelona, Department of Nuclear Medicine, Barcelona, Spain

İlknur Ak Sivriköz

Osmangazi University Faculty of Medicine, Department of Nuclear Medicine, Eskişehir, Turkey

Istvan Szilvasi

Semmelweis University of Medicine, Kútvölgyi Clinical Unit, Isotope Laboratory, Budapest, Hungary

Dragana Sobic Saranovic

University of Belgrade Faculty of Medicine, Clinical Center of Serbia, Center of Nuclear Medicine, Belgrade, Serbia

Mathew L Thakur

Thomas Jefferson University, Department of Radiology, Pennsylvania, United States

Perihan Ünak

Ege University, Institute of Nuclear Sciences, İzmir, Turkey

Seher Ünal

İstanbul University İstanbul Faculty of Medicine, Department of Nuclear Medicine, İstanbul, Turkey

Akın Yıldız

Medstar Antalya Hospital, Clinic of Nuclear Medicine, Antalya, Turkey

© The paper used to print this journal conforms to ISO 9706: 1994 standard (Requirements for Permanence). The National Library of Medicine suggests that biomedical publications be printed on acid-free paper (alkaline paper). Reviewing the articles' conformity to the publishing standards of the Journal, typesetting, reviewing and editing the manuscripts and abstracts in English, creating links to source data, and publishing process are realized by Galenos.

Turkish Society of Nuclear Medicine

Cinnah Caddesi Pilot Sokak No: 10/12 Çankaya 06650 Ankara, Turkey

Phone : +90 312 441 00 45

Fax : +90 312 441 12 95

Web : www.tsnm.org

E-mail : dernekmerkezi@tsnm.org

"Formerly Turkish Journal of Nuclear Medicine"

**Galenos Publisher Contact**

Address: Molla Gürani Mahallesi Kaçamak Sokak No: 21
34093 Fındıkzade-İstanbul-Turkey

Phone: +90 (212) 621 99 25 Fax: +90 (212) 621 99 27

E-mail: info@galenos.com.tr

Web Site: www.galenos.com.tr

Printing at: Özgün Ofset Ticaret Ltd. Şti.

Yeşilce Mah. Aytekin Sk. No: 21 34418 4. Levent/İstanbul

Phone: +90 +90 212 280 00 09

Date of printing: June 2016

ISSN: 2146-1414

ONLINE ISSN: 2147-1959



Molecular Imaging and Radionuclide Therapy (formerly Turkish Journal of Nuclear Medicine) is the official publication of Turkish Society of Nuclear Medicine.

Focus and Scope

Molecular Imaging and Radionuclide Therapy (Mol Imaging Radionucl Ther, MIRT) is a double-blind peer-review journal published in English language. It publishes original research articles, reviews, editorials, short communications, letters, consensus statements, guidelines and case reports with a literature review on the topic, in the field of molecular imaging, multimodality imaging, nuclear medicine, radionuclide therapy, radiopharmacy, medical physics, dosimetry and radiobiology. MIRT is published three times a year (February, June, October). Audience: Nuclear medicine physicians, medical physicists, radiopharmaceutical scientists, radiobiologists.

The editorial policies are based on the "Recommendations for the Conduct, Reporting, Editing, and Publication of Scholarly Work in Medical Journals (ICMJE Recommendations)" by the International Committee of Medical Journal Editors (2013, archived at <http://www.icmje.org/>) rules.

Molecular Imaging and Radionuclide Therapy is indexed in PubMed, PubMed Central (PMC), Emerging Sources Citation Index (ESCI), TUBITAK-ULAKBIM, Gale/Cengage Learning, EBSCO databases, ProQuest Health & Medical Complete, CINAHL, DOAJ, Türkiye Atıf Dizini (Türkiye Citation Index), Turk Medline.

Open Access Policy

This journal provides immediate open access to its content on the principle that making research freely available to the public supports a greater global exchange of knowledge.

Open Access Policy is based on rules of Budapest Open Access Initiative (BOAI) (<http://www.budapestopenaccessinitiative.org/>). By "open access" to [peer-reviewed research literature], we mean its free availability on the public internet, permitting any users to read, download, copy, distribute, print, search, or link to the full texts of these

articles, crawl them for indexing, pass them as data to software, or use them for any other lawful purpose, without financial, legal, or technical barriers other than those inseparable from gaining access to the internet itself. The only constraint on reproduction and distribution, and the only role for copyright in this domain, should be to give authors control over the integrity of their work and the right to be properly acknowledged and cited.

Subscription Information

Manuscripts can only be submitted electronically through the Journal Agent website (<http://www.journalagent.com/mirt/?plng=eng>) after creating an account. This system allows online submission and review.

All published volumes in full text can be reached free of charge through the website <http://mirt.tsnmjournals.org>

Instructions for Authors

Instructions for authors are published in the journal and on the website <http://mirt.tsnmjournals.org>

Correspondence Address

Editor in Chief, Hatice Durak, MD, Professor in Nuclear Medicine
Dokuz Eylül University Faculty of Medicine, Department of Nuclear Medicine
35340 Balçova / İZMİR

Phone : +90 212 621 99 25

Fax : +90 212 621 99 27

e-mail : haticedurak@tsnmjournals.org

Web : <http://mirt.tsnmjournals.org>

The journal is printed on an acid-free paper.

This work is licensed under a Creative Commons Attribution-NonCommercial-NoDerivatives 4.0 International License

Molecular Imaging and Radionuclide Therapy (Mol Imaging Radionucl Ther, MIRT) publishes original research articles, reviews, editorials, short communications, letters, consensus statements, guidelines and case reports with a literature review on the topic, in the field of molecular imaging, multimodality imaging, nuclear medicine, radionuclide therapy, radiopharmacy, medical physics, dosimetry and radiobiology. MIRT is published by the Turkish Society of Nuclear Medicine three times a year (February, June, October). The journal is printed on an acid-free paper.

Molecular Imaging and Radionuclide Therapy is indexed in PubMed, PubMed Central (PMC), Emerging Sources Citation Index (ESCI), TUBITAK-ULAKBIM, Gale/Cengage Learning, EBSCO databases, ProQuest Health & Medical Complete, CINAHL, DOAJ, Türkiye Atıf Dizini (Türkiye Citation Index), Turk Medline.

Molecular Imaging and Radionuclide Therapy does not charge any article submission or processing charges.

GENERAL INFORMATION

MIRT commits to rigorous peer review, and stipulates freedom from commercial influence, and promotion of the highest ethical and scientific standards in published articles. Neither the Editor(s) nor the publisher guarantees, warrants or endorses any product or service advertised in this publication. All articles are subject to review by the editors and peer reviewers. If the article is accepted for publication, it may be subjected to editorial revisions to aid clarity and understanding without changing the data presented.

Manuscripts must be written in English and must meet the requirements of the journal. The journal is in compliance with the uniform requirements for manuscripts submitted to biomedical journals published by the International Committee of Medical Journal Editors (NEJM 1997; 336:309-315, updated 2001). Manuscripts that do not meet these requirements will be returned to the author for necessary revision before the review. Authors of manuscripts requiring modifications have a maximum of two months to resubmit the revised text. Manuscripts returned after this deadline will be treated as new submissions.

It is the authors' responsibility to prepare a manuscript that meets ethical criteria. The Journal adheres to the principles set forth in the Helsinki Declaration October 2008. (<http://www.wma.net/en/30publications/10policies/b3/index.html>) and holds that all reported research involving "Human beings" conducted in accordance with such principles. Reports describing data obtained from research conducted in human participants must contain a statement in the MATERIALS AND METHODS section indicating approval by the ethical review board and affirmation that INFORMED CONSENT was obtained from each participant.

- All manuscripts reporting experiments using animals must include a statement in the MATERIALS AND METHODS section giving assurance that all animals have received humane care in compliance with the Guide for the Care and Use of Laboratory Animals (www.nap.edu) and indicating approval by the ethical review board.
- Case reports should be accompanied by INFORMED CONSENT and the identity of the patient should be hidden.
- Subjects must be identified only by number or letter, not by initials or names. Photographs of patients' faces should be included only if scientifically relevant. Authors must obtain written consent from the patient for use of such photographs.
- If the proposed publication concerns any commercial product, the author must include in the cover letter a statement indicating that the author(s) has (have) no financial or other interest with the product or explaining the nature of any relations (including consultancies) between the author(s) and editor the manufacturer or distributor of the product.

MANUSCRIPT CATEGORIES

1. Original Articles

2. Short Communications are short descriptions of focused studies with important, but very straightforward results. These manuscripts should be no longer than 2000 words, and include no more than two figures and tables and 20 references.

3. Reviews address important topics in the field. Authors considering the submission of uninvited reviews should contact the editor in advance to determine if the topic that they propose is of current potential interest to the Journal. Reviews will be considered for publication only if they are written by authors who have at least three published manuscripts in the international peer reviewed journals and these studies should be cited in the review. Otherwise only invited reviews will be considered for peer review from qualified experts in the area.

4. Editorials are usually written by invitation of the editor by the editors on current topics or by the reviewers involved in the evaluation of a submitted manuscript and published concurrently with that manuscript.

5. Case Report and Literature Reviews are descriptions of a case or small number of cases revealing a previously undocumented disease process, a unique unreported manifestation or treatment of a known disease process, unique unreported complications of treatment regimens or novel and important insights into a condition's pathogenesis, presentation, and/or management. The journal's policy is to accept case reports only if accompanied by a review of the literature on the related topic. They should include an adequate number of images and figures.

6. Consensus Statements or Guidelines may be submitted by professional societies. All such submissions will be subjected to peer review, must be modifiable in response to criticisms, and will be published only if they meet the Journal's usual editorial standards. These manuscripts should typically be no longer than 4000 words and include no more than six figures and tables and 120 references.

7. Letters to the Editor may be submitted in response to work that has been published in the Journal. Letters should be short commentaries related to specific points of agreement or disagreement with the published work. Letters should be no longer than 500 words with no more than five complete references, and may not include any figures or tables.

Note on Prior Publication

Articles are accepted for publication on the condition that they are original, are not under consideration by another journal, or have not been previously published. Direct quotations, tables, or illustrations that have appeared in copyrighted material must be accompanied by written permission for their use from the copyright owner and authors. Materials previously published in whole or in part shall not be considered for publication. At the time of submission, authors must report that the manuscript has not been published elsewhere. Abstracts or posters displayed at scientific meetings need not be reported.

MANUSCRIPT SUBMISSION PROCEDURES

MIRT only accepts electronic manuscript submission at the web site www.mirt.tsnmjournals.org. After logging on to the website Click the 'online manuscript submission' icon. All corresponding authors should be provided with a password and a username after entering the information required. If you already have an account from a previous submission, enter your username and password to submit a new or revised manuscript. If you have forgotten your username and/or password, please send an e-mail to the editorial office for assistance. After logging on to the article submission system please read carefully the directions of the system to give all needed information and attach the manuscript, tables and figures and additional documents.

INSTRUCTIONS TO AUTHORS

All Submissions Must Include:

1. Completed Copyright Assignment & Disclosure of Potential Conflict of Interest Form; This form should be downloaded from the website (provided in the author section), filled in thoroughly and uploaded to the website during the submission.
2. Informed consent (for case reports); Authors must complete the online submission forms. If you are unable to successfully upload the files please contact the editorial office by e-mail.

There is no submission fee for MIRT.

MANUSCRIPT PREPARATION

General Format

The Journal requires that all submissions be submitted according to these guidelines:

- Text should be double spaced with 2.5 cm margins on both sides using 12-point type in Times Roman font.
- All tables and figures must be placed after the text and must be labeled.
- Each section (abstract, text, references, tables, figures) should start on a separate page.
- Manuscripts should be prepared as a word document (*.doc) or rich text format (*.rtf).
- Please make the tables using the table function in Word.
- Abbreviations should be defined in parenthesis where the word is first mentioned and used consistently thereafter.
- Results should be expressed in metric units. Statistical analysis should be done accurately and with precision. Please consult a statistician if necessary.

Title Page

The title page should be a separate form from the main text and should include the following:

- Full title (in English and in Turkish) Turkish title will be provided by the editorial office for the authors who are not Turkish speakers.
- Authors' names and institutions.
- Short title of not more than 40 characters for page headings.
- At least three and maximum eight key words. (in English and in Turkish) Do not use abbreviations in the key words. Turkish key words will be provided by the editorial office for the authors who are not Turkish speakers. If you are not a native Turkish speaker, please re enter your English keywords to the area provided for the Turkish keywords. English key words should be provided from <http://www.nlm.nih.gov/mesh> (Medical Subject Headings) while Turkish key words should be provided from <http://www.bilimterimleri.com>.
- Word count (excluding abstract, figure legends and references).
- Corresponding author's e-mail and address, telephone and fax numbers.
- Name and address of person to whom reprint requests should be addressed.

Original Articles

Authors are required to state in their manuscripts that ethical approval from an appropriate committee and informed consents of the patients were obtained. These documents may be asked by the reviewers or the editorial board during the submission process.

- **Abstract:** (in English and in Turkish) Original Articles should be submitted with a structured abstract of no more than 250 words. All information reported in the abstract must appear in the manuscript. The abstract should not include references. Please use complete sentences for all sections of the abstract. Structured abstract should include background, objective, methods, results and conclusions. Turkish

abstract will be provided by the editorial office for the authors who are not Turkish speakers. If you are not a native Turkish speaker, please re enter your English abstract to the area provided for the Turkish abstract.

- Introduction
- Materials and Methods
- Results
- Discussion
- Study Limitations
- Conclusion
- **Acknowledgement:** May be given for contributors who are not listed as authors, or for grant support of the research.
- **References:** References should be cited in numerical order (in parentheses) in the text and listed in the same numerical order at the end of the manuscript on a separate page or pages. The author is responsible for the accuracy of references. Examples of the reference style are given below. Further examples will be found in the articles describing the Uniform Requirements for Manuscripts Submitted to Biomedical Journals (Ann Intern Med.1988; 208:258-265, Br Med J. 1988; 296:401-405). The titles of journals should be abbreviated according to the style used in the Index Medicus. Journal Articles and Abstracts: Surnames and initials of author's name, title of the article, journal name, date, volume number, and pages. All authors should be listed regardless of number. The citation of unpublished papers, observations or personal communications is not permitted. Citing an abstract is not recommended. **Books:** Surnames and initials of author's names, chapter title, editor's name, book title, edition, city, publisher, date and pages.

Sample References

Journal Article: Sayit E, Söylev M, Capa G, Durak I, Ada E, Yılmaz M. The role of technetium-99m-HMPAO-labeled WBC scintigraphy in the diagnosis of orbital cellulitis. *Ann Nucl Med* 2001;15:41-44.

Article with DOI Number: Erselcan T, Hasbek Z, Tandogan I, Gumus C, Akkurt I. Modification of Diet in Renal Disease equation in the risk stratification of contrast induced acute kidney injury in hospital inpatients. *Nefrologia* 2009 doi: 10.3265/Nefrologia.2009.29.5.5449.en.full.

Article in a journal published ahead of print: Ludbrook J. Musculo-venous pumps in the human lower limb. *Am Heart J* 2009;00:1-6. (accessed 20 February 2009).

Book Chapters: Lang TF, Duryea J. Peripheral Bone Mineral Assessment of the Axial Skeleton: Technical Aspects. In: Orwoll ES, Bliizotes M (eds). *Osteoporosis: Pathophysiology and Clinical Management*. New Jersey, Humana Pres Inc, 2003;83-104.

Books: Greenspan A. *Orthopaedic Radiology a Practical Approach*. 3th ed. Philadelphia, Lippincott Williams Wilkins 2000, 295-330.

Website: Smith JR. 'Choosing Your Reference Style', *Online Referencing* 2(3), <http://orj.sagepub.com> (2003, accessed October 2008).

- Tables

Tables must be constructed as simply as possible. Each table must have a concise heading and should be submitted on a separate page. Tables must not simply duplicate the text or figures. Number all tables in the order of their citation in the text. Include a title for each table (a brief phrase, preferably no longer than 10 to 15 words). Include all tables in a single file following the manuscript.

- Figure Legends

Figure legends should be submitted on a separate page and should be clear and informative.

INSTRUCTIONS TO AUTHORS

- Figures

Number all figures (graphs, charts, photographs, and illustrations) in the order of their citation in the text. At submission, the following file formats are acceptable: AI, EMF, EPS, JPG, PDF, PPT, PSD, TIF. Figures may be embedded at the end of the manuscript text file or loaded as separate files for submission. All images MUST be at or above intended display size, with the following image resolutions: Line Art 800 dpi, Combination (Line Art + Halftone) 600 dpi, Halftone 300 dpi. Image files also must be cropped as close to the actual image as possible.

Review Articles:

- Title page (see above)
- Abstract: Maximum 250 words; without structural divisions; in English and in Turkish. Turkish abstract will be provided by the editorial office for the authors who are not Turkish speakers. If you are not a native Turkish speaker, please re enter your English abstract to the area provided for the Turkish abstract.
- Text
- Conclusion
- Acknowledgements (if any)
- References

Case Report and Literature Review:

- Title page (see above)
- Abstract: Approximately 100-150 words; without structural divisions; in English and in Turkish. Turkish abstract will be provided by the editorial office for the authors who are not Turkish speakers. If you are not a native Turkish speaker, please re-enter your English abstract to the area provided for the Turkish abstract.
- Introduction
- Case report
- Literature Review and Discussion
- References

Editorial:

- Title page (see above)
- Abstract: Maximum 250 words; without structural divisions; in English and in Turkish. Turkish abstract will be provided by the editorial office for the authors who are not Turkish speakers. If you are not a native Turkish speaker, please re enter your English abstract to the area provided for the Turkish abstract.
- Text
- References

Letters to the Editor:

- Title page (see above)
- Short comment to a published work, no longer than 500 words, no figures or tables.
- References no more than five.

Proofs and Reprints

Proofs and a reprint order are sent to the corresponding author. The author should designate by footnote on the title page of the manuscript the name and address of the person to whom reprint requests should be directed. The manuscript when published will become the property of the journal.

Archiving

The editorial office will retain all manuscripts and related documentation (correspondence, reviews, etc.) for 12 months following the date of publication or rejection.

Submission Preparation Checklist

As part of the submission process, authors are required to check off their submission's compliance with all of the following items, and submissions may be returned to authors that do not adhere to these guidelines.

1. The submission has not been previously published, nor is it before another journal for consideration (or an explanation has been provided in Comments to the Editor).
2. The submission file is in Microsoft Word, RTF, or WordPerfect document file format. The text is double-spaced; uses a 12-point font; employs italics, rather than underlining (except with URL addresses); and the location for all illustrations, figures, and tables should be marked within the text at the appropriate points.
3. Where available, URLs for the references will be provided.
4. All authors should be listed in the references, regardless of the number.
5. The text adheres to the stylistic and bibliographic requirements outlined in the Author Guidelines, which is found in About the Journal.
6. English keywords should be provided from <http://www.nlm.nih.gov/mesh> (Medical Subject Headings), while Turkish key words should be provided from <http://www.bilinterimleri.com>
7. The title page should be a separate document from the main text and should be uploaded separately.
8. The "Affirmation of Originality and Assignment of Copyright/The Disclosure Form for Potential Conflicts of Interest Form" should be downloaded from the website, filled thoroughly and uploaded during the submission of the manuscript.

TO AUTHORS

Copyright Notice

The author(s) hereby affirms that the manuscript submitted is original, that all statement asserted as facts are based on author(s) careful investigation and research for accuracy, that the manuscript does not, in whole or part, infringe any copyright, that it has not been published in total or in part and is not being submitted or considered for publication in total or in part elsewhere. Completed Copyright Assignment & Affirmation of Originality Form will be uploaded during submission.

By signing this form;

1. Each author acknowledges that he/she participated in the work in a substantive way and is prepared to take public responsibility for the work.
2. Each author further affirms that he or she has read and understands the "Ethical Guidelines for Publication of Research".
3. The author(s), in consideration of the acceptance of the manuscript for publication, does hereby assign and transfer to the Molecular Imaging and Radionuclide Therapy all of the rights and interest in and the copyright of the work in its current form and in any form subsequently revised for publication and/or electronic dissemination.

Privacy Statement

The names and email addresses entered in this journal site will be used exclusively for the stated purposes of this journal and will not be made available for any other purpose or to any other party.

Peer Review Process

1. The manuscript is assigned to an editor, who reviews the manuscript and makes an initial decision based on manuscript quality and editorial priorities.
2. For those manuscripts sent for external peer review, the editor assigns at least two reviewers to the manuscript.
3. The reviewers review the manuscript.
4. The editor makes a final decision based on editorial priorities, manuscript quality, and reviewer recommendations.
5. The decision letter is sent to the author.

Review

- 50** Use of Positron Emission Tomography/Computed Tomography in Radiation Treatment Planning for Lung Cancer
Akciğer Kanserlerinde Radyoterapi Planlamada Pozitron Emisyon Tomografisi/Bilgisayarlı Tomografi Kullanımı
Kezban Berberoğlu; İstanbul, Turkey

Original Articles

- 63** Morphologic and Metabolic Comparison of Treatment Responsiveness with ¹⁸F-fluorodeoxyglucose-Positron Emission Tomography/Computed Tomography According to Lung Cancer Type
Akciğer Kanseri Tipine Göre ¹⁸Florodeoksiglikoz-Pozitron Emisyon Tomografisi/Bilgisayarlı Tomografi ile Tedavi Yanıtının Morfolojik ve Metabolik Karşılaştırılması
Mehmet Fatih Börksüz, Taner Erselcan, Zekiye Hasbek, Birsen Yücel, Bülent Turgut; Aksaray, Muğla, Sivas, Turkey
- 70** Evaluation of Silent Myocardial Ischemia with Single-Photon Emission Computed Tomography/Computed Tomography in Asymptomatic Subjects with Diabetes and Pre-Diabetes
Asemptomatik Diyabetik ve Pre-Diyabetik Hastalarda Miyokardiyal Sessiz İskeminin Tek Foton Emisyon Bilgisayarlı Tomografisi/Bilgisayarlı Tomografi ile Değerlendirilmesi
Elif Özdemir, Şefika Burçak Polat, Nilüfer Yıldırım, Şeyda Türkölmez, Reyhan Ersoy, Tahir Durmaz, Telat Keleş, Engin Bozkurt, Bekir Çakır; Ankara, Turkey
- 79** Is Very High Thyroid Stimulating Hormone Level Required in Differentiated Thyroid Cancer for Ablation Success?
Diferansiyel Tiroid Kanserlerinde Ablasyon Başarısı İçin Tiroid Stimüle Edici Hormon Seviyesinin Çok Yüksek Olması Gerekli midir?
Zekiye Hasbek, Bülent Turgut; Sivas, Turkey
- 85** Recurrence Incidence in Differentiated Thyroid Cancers and the Importance of Diagnostic Iodine-131 Scintigraphy in Clinical Follow-up
Diferansiyel Tiroid Karsinomunda Rekürrens Sıklığı ve Klinik İzlemede Tanısal İyot-131 Sintigrafisinin Önemi
Filiz Hatipoğlu, İnanç Karapolat, Özgür Ömür, Ayşegül Akgün, Ahmet Yanarateş, Kamil Kumanlıoğlu; İzmir, Turkey

Case Reports

- 91** Hypermetabolic Calcified Lymph Nodes on ¹⁸F-fluorodeoxyglucose-Positron Emission Tomography/Computed Tomography in a Case of Treated Ovarian Cancer Recurrence: Residual Disease or Benign Formation?
Tedavi Edilmiş Over Kanseri Nüksünde ¹⁸Florodeoksiglikoz-Pozitron Emisyon Tomografisi/Bilgisayarlı Tomografi ile Saptanan Hipermetabolik Kalsifiye Lenf Nodları: Rezidüel Hastalık mı? Benign Oluşum mu?
Alexandra Nikaki, Athanasios Alexopoulos, Fani Vlachou, Vasiliki Filippi, Ioannis Andreou, Vasiliki Rapti, Konstantinos Gogos, Konstantinos Dalianis, Roxani Efthymiadou, Vassilios Prassopoulos; Athens, Greece
- 97** Sentinel Lymph Node Detection by 3D Freehand Single-Photon Emission Computed Tomography in Early Stage Breast Cancer
Erken Evre Meme Kanserinde 3D Freehand Tek Foton Emisyon Bilgisayarlı Tomografi ile Sentinel Lenf Nodu Tespiti
Salih Sinan Gültekin, Ahmet Oğuz Hasdemir, Serhat Tokgöz, Gülay Özgehan, Hakan Güzel, Cüneyt Yücesoy, Emine Öztürk, Ata Türker Arıkkö; Ankara, Turkey
- 102** Kikuchi Disease with Generalized Lymph Node, Spleen and Subcutaneous Involvement Detected by Fluorine-18-Fluorodeoxyglucose Positron Emission Tomography/Computed Tomography
Flor-18-Florodeoksiglukoz Pozitron Emisyon Tomografisi/Bilgisayarlı Tomografi ile Saptanan Yaygın Lenf Nodu, Dalak ve Deri Altı Tutulumu Olan Kikuchi Hastalığı
Alshaima Alshammari, Evangelia Skoura, Nafisa Kazem, Rasha Ashkanani; Jabriya, Kuwait, London, United Kingdom



Use of Positron Emission Tomography/Computed Tomography in Radiation Treatment Planning for Lung Cancer

Akciğer Kanserlerinde Radyoterapi Planlamada Pozitron Emisyon Tomografi/Bilgisayarlı Tomografi Kullanımı

Kezban Berberoğlu

Anadolu Medical Center, Clinic of Nuclear Medicine, İstanbul, Turkey

Abstract

Radiotherapy (RT) plays an important role in the treatment of lung cancer. Accurate diagnosis and staging are crucial in the delivery of RT with curative intent. Target miss can be prevented by accurate determination of tumor contours during RT planning. Currently, tumor contours are determined manually by computed tomography (CT) during RT planning. This method leads to differences in delineation of tumor volume between users. Given the change in RT tools and methods due to rapidly developing technology, it is now more significant to accurately delineate the tumor tissue. F18 fluorodeoxyglucose positron emission tomography/CT (F18 FDG PET/CT) has been established as an accurate method in correctly staging and detecting tumor dissemination in lung cancer. Since it provides both anatomic and biologic information, F18 FDG PET decreases inter-user variability in tumor delineation. For instance, tumor volumes may be decreased as atelectasis and malignant tissue can be more accurately differentiated, as well as better evaluation of benign and malignant lymph nodes given the difference in FDG uptake. Using F18 FDG PET/CT, the radiation dose can be escalated without serious adverse effects in lung cancer. In this study, we evaluated the contribution of F18 FDG PET/CT for RT planning in lung cancer.

Keywords: F18 fluorodeoxyglucose positron emission tomography/computed tomography, radiotherapy planning, non-small cell lung cancer, small cell lung cancer

Öz

Akciğer kanserlerinin tedavisinde radyoterapi önemli rol oynar. Küratif radyoterapinin uygun biçimde verilebilmesi için doğru tanı ve evrelendirme yapılması şarttır. Radyoterapi planlamada tümör sınırlarının doğru biçimde belirlenmesi ile coğrafik kayıpların önüne geçilebilir. Günümüzde radyoterapi planlamada bilgisayarlı tomografi (BT) görüntüleri kullanılarak tümör sınırları manuel olarak belirlenmektedir. Bu yöntem, kullanıcılar arasında tümör volümlerinin belirlenmesinde farklılıklara yol açmaktadır. Hızla gelişen teknoloji sayesinde radyoterapi cihazlarının ve yöntemlerinin değişmesi uygun tedavinin verilebilmesinde gerçek tümör dokusunun gösterilmesinin önemini artırmıştır. F18 florodeoksiglukoz pozitron emisyon tomografi/BT'nin (F18 FDG PET/BT) akciğer kanserlerinde doğru evreleme ve tümör yayılımı tespit etmede güvenilir bir yöntem olduğu bildirilmiştir. F18 FDG PET anatomik bilgilere ilave olarak biyolojik bilgileri de sağladığından klinisyenler arasında farklılığı anlamlı biçimde azaltmaktadır. Örneğin tümör dokusunu atelektazik alandan ayırarak ve boyutları benign nedenlerle büyümüş lenf nodlarını belirleyerek tümör volümlerini azaltmakta veya boyutları küçük ancak FDG tutulumu gösteren metastatik lenf nodlarını göstererek doğru alanın ışınlanmasına olanak sağlamaktadır. F18 FDG PET/BT ile akciğer kanserlerinde ciddi yan etkilere yol açmadan doz artırımını yapılabilir. Bu yazıda akciğer kanserlerinde radyoterapi planlamasının F18 FDG PET/BT ile yapılmasının katkısı değerlendirilmiştir.

Anahtar Kelimeler: F18 florodeoksiglukoz pozitron emisyon tomografi/bilgisayarlı tomografi, radyoterapi planlama, küçük hücreli dışı akciğer kanseri, küçük hücreli akciğer kanseri

Address for Correspondence: Kezban Berberoğlu MD, Anadolu Medical Center, Clinic of Nuclear Medicine, İstanbul, Turkey
Phone: +90 532 584 62 56 E-mail: kezbanberberoglu@hotmail.com **Received:** 26.11.2015 **Accepted:** 01.02.2016

Introduction

External beam radiotherapy (RT) plays an important role in the management of non-small cell lung cancer (NSCLC) and small cell lung cancer (SCLC) (1,2). In the delivery of RT with curative intent, an optimum treatment plan will deliver a sufficiently high dose of radiation to achieve high tumor control while delivering the least possible dose to the smallest possible volume of critical normal tissues to reduce the side effects of RT. The introduced RT techniques such as three-dimensional conformal RT (3D-CRT), intensity modulated radiation therapy (IMRT) (3), and image-guided radiation therapy (IGRT) have improved the accuracy of radiation delivery, leading to improved loco-regional control with reduced morbidity by facilitating delivery of a higher radiation dose to the tumor while sparing more normal tissue (4,5). Before a treatment decision is made, accurate diagnosis and staging are essential parts of the RT treatment plan. The staging and diagnosis of the disease also play a crucial role in the success of definitive RT. Thus, feasible systemic treatments are enabled instead of unnecessary local treatments in patients with distant metastasis owing to accurate staging. The effectiveness of radiation therapy for lung cancer definitive treatment is limited by the radio-sensitivity of surrounding normal structures, by the difficulty in delineating the extent of malignant tissue using conventional imaging techniques, and by the identification of distant metastatic disease. Accurate and precise target delineation is necessary in order to take full advantage of these modern RT techniques. In addition, surgical resection is the standard of care for stage I and II NSCLC; however, significant co-morbidities may preclude surgical resection in those who are not able to tolerate the procedure. There is emerging data on the potential of ablative RT, called the stereotactic body radiation therapy (SBRT), in an effort to reduce morbidity and achieve better local control in a select group of patients. Herein we review the potential role of positron emission tomography (PET) imaging as a prognostic indicator in treatment planning and in the assessment of response to SBRT. Accurate delineation of target volume and preservation of peripheral critical organs determine treatment success in not only IMRT/volumetric modulated arc therapy but also SBRT. Target volumes and treatment volumes in RT planning are primarily determined by structural imaging with CT, contrast CT or MRI, which together with clinical judgment are used to estimate the likely extension of microscopic disease in each case and thereby define the clinical target volume (CTV). Currently computed tomography (CT) is still being used for the determination of tumor volume and to obtain electron density information that is necessary for organ dose calculation during treatment planning. In a clinical study where the tumor contour was drawn by radiation oncologists manually, there were inter-user differences between radiation oncologists in the determination of tumor volumes (6). Anatomic imaging methods can be insufficient

for assessment of some tumors and lymph nodes, and it is observed that radiation field might not include the tumor despite radiation dose escalation (7). Feasibility studies have found that the use of F18 fluorodeoxyglucose-PET/CT (F18-FDG) for planning three-dimensional conformal radiation therapy improves the standardization of volume delineation as compared to CT alone in several types of cancers that are well imaged on PET (8). FDG-PET/CT was formed by the fusion of CT that allows anatomic information, and FDG-PET that provides biological information. Thus, both anatomic and biologic information is acquired together. FDG-PET/CT significantly decreases the delineation differences between oncologists, and it provides proper staging by identifying tumor and lymph nodes and hence determines gross target volume (GTV) more accurately during RT planning process. In addition, it was shown that PET/CT increases the sensitivity and accuracy in determining nodal GTVs than those detected by CT alone. The contribution of FDG-PET/CT to RT planning has been investigated in various cancer types (9). Currently, the widespread use of FDG-PET/CT allows RT planning by this method (10). Functional/biologic imaging by FDG-PET/CT changes RT planning due to several reasons. The most important ones are:

1. Detection of lesions that are not observed by CT and MR (identification of small lymph nodes and distant metastases),
2. Reduction of tumor volumes by determination of fields without tumor such as atelectasis,
3. Allowing dose heterogeneity within one target by determining biologic differences within the tumor,
4. Superior ability in assessing the tumor after chemo-RT and during treatment,
5. "Response modulated RT" planning based on changing target volumes during the course of treatment (11,12).

Radiotherapy Planning in Non-Small Cell Lung Cancer by Fluorodeoxyglucose Positron Emission Tomography/Computed Tomography

Lung cancer is the leading cause of cancer mortality. Five-year life expectancy is 14% in patients diagnosed with lung cancer, and surgery is indicated in approximately 1/3rd (13). Surgery is the primary treatment for patients with early-stage disease. However, RT plays a significant role in those who cannot be operated due to medical and technical reasons. Disease control can be achieved by delivering the maximum radiation dose to the tumor and decreasing the dose to peripheral tissues; in NSCLC, this can be achieved via novel RT techniques such as IMRT, IGRT, and SBRT. RT planning by CT is a standard approach. Planning is performed by using anatomic information obtained by CT. When PET is used, biologic data can be included in planning as well, which allows dose escalation to the GTVs.

Staging

Staging is the most critical process in NSCLC, since both treatment strategy and prognosis are subject to change according to disease stage. FDG-PET/CT is more accurate than CT in showing mediastinal and distant metastases, and this imaging platform changes the treatment plan in approximately 1/3rd of patients (14). The sensitivity of FDG-PET/CT in mediastinal staging is higher than CT due to increased metabolic uptake of lymph nodes in FDG-PET/CT that were otherwise noted to be of normal size by CT. FDG-PET/CT can differentiate a metabolic active tumor from atelectasis (15). In addition, RT target volume can also be determined by detecting necrotic regions in the tumor. Thus, maximum radiation can be applied to different regions within the tumor by adjusting the intra-target dose, while decreasing the radiation dose that peripheral tissues will receive. As a result, fibrosis and long-term side effects will decrease (16). Patients can be operated if there is no lymph node involvement (N0) or if there is only hilar lymph node involvement (N1) in NSCLC. SBRT provides good local control in non-operable patients with T1-2 tumor and without lymph node metastasis (N0) (80 Gray in 6-8 fractions; 30-60 Gy in 3-5 fractions) (17). For this reason, the highly accurate mediastinal staging provided by FDG-PET/CT is critical for early stage NSCLC patients who are candidates for SBRT. Li et al. (17) evaluated 200 patients by FDG-PET/CT before the operation in their multi-centered study. They compared PET and the histopathologic results of surgery specimens. The sensitivity rate (83%) and negative predictive value (NPV) (91%) of PET/CT were found to be very high for mediastinal lymph node staging. Treatment volumes change owing to the presence of non-enlarged lymph nodes with increased FDG uptake. Hellwig et al. (18) reported the sensitivity rate of CT and FDG-PET as 56% and 83% for all stages, respectively. Enlarged nodal size on CT showed a sensitivity of PET of 90% while sensitivity was 70% in normal lymph node sizes on CT. Routine elective nodal radiation is not recommended due to the high NPV of FDG-PET/CT in detecting mediastinal lymph node metastasis (19). SBRT can be a treatment option for patients if mediastinal lymph node metastasis is not detected in FDG-PET study. Selective lymph node radiation, which refers to the irradiation of lymph nodes with increased FDG-PET uptake, is a reliable method that provides local control in lymph nodes with decreased target volumes (16,20). Hwangbo et al. (21) found that mediastinal staging by FDG-PET/CT led to false positive results in approximately 30% of patients. Therefore, pathologic evaluation with mediastinoscopy or endoscopic ultrasound (EUS-FNAB) guided fine needle aspiration biopsy may be more suitable. The sensitivity of EUS-FNAB and that of FDG-PET/CT are similar in the detection of mediastinal metastasis (EUS-FNAB: 97.9%, FDG-PET: 96.3%) in squamous cell carcinoma while EUS-FNAB has a higher sensitivity in adenocarcinoma patients (EUS-FNAB: 94.6%, FDG-PET: 77.8%) (21).

A dosimetric study of van Der Wel et al. (20) evaluating 21 patients with N2 and N3 NSCLC showed that using FDG-PET/CT in radiation treatment planning process the esophagus and the lungs could be kept in the low dose area while the tumor received a high dose. FDG-PET/CT is one of the most important methods for the detection of NSCLC patients who are candidates for definitive RT. FDG-PET/CT affects staging by detection of distant metastasis and locally advanced disease, thus improving the success rates of cancer treatment with curative intent such as RT and chemotherapy (22). In a prospective study by Mac Manus et al. (23) on 153 patients, FDG-PET/CT changed treatment plan in 30% of patients to palliative treatment who were initially planned for curative-intent RT by conventional staging. This alteration was due to the detection of distant metastasis and extensive intrathoracic disease in 20% and 10% of patients, respectively. Staging with PET predicts life expectancy more accurately than conventional staging in patients planned for curative-intent definitive RT. It allows prevention of unnecessary treatment for patients with a short life expectancy. The accuracy of staging with PET/CT in patients with NSCLC is higher and it allows radiation oncologists to treat the malignant tissue alone. In a prospective study including 105 NSCLC patients, the treatment strategy for 26% of the patients was changed from curative therapy to palliation after staging with FDG-PET, overall, the treatment plan was changed in 67% of the entire patient group (24). In another study including 153 NSCLC patients, it was observed that disease staging changed in 33% of the patients and target volumes changed in 25% of the patients after use of FDG-PET (25). It was further shown that the use of FDG-PET study for the detection of tumor volumes significantly decreased the differences in contouring between radiation oncologists. FDG also led to intra-observer changes, as the same oncologist contoured the same target differently when also using FDG PET (26).

Definition of Volumes Delineated in Radiotherapy Planning

The definitions related to tumor localization were described in International Commission on Radiation Units (ICRU) 29th, 50th, 62nd, 71st and 83rd reports in detail ICRU. In this study, the definition of target volumes was made by using these protocols (Figure 1).

Gross Tumor Volume GTV: The visible tumor volume that can be felt by hand and can be detected by methods such as CT or MR.

Clinical Target Volume: In various studies, it was shown that there were undetectable subclinical malignant cells around the gross tumor. Thus, it was considered that these areas should also be included in the treatment volume. The treatment volume is determined by the radiation oncologist based on the aim of treatment (cure versus palliation).

CTV=GTV + subclinical disease area

Planning Target Volume: Patient and machine factors are considered in the delineation of the planning target volume (PTV), which is a geometrical definition. Accurate selection of radiation areas and sizes in order to create the desired dose in CTV depends on the definition of PTV by considering error margins. PTV volume and shape are determined by the selected therapy techniques such as SBRT, tumor location and set-up errors that depend on the previously defined CTV. In addition, PTV is dependent on tumor location that can influence assessment with respiration or digestive organ movement such as peristalsis, as well as on patient set-up during treatment planning session and beam inaccuracies. The required confidence margins should be added to therapy plan to minimize these problems. Internal margins include physiological alterations in position, volume and shape of the tumor according to anatomical reference points (i.e. bladder and rectum become full differently in each treatment, respiration, intestine and heart movements). Set-up margin includes patient-specific clinical and instrument specific mechanical and dosimetric factors besides unavailability of the same position for the patient and radiation area according to coordinate systems of therapy instrument.

$PTV = CTV + \text{internal margin (IM)} + \text{set-up margin (SM)}$.

Internal Target Volume: This is defined both in ICRU 62 and ICRU 50, and includes respiration, digestion, heart and other organ movements in addition to CTV.

$ITV = CTV + IM$

Planning Organ at Risk Volume: Therapy planning and total dose should be also decided by considering radiation sensitivities of critical organs and early/late side effects. Side effects can manifest in the long-term in some organs

such as the spinal cord, and permanent damage can occur with high doses. Early side effects such as mucositis and diarrhea may lead to interruption of therapy. Generally, the dose limits of specific tissues and organs that can be tolerated without side effects should be determined and these doses should not be exceeded. IM and SM should be added while determining "planning organ at risk volume" (PVR) that can affect the dose area and therapy planning significantly.

$PRV = OAR + IM + SM$

Effect of Fluorodeoxyglucose Positron Emission Tomography on Target Volume Determination

FDG-PET/CT leads to significant alterations in target volume size and shape as shown in various studies (15,20,27,28,29,30,31,32,33).

In a recent review reported by Chi and Nguyen (34), it was observed that target volumes changed more than 20% while staging changed 20-50% as a result of treatment planning with FDG-PET. The most significant alteration was related to the differentiation of atelectasis from tumor tissue in PET images (Figure 2), and detection of lymph node metastases by observing increased FDG uptake in small-sized lymph nodes on CT (15,27,28,29,30,33) (Figure 3). Bradley et al. (29) showed that there was a 58% change in the delineation of tumor volume when planned using FDG-PET/CT in stage III NSCLC patients along with a 31% change in disease stage. The ability to identify and differentiate atelectasis led to a decrease in GTV delineation in 3 out of 24 patients planned for 3D conformal RT, while the ability to identify small lymph node metastases via high FDG uptake led to a GTV increase in 10 patients as well as detecting additional parenchymal disease in one patient. Furthermore, the dosage to the normal lung and esophagus decreases with a small GTV by excluding atelectasis. Similar studies showed that doses to the heart, esophagus, spinal cord and normal lungs decreased due to alterations of the target volume when using FDG-PET/CT (27,28,30,31,33). Although an increase in dose to peripheral tissue was observed in patients with greater GTV volume due to mediastinal lymph nodes detected by FDG-PET/CT, this increase was not found to be clinically significant in all patients. In a study of van Der Wel et al. (20), it was shown that nodal GTV decreased and thus, the dose that esophagus and normal received took decreased by FDG-PET/CT in N2-3 NSCLC patients. In a study performed in our clinic including 25 patients with lung cancer, a change was detected in 96% of the patients when target volumes were delineated by using F18 FDG-PET/CT versus CT alone. GTV and CTV volumes delineated by using FDG-PET/CT were lower than the volumes obtained by CT alone in 64% of the patients. This was due to PET/CT's enabling differentiation of the tumor from atelectasis in the lung (35).

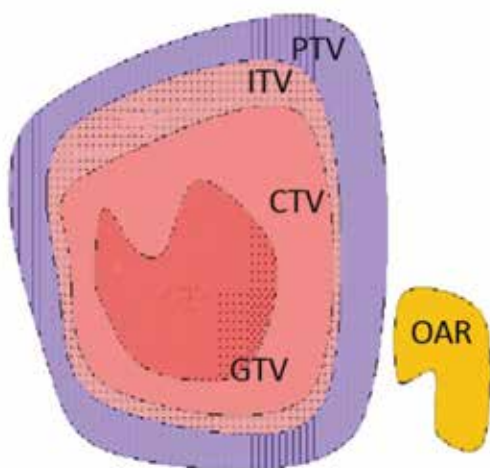


Figure 1. International Commission on Radiation Units 62: Treatment volume definitions

PTV: Planning target volume, CTV: Clinical target volume, GTV: Gross tumor volume

Delineation of Target Volumes by Fluorodeoxyglucose Positron Emission Tomography

Once PET and CT images are obtained and fused, tumor and target volume delineation are the most important steps to follow. Individual view assessment for each patient and determination of tumor contours are required because of the differences in bio-distribution, dynamic and screening features of screening agents used in nuclear medicine. Thus, a standard use and algorithm of

PET for the detection of target volumes is not available. Accurate and consistent detection of target volumes by PET is affected by certain factors. The first one is the limited spatial resolution of PET for the detection of GTV (it is approximately 4.5 mm in the latest generation PET/CT scanners) and partial difficulty in the determination of lesions due to poor resolution. The small lesions can be detected if only they have high FDG uptake while almost all of the lesions larger than 1 cm or those with increased FDG uptake 4 times greater than background activity can

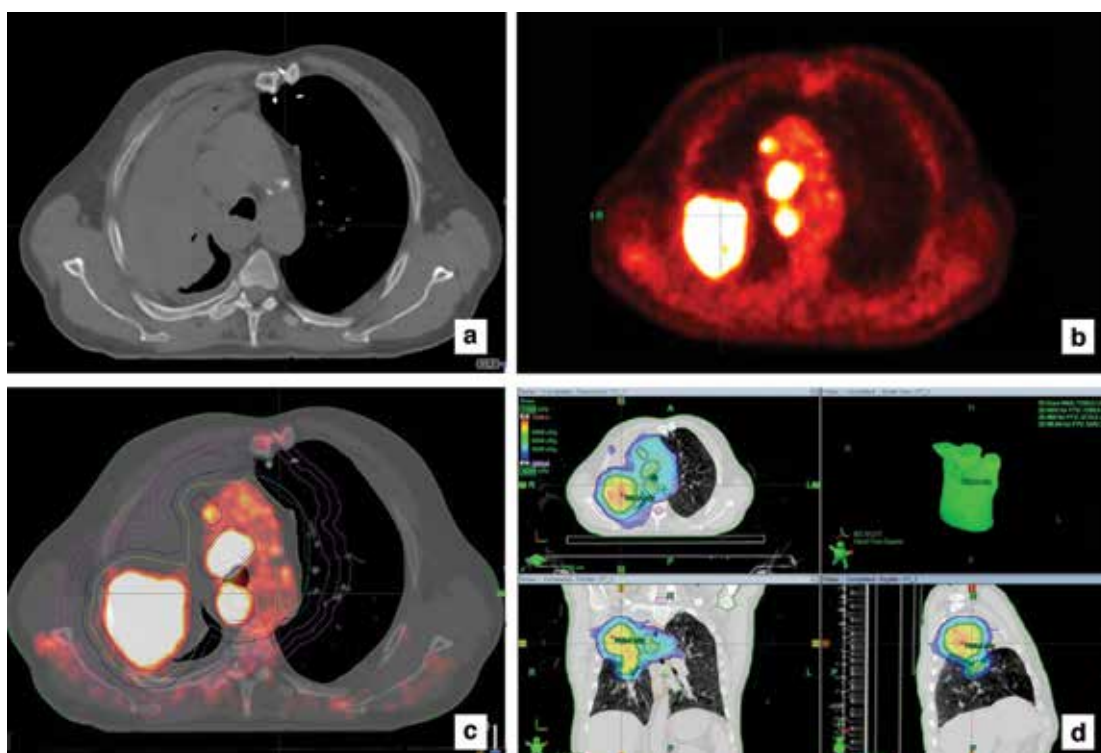


Figure 2. Non-small cell lung cancer, a) The atelectatic field cannot be separated from the tumor tissue in computed tomography, b) Positron emission tomography images showed increased fluorodeoxyglucose uptake in the tumor tissue, c and d) It was observed that there was a significant difference in target volumes formed by positron emission tomography/computed tomography fusion images

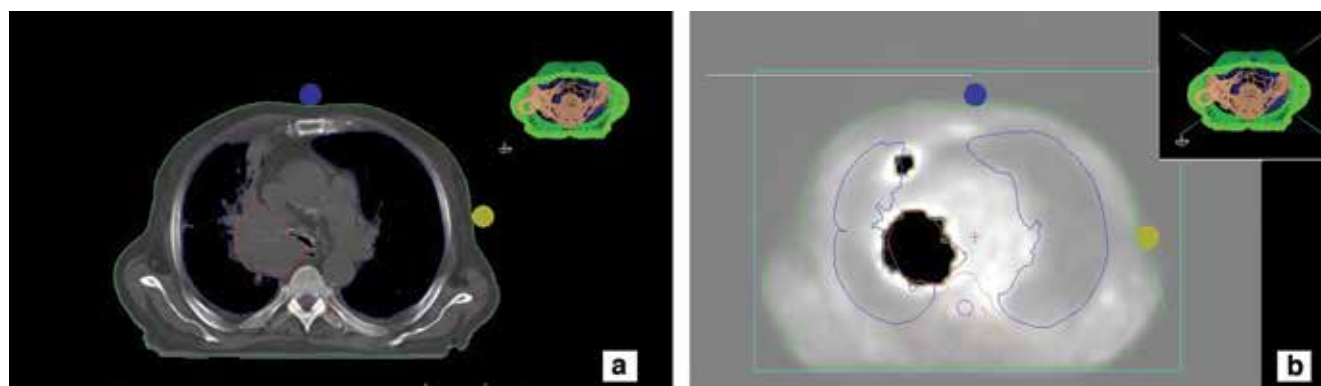


Figure 3. a) A normal-sized mediastinal lymph node in computed tomography images, b) Increased activity uptake was seen in positron emission tomography images, gross tumor volume included

be detected. The detection of tumor contours by visual assessment is subjective, and hence proper delineation varies according to physician experience; certain lesions can be obscured due to partial poor spatial resolution. In addition, the proper assessment may be affected by view window selection, color scale, lesion/background ratio and high uptake in neighboring normal structures in PET images. These problems can be minimized by fusing PET and CT images. The tumor can be detected more clearly by obtaining more information with fused images of PET and CT imaging. PET images can also be used for RT planning in patients with FDG-PET staging and who are suitable for RT with curative intent (29). Ideally, PET staging images of RT candidates can be used directly in treatment planning if the views are acquired with the patient in the treatment position with suitable immobilization (36). If there is no PET/CT instrument in the department, PET and CT image fusion can be performed afterward, only if reference markers were used (37). If PET imaging are not acquired in the treatment position (i.e. if arms are not above the head) or if there has been a significant time lapse since staging PET images, then it is recommended that PET should be repeated in the accurate position. Target volumes can be delineated by visual assessment, experience and initiative of the physician as well as mathematical modeling methods using PET data obtained by semi-quantitative calculations in RT planning. Methods used for the detection of target volumes are as follows:

1. Visual Assessment

It is observed that standardized uptake value (SUV_{max}) and other similar parameters are being used in almost all studies in which RT planning is performed by visual assessment. Visual method is not defined in the literature, thus, it is recommended that a detailed protocol should be outlined by the centers that will use this method. Anatomic labels should confirm the suitability of PET/CT and fusion images, and the radiation oncologist and the nuclear medicine specialist should select the suitable diagnostic window before beginning the RT planning process by visual assessment. In a study by Doll et al. (38) including 44 international and different disciplines, it was shown that tumor volumes were determined most accurately in teams including nuclear medicine doctor and radiation oncologist.

2. Automatic or Semi-Automatic Methods

Methods that are more objective were investigated using automatic and semi-automatic methods in order to decrease the inter-user variability in the detection of target tumor volumes by FDG-PET/CT. However, these methods could not differentiate neoplastic tissue from physiologic and inflammatory processes since FDG is not a tumor-specific substance. Tumor volumes required revision in

studies using real patient data while these methods yielded good results in studies using phantom data. It should be remembered that FDG is involved in macrophages and granulation tissue beside tumor cells. FDG-PET is a map showing three-dimensional glucose distribution, but it is not a map showing cancer cells (39).

2.1. Standardized Uptake Value

SUV_{max} is the most compatible and reliable quantitative parameter commonly used for the assessment of tumor activity in clinical practice [SUV_{max} : Maximum activity concentration/(injected dose/weight)]. Eighty-seven patients with pulmonary nodules were included in the study. Lesions were confirmed by pathological assessment and followed up for at least 2 years. When the threshold value for SUV was considered as 2.5 for the diagnosis of lung cancer, the sensitivity, specificity and accuracy were 97%, 82%, and 92%, respectively (40). Therefore, SUV threshold value is recommended as 2.5 for the detection of GTV during RT planning (41).

2.2. Thresholding Method

In the most common thresholding approach, it is accepted that selection of the field with constant percent uptake levels according to maximum activity value of tumor helps to determine tumor contour (42). In the studies in which constant threshold value was accepted as 40-50%, it was observed that this threshold value led to serious errors in lesion-size, homogeneity, and lesion/background contrast-dependent volume calculations (43). This approach was shown to decrease GTV significantly in primary NSCLC patients who showed large, non-homogeneous activity uptake by comparing various contouring methods (44). Thus, more studies are required for the detection of gross tumor contours by contrast-dependent adaptive thresholding methods.

2.3. Background Cut-off Method and Source/Background Plan Algorithms

In the background cut-off method, which is another automatic contouring method, tumor volumes are formed by drawing the field above the detected value (i.e. the fields showing 3 standard deviations from background activity for increase uptake level, fields above 2.5 SUV) (45). The advantage of this method is the detection of contours separately from heterogeneous FDG uptake in the lesion. However, the accuracy of this background cut-off approach depends on the accuracy of the statistical method used for this method. Contrast-oriented thresholding algorithm is obtained by calculating the effects of background FDG concentration on tumor volumes for the detection of GTV by PET in NSCLC patients (46). This approach showed that the GTV decreased as compared to the volumes obtained by CT alone, and it was compatible with pathologic tumor volume. This study detected a significant difference in pathologic tumor volume for tumors located in the lower lobes, as a result of breathing

motion. It was predicted that these mistakes can be prevented by three-dimensional PET imaging. In a study, in which source/background ratio determined by auto-segmentation approach was used, the results were compatible with pathologic tumor size in 33 NSCLC patients (47).

2.4. Gradient-Based Approach

PET-GTV detected by gradient-based approach is recommended in order to minimize statistical image noise and resolution blur (48). In a phantom study by Werner-Wasik et al. (49), gradient-based approach produced results that were more accurate as compared to other methods in terms of PET-GTV detection. In addition, this method was also compared with other methods in which GTV was

determined by comparing to surgical samples (50,51). A study including 10 patients who had undergone lobectomy for stage I-II NSCLC found that PET-GTV detected by 40-50% constant threshold and source/background ratio methods was better than GTV detected visually on CT images (50). In another study including 19 patients, tumor volumes detected by the gradient-based approach in PET/CT images obtained during normal breathing before surgery were highly compatible with surgical pathologic results (51).

2.5. Automatic Methods

Full-automatic thresholding methods were developed for the detection of tumor volumes by FDG-PET in lung cancer

Table 1. Methods of gross tumor volume delineation on positron emission tomography in correlation with surgical specimens

1.1.1.1.1.1	Patient Number	Method of GTV delineation on PET	Correlation between CT, PET, PET/CT and pathologic tumor size
Lin et al. (46)	37	Halo for tumor observed in fused PET/CT images	Stronger correlation between GTV and pathologic tumor dimensions were observed with PET/CT Mean SUV of the external margin of halo was 2.41±0.73 T stage and histology significantly influenced SUV at the edge of halo
Yu et al. (52)	52	SUV of 2.5	FDG-PET/CT had significantly better correlation with surgical specimens than CT or PET alone, especially in the presence of atelectasis
Yu et al. (53)	15	SUV threshold of 3.0±1.6	Best correlation between PET GTV and actual tumor was found at the SUV threshold of 3.0±1.6
Wu et al. (54)	31	Thresholding with 20-55% SUV _{max}	Maximal tumor dimension was more accurately predicted by CT at the window-level of 1.600 and -300 HU than PET GTVs (best correlation with pathologic tumor volume at 50% SUV _{max})
Schaefer et al. (55)	15	Tumor threshold=A *mean SUV70% + B *background	Pathologic tumor volume: 39±51 ml PET tumor volume: 48±62 ml CT tumor volume: 60.6±86.3 ml Both CT and PET volumes were highly correlated with pathological volumes (p<0.001). Increased variation between PET and pathological tumor volumes were observed in lower lobes.
van Baardwijk et al. (47)	33	Source-to-background ratio autosegmentation	Maximal tumor diameter of the PET GTV was highly correlated with that in surgical specimens (CC: 0.90). Auto-segmented GTVs were smaller than manually contoured GTVs on PET/CT
Wanet et al. (50)	10	Gradient based method Fixed threshold at 40 and 50% of the SUV _{max} Adaptive thresholding based on the source-to-background ratio	Comparison of both CT and PET/CT Gradient-based method led to the best estimation of the GTV PET GTVs were smaller than CT GTVs in general
Cheebsumon et al. (51)	19	Absolute SUV cut-off (2.5) Fixed threshold at 50% and 70% SUV _{max} Adaptive thresholding 41-70% SUV _{max} Contrast oriented algorithm Source to background ratio Gradient based method	Adaptive 50% gradient- based methods generated the most consistent maximal tumor dimension, which had a fair correlation with pathological tumor size

SUV_{max}: Maximum standard uptake value, GTV: Gross tumor volume, PET: Positron emission tomography, CT: Computed tomography

patients. Automatic thresholding methods using source/background algorithm is one of the most frequently used methods. If automatic contouring is performed using only functional images for RT planning, serious errors may occur. Primarily, it is important to match the images obtained by CT and the other anatomic imaging methods before determining tumor volume by automatic segmentation. Afterward, these should be revised by the planner since pathologic and physiologic distribution of the radioactive substance cannot be differentiated by automatic thresholding methods.

IA standardized automatic method for the delineation of GTV has not been established yet, although the methods discussed above have been reported for the detection of tumor volume. The concordance of real tumor volume obtained by surgery and different GTV detection methods in NSCLC patients are summarized in Table 1 (34).

Tumor Movement: Radiotherapy Planning by Gated Positron Emission Tomography/Computed Tomography

Organ movement and thus, tumor motion due to respiration, cardiac cycle, and other factors, is a significant issue in the delineation of the target tumor volume in thoracic malignancies. Calculations in RT planning should be performed by taking organ movements into consideration (56). A more accurate treatment can be delivered by following organ movement. If the tumor volume moves out of the contours, a part of the tumor can remain in the low-dose field due to organ motion. A few non-randomized studies described adverse effects related to average lung dose, despite the belief that high doses are advantageous for lung cancer patients (57). The peripheral healthy tissue can be preserved while increasing the dose to the tumor, and a smaller margin can be used to create the PTV by four-dimensional (4D) RT. PET, as well as CT images, can be recorded synchronized with the respiratory cycle in 4D Gated PET/CT imaging. Images are formed by taking a specific phase of 4D PET/CT respiration cycle as a reference point, and image of the tumor that moves with breathing can be obtained (58). Therefore, tumor contours can be delineated more accurately and normal tissues can be preserved better. 4D Gated PET/CT corrects for movement-dependent motion blur and shows the functionally active field of the tumor that is mobilized with respiration more clearly. In a study by Lamb et al. (59), tumor volumes of 4 lesions in the lower lobes of 3 patients were delineated, calculated by both 4D CT and 4D Gated PET/CT, and were compared. In this study, GTVs obtained by 4D PET/CT were 30% smaller in volume than those obtained by 4D CT. In the same study, the difference between the target tumor volumes obtained by 4D CT and normal PET images was deemed as minor. Gated PET allows more accurate GTV detection than 4D CT for SBRT planning, especially in tumors

located in the lower lobes, which have more movement. 4D CT has a decreased accuracy of tumor motion assessment in lower lobe lesions, due to the proximity of the tumor to soft tissues such as the liver on the right and the spleen and stomach on the left. Tumor motion is the most significant obstacle to the planning of conformal RT. The treating system should be compatible with the differences due to tumor motion (real time monitoring) at all times (60) or the radiation dose should be delivered only at a specific phase of the respiratory cycle. As a result, the definition of three-dimensional conformal RT is termed as a four-dimensional or gated radiation therapy.

Clinical Results of Radiotherapy Planning Performed by Positron Emission Tomography/Computed Tomography

The literature indicates that FDG-PET/CT significantly decreases clinical tumor volumes in patients with large lymph nodes without FDG uptake and atelectasis due to its high diagnostic accuracy in NSCLC. FDG-PET/CT was also observed to have a prognostic value since the SUV_{max} value is reported to predict survival in primary NSCLC patients. In addition, the pre- and post-RT SUV_{max} values were found to correlate with overall survival and disease-free survival. High SUV_{max} values were associated with poor survival in primary lung tumors and with the presence of lymph node metastasis (61). High glucose uptake of the tumor is related to its high metastatic potential. Mac Manus et al. (62) investigated the role of FDG-PET in the assessment of response to RT. In this study, screening was performed by FDG-PET for 88 NSCLC patients before and after chemotherapy (on average 70 days after RT initiation, 60 Gy, 30 fractions for 6 weeks). The complete metabolic response was obtained in 45% of the patients while a partial metabolic response was obtained in 36% of the patients by FDG-PET after treatment. The mean survival was 31 months and 11 months in the group with a complete metabolic response and in the group without response, respectively. One-year survival was determined as 93% and 47% in the group with complete response and without response, respectively. This study detected that the results were statistically significant despite confounders such as inflammation due to RT. There are significant differences in SUV_{max} changes during RT between the group that showed metabolic response and the group with no response. Overall survival was higher in the group with a metabolic response. The decrease ratio in SUV_{max} value directly correlated with disease-free survival (63). FDG-PET/CT plays an important role in the detection of recurrent disease. Metabolic evaluation by PET/CT in NSCLC has a high accuracy rate after treatment (78-98%) (64). Investigations can be performed as early as 6 weeks post treatment due to pneumonia and inflammation that may occur after RT, but the recommended interval is frequently 3-6 months.

Metabolic response assessment is an important parameter for the detection of local failure and survival. The detection of residual metabolic activity allows for the possibility of additional planning (Figure 4). In a study by Velasquez et al. (65), PET images were assessed before and after radical chemotherapy in 101 non-operated NSCLC patients. The overall survival was significantly decreased in the group showing residual metabolic uptake in the post-treatment PET study. There was an association between detection of residual increased metabolic uptake after RT in large tumors and tumors with high SUV_{max} value. The clinical results of stage II-III NSCLC patients whose disease volumes were identified by FDG-PET/CT and who were treated with RT were reported in two recent studies (66,67). In a pilot study including 32 patients treated with RT, only one local failure and one local progression were detected (66). The recurrence was in a lymph node. When the treatment plans were revisited, it was observed that this lymph node was FDG positive but was not included in the treatment volume. In another study on 137 stage III NSCLC patients and PET-positive areas, local recurrence was reported as 14.6% and distant metastases as 16.8% (67). These findings showed that clinical results of patients with stage II and III disease whose RT were planned by PET were as good as of those planned by using CT (68). Furthermore, the dose to the primary lesion can be increased while preserving the normal tissue in locally advanced NSCLC by using PET. Therefore, local control can be increased as well as survival, as was suggested by Aupérin et al. (69) in a meta-analysis.

Radiotherapy Planning by Fluorodeoxyglucose Positron Emission Tomography/Computed Tomography in Small Cell Lung Cancer Staging

SCLC consists of approximately 20-25% of lung cancers. It is often diagnosed at an advanced stage with distant metastases and exhibits an aggressive clinical behavior (70). In spite of aggressive treatment, it carries a poor prognosis (9). Accurate staging in SCLC is the most important factor in determining the most appropriate method of treatment. It is difficult to determine disease spread and especially to assess the involvement of mediastinal lymph nodes. Fischer et al. (71) compared FDG-PET/CT as a staging tool with standardized staging modalities (CT and bone scintigraphy) in their prospective study including 29 SCLC patients. In this study, PET/CT changed the plan in five of 29 patients (17%), and it was shown that this method increased the accuracy of tumor definition. In another study, 8.3-9.5% of patients were up-staged to advanced stages with the addition of FDG-PET/CT (72,73). Arslan et al. (74) evaluated the accuracy of staging by FDG-PET/CT and CT, and its relation to overall survival. When compared to staging by CT, staging by FDG-PET/CT up-staged nine of 25 patients (36%), while down-staging two patients (8%). In addition, a significant survival difference was predicted ($p=0.019$) by using FDG-PET/CT in the staging process, but there was no difference in those in which CT had been used ($p=0.055$). These studies recommend the use of FDG-PET/CT for initial staging in SCLC during limited stage.

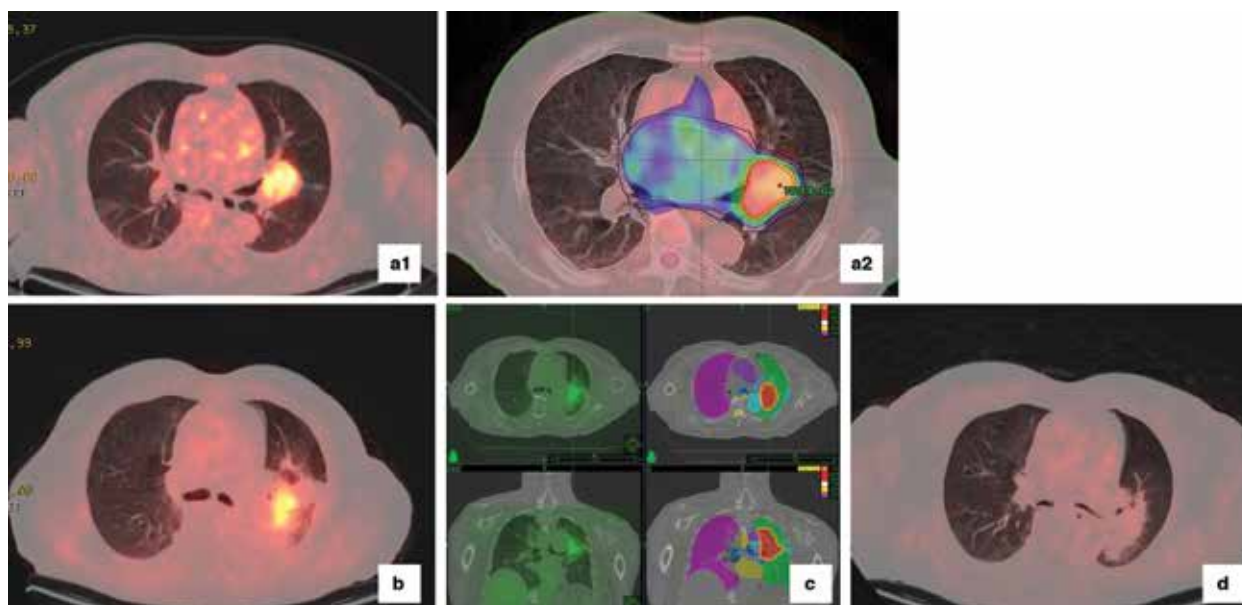


Figure 4. Non-small cell lung cancer, 82 y.o., M patient, a1) Abnormal increased metabolic activity was observed in the mass identified in the left parahilar region and, a2) Intensity modulated radiation therapy planning images by these views, b) Increased metabolic activity compatible with residual mass was seen in positron emission tomography/computed tomography that was applied for treatment-control after four months, c) Plan images belonged to stereotactic body radiation therapy that was applied to the residual mass, d) Pathologic activity was not observed in positron emission tomography/computed tomography after one year (complete metabolic response)

Determination of Tumor Volumes by Fluorodeoxyglucose Positron Emission Tomography/Computed Tomography

There are less studies in which tumor volumes were determined by FDG-PET/CT in SCLC patients when compared to NSCLC. Nevertheless, it can contribute to the treatment planning process by determining tumor volumes more accurately as in NSCLC.

Radiotherapy Planning for the Field Involved Lymph Node with Fluorodeoxyglucose Positron Emission Tomography/Computed Tomography

Elective nodal radiation of mediastinal lymph nodes in SCLC patients with limited disease decreases nodal failure rate. However, some physicians are reluctant to offer elective nodal radiation due to serious adverse effects as a result of large field of radiation. Baas et al. (75) evaluated involved field RT in early stage SCLC patients diagnosed by CT in their phase II study. Mean survival was 19.5 months with acceptable adverse effects. De Ruyscher et al. (76) investigated involved field RT in early stage SCLC patients diagnosed by CT in their phase II study. They assessed general survival and isolated lymph node failure rates, which was described as relapse in local lymph nodes out of target volumes in patients who had no failure identified in the treatment field. In this study, isolated lymph node metastases that were not included in the treatment field was found to be unexpectedly high (11%). Involved field RT was considered as controversial by International Atomic Energy Agency (IAEA) when these findings were evaluated, and further prospective clinic studies were suggested (77). FDG-PET/CT can be used in order to determine the requirement of elective nodal radiation. Two recent studies assessed the requirement for elective nodal radiation after staging by FDG-PET/CT (78,79). In a prospective study, van Loon et al. (78) assessed involved field RT by FDG-PET in 60 patients with limited stage SCLC disease. The mean overall survival was 19 months and isolated nodal failure rate was 3%. The isolated nodal failure rate was significantly lower in the group planned by FDG-PET as compared to the group planned by CT (11% vs. 3%). Shirvani et al. (79) evaluated 60 patients with limited stage SCLC who were staged by FDG-PET and were treated with IMRT involved field RT. The 2-years survival rate was calculated as 58%, and isolated nodal failure was detected in one patient (3%). These studies concluded that involved field RT could be used reliably instead of elective nodal radiation in patients staged by F18 FDG-PET. In this way, the toxicity can be decreased or adjusted by not irradiating the PET negative lymph nodes. Involved field RT by FDG-PET in SCLC is a current discussion subject and the use of involved field RT instead of elective nodal radiation should be assessed by further prospective studies. Another role of FDG-PET in SCLC is the evaluation

of response to treatment. It was found that assessment success of FDG-PET in patients who received chemotherapy and RT was high (80).

Conclusion

In conclusion, the most important contribution of FDG-PET to the management of SCLC is in the accuracy of staging. Although RT use with the help of FDG-PET in this patient group is controversial, involved field radiation is an attention-grabbing method. FDG-PET treatment planning can change treatment strategy of SCLC patients with limited disease.

Ethics

Peer-review: Externally peer-reviewed.

References

1. Onishi H, Shirato H, Nagata Y, Hiraoka M, Fujino M, Gomi K, Niibe Y, Karasawa K, Hayakawa K, Takai Y, Kimura T, Takeda A, Ouchi A, Hareyama M, Kokubo M, Hara R, Itami J, Yamada K, Araki T. Hypofractionated stereotactic radiotherapy (HypoFXSRT) for stage I non-small cell lung cancer: updated results of 257 patients in a Japanese multi-institutional study. *J Thorac Oncol* 2007;2(Suppl 3):94-100.
2. Grills IS, Mangona VS, Welsh R, Chmielewski G, McInerney E, Martin S, Wloch J, Ye H, Kestin LL. Outcomes after stereotactic lung radiotherapy or wedge resection for stage I non-small-cell lung cancer. *J Clin Oncol* 2010;28:928-935.
3. Dogan N, Leybovich LB, Sethi A, Emami B. Improvement of dose distributions in abutment regions of intensity modulated radiation therapy and electron fields. *Med Phys* 2002;29:38-44.
4. Zelefsky MJ, Leibel SA, Kutcher GJ, Fuks Z. Three-dimensional conformal radiotherapy and dose escalation: where do we stand? *Semin Radiat Oncol* 1998;8:107-114.
5. Hanks GE, Hanlon AL, Schultheiss TE, Pinover WH, Movsas B, Epstein BE, Hunt MA. Dose escalation with 3D conformal treatment: five year outcomes, treatment optimization, and future directions. *Int J Radiat Oncol Biol Phys* 1998;41:501-510.
6. Van de Steene J, Linthout N, de Mey J, Vinh-Hung V, Claassens C, Noppen M, Bel A, Storme G. Definition of gross tumor volume in lung cancer: inter-observer variability. *Radiother Oncol* 2002;62:37-49.
7. van Herk M, Remeijer P, Lebesque JV. Inclusion of geometric uncertainties in treatment plan evaluation. *Int J Radiat Oncol Biol Phys* 2002;52:1407-1422.
8. Lardinois D, Weder W, Hany TF, Kamel EM, Korom S, Seifert B, von Schulthess GK, Steinert HC. Staging of non-small-cell lung cancer with integrated positron-emission tomography and computed tomography. *N Engl J Med* 2003;348:2500-2507.
9. Lammering G, De Ruyscher D, van Baardwijk A, Baumert BG, Borger J, Lutgens L, van den Ende P, Ollers M, Lambin P. The use of FDG-PET to target tumors by radiotherapy. *Strahlenther Onkol* 2010;186:471-481.
10. Baum RP, Hellwig D, Mezzetti M. Position of nuclear medicine modalities in the diagnostic workup of cancer patients: lung cancer. *Q J Nucl Med Mol Imaging* 2004;48:119-142.
11. Weber WA, Wieder H. Monitoring chemotherapy and radiotherapy of solid tumors. *Eur J Nucl Med Mol Imaging* 2006;33(Suppl 1):27-37.
12. Ling CC, Li XA. Over the next decade the success of radiation treatment planning will be judged by the immediate biological response of tumor cells rather than by surrogate measures such as dose maximization and uniformity. *Med Phys* 2005;32:2189-2192.

13. Rubin P. *Clinical Oncology*, 8th ed. Philadelphia, Saunders 2001.
14. Kernstine KH, Mclaughlin KA, Menda Y, Rossi NP, Kahn DJ, Bushnell DL, Graham MM, Brown CK, Madsen MT. Can FDG-PET reduce the need for mediastinoscopy in potentially resectable non-small cell lung cancer? *Ann Thorac Surg* 2002;73:394-401.
15. Nestle U, Walter K, Schmidt S, Licht N, Nieder C, Motaref B, Hellwig D, Niewald M, Ukena D, Kirsch CM, Sybrecht GW, Schnabel K. 18F-deoxyglucose positron emission tomography (FDG-PET) for the planning of radiotherapy in lung cancer: high impact in patients with atelectasis. *Int J Radiat Oncol Biol Phys* 1999;44:593-597.
16. De Ruyscher D, Wanders S, Minken A, Lumens A, Schiffelers J, Stultiens C, Halders S, Boersma L, Baardwijk Av, Verschueren T, Hochstenbag M, Snoep G, Wouters B, Nijsten S, Bentzen SM, Kroonenburgh Mv, Ollers M, Lambin P. Effects of radiotherapy planning with a dedicated combined PET-CT-simulator of patients with non-small cell lung cancer on dose limiting normal tissues and radiation dose escalation: a planning study. *Radiother Oncol* 2005;77:5-10.
17. Li X, Zhang H, Xing L, Ma H, Xie P, Zhang L, Xu X, Yue J, Sun X, Hu X, Chen M, Xu W, Chen L, Yu J. Mediastinal lymph nodes staging by 18F-FDG PET/CT for early stage non-small cell lung cancer: a multi center study. *Radiother Oncol* 2012;102:246-250.
18. Hellwig D, Baum RP, Kirsch C. FDG-PET, PET/CT and conventional nuclear medicine procedures in the evaluation of lung cancer: a systematic review. *Nuklearmedizin* 2009;48:59-69.
19. Senan S, De Ruyscher D, Giraud P, Mirimanoff R, Budach V; Radiotherapy Group of European Organization for Research and Treatment of Cancer. Literature-based recommendations for treatment planning and execution in high-dose radiotherapy for lung cancer. *Radiother Oncol* 2004;71:139-146.
20. van Der Wel A, Nijsten S, Hochstenbag M, Lamers R, Boersma L, Wanders R, Lutgens L, Zimny M, Bentzen SM, Wouters B, Lambin P, De Ruyscher D. Increased therapeutic ratio by 18FDG-PET-CT planning in patients with clinical CT stage N2/N3M0 non-small cell lung cancer: a modeling study. *Int J Radiat Oncol Biol Phys* 2005;61:649-655.
21. Hwangbo B, Kim SK, Lee HS, Lee HS, Kim MS, Lee JM, Kim HY, Lee GK, Nam BH, Zo JI. Application of endobronchial ultrasound-guided transbronchial needle aspiration following integrated PET/CT in mediastinal staging of potentially operable non-small cell lung cancer. *Chest* 2009;135:1280-1287.
22. Mac Manus MP, Wong K, Hicks RJ, Matthews JP, Wirth A, Ball DL. Early mortality after radical radiotherapy for non-small-cell lung cancer: comparison of PET-staged and conventionally staged cohorts treated at a large tertiary referral center. *Int J Radiat Oncol Biol Phys* 2002;52:351-361.
23. Mac Manus MP, Hicks RJ, Ball DL, Kalff V, Matthews JP, Salminen E, Khaw P, Wirth A, Rischin D, McKenzie A. F-18 fluorodeoxyglucose positron emission tomography staging in radical radiotherapy candidates with non-small cell lung carcinoma: powerful correlation with survival and high impact on treatment. *Cancer* 2001;92:886-895.
24. Kalff V, Hicks RJ, MacManus MP, Binns DS, McKenzie AF, Ware RE, Hogg A, Ball DL. Clinical impact of (18)F fluorodeoxyglucose positron emission tomography in patients with non-small-cell lung cancer: a prospective study. *J Clin Oncol* 2001;19:111-118.
25. Hicks RJ, Kalff V, MacManus MP, Ware RE, Hogg A, McKenzie AF, Matthews JP, Ball DL. (18)F-FDG PET provides high impact and powerful prognostic stratification in staging newly diagnosed non-small-cell lung cancer. *J Nucl Med* 2001;42:1596-1604.
26. Fox JL, Rengan R, O'Meara W, Yorke E, Erdi Y, Nehmeh S, Leibel SA, Rosenzweig KE. Does registration of PET and planning CT images decrease interobserver and intraobserver variation in delineating tumor volumes for non-small-cell lung cancer? *Int J Radiat Oncol Biol Phys* 2005;62:70-75.
27. Erdi YE, Rosenzweig K, Erdi AK, Macapinlac HA, Hu YC, Braban LE, Humm JL, Squire OD, Chui CS, Larson SM, Yorke ED. Radiotherapy treatment planning for patients with non-small cell lung cancer using positron emission tomography (PET). *Radiother Oncol* 2002;62:51-60.
28. Mah K, Caldwell CB, Ung YC, Danjoux CE, Balogh JM, Ganguli SN, Ehrlich LE, Tirona R. The impact of 18 FDG-PET on target and critical organs in CT-based treatment planning of patients with poorly defined non-small-cell lung carcinoma: a prospective study. *Int J Radiat Oncol Biol Phys* 2002;52:339-350.
29. Bradley J, Thorstad WL, Mutic S, Miller TR, Dehdashti F, Siegel BA, Bosch V, Bertrand RJ. Impact of FDG-PET on radiation therapy volume delineation in non-small-cell lung cancer. *Int J Radiat Oncol Biol Phys* 2004;59:78-86.
30. Ceresoli G, Cattaneo GM, Castellone P, Rizzos G, Landoni C, Gregorc V, Calandrino R, Villa E, Messa C, Santoro A, Fazio F. Role of computed tomography and [18F] fluorodeoxyglucose positron emission tomography image fusion in conformal radiotherapy of non-small cell lung cancer: a comparison with standard techniques with and without elective nodal irradiation. *Tumori* 2007;93:88-96.
31. Vanuytsel LJ, Vansteenkiste JF, Stroobants SG, De Leyn PR, De Wever W, Verbeke EK, Gatti GG, Huyskens DP, Kutcher GJ. The impact of 18F-fluoro-2-deoxy-D-glucose positron emission tomography (FDG-PET) lymph node staging on the radiation treatment volumes in patients with non-small cell lung cancer. *Radiother Oncol* 2000;55:317-324.
32. Faria SL, Menard S, Devic S, Sirois C, Souhami L, Lisbona R, Freeman CR. Impact of FDG-PET/CT on radiotherapy volume delineation in non-small-cell lung cancer and correlation of imaging stage with pathologic findings. *Int J Radiat Oncol Biol Phys* 2008;70:1035-1038.
33. Yin LJ, Yu XB, Ren YG, Gu GH, Ding TG, Lu Z. Utilization of PET-CT in target volume delineation for three-dimensional conformal radiotherapy in patients with non small cell lung cancer and atelectasis. *Multidiscip Respir Med* 2013;8:21.
34. Chi A, Nguyen NP. The utility of positron emission tomography in the treatment planning of image-guided radiotherapy for non-small cell lung cancer. *Front oncol* 2014;4:273.
35. Baş Ayata H, Güden M, Berberoğlu K, Küçük N, Ceylan C, Kiliç A. Akciğer tümörlü hastalarda hedef völümün belirlenmesinde PET-BT ve BT görüntü karşılaştırılması. *Türk Onkoloji Derg* 2010;25:1;11-19.
36. Messa C, Di Muzio N, Picchio M, Gilardi MC, Bettinardi V, Fazio F. PET/CT and radiotherapy. *Q J Nucl Med Mol Imaging* 2006;50:4-14.
37. Deniaud-Alexandre E, Touboul E, Lerouge D, Grahek D, Foulquier JN, Petegnief Y, Grès B, El Balaa H, Keraudy K, Kerrou K, Montravers F, Milleron B, Lebeau B, Talbot JN. Impact of computed tomography and 18F-deoxyglucose coincidence detection emission tomography image fusion for optimization of conformal radiotherapy in non-small-cell lung cancer. *Int J Radiat Oncol Biol Phys* 2005;63:1432-1441.
38. Doll C, Duncker-Rohr V, Rücker G, Mix M, MacManus M, De Ruyscher D, Vogel W, Eriksen JG, Oyen W, Grosu AL, Weber W, Nestle U. Influence of experience and qualification on PET-based target volume delineation. When there is no expert—ask your colleague. *Strahlenther Onkol* 2014;190:555-562.
39. Kubota R, Yamada S, Kubota K, Ishiwata K, Tamahashi N, Ido T. Intratumoral distribution of fluorine-18-fluorodeoxyglucose in vivo: high accumulation in macrophages and granulation tissues studied by microautoradiography. *J Nucl Med* 1992;33:1972-1980.
40. Duhaylongsod FG, Lowe VJ, Patz EF Jr, Vaughn AL, Coleman RE, Wolfe WG. Detection of primary and recurrent lung cancer by means of F-18 fluorodeoxyglucose positron emission tomography (FDGPET). *J Thorac Cardiovasc Surg* 1995;110:130-139.
41. Paulino AC, Johnstone PA. FDG-PET in radiotherapy treatment planning: Pandora's box? *Int J Radiat Oncol Biol Phys* 2004;59:4-5.
42. Yaremko B, Riauka T, Robinson D, Murray B, Alexander A, McEwan A, Roa W. Thresholding in PET images of static and moving targets. *Phys Med Biol* 2005;50:5969-5982.
43. Yaremko B, Riauka T, Robinson D, Murray B, McEwan A, Roa W. Threshold modification for tumour imaging in non-small-cell lung cancer using positron emission tomography. *Nucl Med Commun* 2005;26:433-440.

44. Nestle U, Kremp S, Schaefer-Schuler A, Sebastian-Welsch C, Hellwig D, Rube C, Kirsch CM. Comparison of different methods for delineation of 18F-FDG PET-positive tissue for target volume definition in radiotherapy of patients with non-small cell lung cancer. *J Nucl Med* 2005;46:1342-1348.
45. Zasadny KR, Kison PV, Francis IR, Wahl RL. FDG-PET Determination of metabolically active tumor volume and comparison with CT. *Clin Positron Imaging* 1998;1:123-129.
46. Lin S, Han B, Yu L, Shan D, Wang R, Ning X. Comparison of PET-CT images with the histological picture of a resectable primary tumor for delineating GTV in non small cell lung cancer. *Nucl Med Commun* 2011;36:479-485.
47. van Baardwijk A, Bosmans G, Boersma L, Buijsen J, Wanders S, Hochstenbag M, van Suylen RJ, Dekker A, Dehing-Oberije C, Houben R, Bentzen SM, van Kroonenburgh M, Lambin P, De Ruyscher D. PET-CT-based auto-contouring in non-small-cell lung cancer correlates with pathology and reduces inter observer variability in the delineation of the primary tumor and involved nodal volumes. *Int J Radiat Oncol Biol Phys* 2007;68:771-778.
48. Geets X, Lee JA, Bol A, Lonnew M, Gregoire V. A gradient-based method for segmenting FDG-PET images: methodology and validation. *Eur J Nucl Med Mol Imaging* 2007;34:1427-1438.
49. Werner-Wasik M, Nelson AD, Choi W, Arai Y, Faulhaber PF, Kang P, Almeida FD, Xiao Y, Ohri N, Brockway KD, Piper JW, Nelson AS. What is the best way to contour lung tumors on PET scans? Multiobserver validation of a gradient-based method using a NSCLC digital PET phantom. *Int J Radiat Oncol Biol Phys* 2012;82:1164-1171.
50. Wanet M, Lee JA, Weynand B, De Bast M, Poncelet A, Lacroix V, Coche E, Grégoire V, Geets X. Gradient-based delineation of the primary GTV on FDG-PET in non-small cell lung cancer: a comparison with threshold-based approaches, CT and surgical specimens. *Radiother Oncol* 2011;98:117-125.
51. Cheebsumon P, Boellaard R, de Ruyscher D, van Elmpt W, van Baardwijk A, Yaqub M, Hoekstra OS, Comans EF, Lammertsma AA, van Velden FH. Assessment of tumour size in PET/CT lung cancer studies: PET and CT based methods compared to pathology. *EJNMMI Res* 2012;2:56.
52. Yu HM, Liu YF, Hou M, Liu J, Li XN, Yu JM. Evaluation of gross tumor size using CT, 18F-FDG PET, integrated 18F-FDG PET/CT and pathological analysis in non-small cell lung cancer. *Eur J Radiol* 2009;72:104-113.
53. Yu J, Li X, Xing L, Mu D, Fu Z, Sun X, Sun X, Yang G, Zhang B, Sun X, Ling CC. Comparison of tumor volumes as determined by pathologic examination and FDG-PET/CT images of non-small cell lung cancer: a pilot study. *Int J Radiat Oncol Biol Phys* 2009;75:1468-1474.
54. Wu K, Ung YC, Hornby J, Freeman M, Hwang D, Tsao MS, Dahele M, Darling G, Maziak DE, Tirona R, Mah K, Wong CS. PET CT thresholds for radiotherapy target definition in non-small-cell lung cancer: how close are we to the pathologic findings? *Int J Radiat Oncol Biol Phys* 2010;77:699-706.
55. Schaefer A, Kim YJ, Kremp S, Mai S, Fleckenstein J, Bohnenberger H, Schäfers HJ, Kuhnigk JM, Bohle RM, Rube C, Kirsch CM, Grgic A. PET-based delineation of tumour volumes in lung cancer: comparison with pathological findings. *Eur J Nucl Med Mol Imaging* 2013;40:1233-1244.
56. Webb S. Motion effects in (intensity modulated) radiation therapy: a review. *Phys Med Biol* 2006;51:403-425.
57. Rengan R, Rosenzweig KE, Venkatraman E, Koutcher LA, Fox JL, Nayak R, Amols H, Yorke E, Jackson A, Ling CC, Leibel SA. Improved local control with higher doses of radiation in large-volume stage III non-small-cell lung cancer. *Int J Radiat Oncol Biol Phys* 2004;60:741-747.
58. Nehmeh SA, Erdi YE, Pan T, Yorke E, Mageras GS, Rosenzweig KE, Schoder H, Mostafavi H, Squire O, Pevsner A, Larson SM, Humm JL. Quantitation of respiratory motion during 4D-PET/CT acquisition. *Med Phys* 2004;31:1333-1338.
59. Lamb JM, Robinson C, Bradley J, Laforest R, Dehdashti F, White BM, Wuenschel S, Low DA. Generating lung tumor internal target volumes from 4D-PET maximum intensity projections. *Med Phys* 2011;38:5732-5737.
60. Jeremic B. Incidental irradiation of nodal regions at risk during limited-field radiotherapy (RT) in dose-escalation studies in non-small cell lung cancer (NSCLC). Enough to convert no-elective into elective nodal irradiation (ENI)? *Radiother Oncol* 2004;71:123-125.
61. Liao CT, Chen JH, Liang JA, Yeh JJ, Kao CH. Meta-analysis study of lymph node staging by 18F-FDG PET/CT scan in non-small cell lung cancer. Comparison of TB and non-TB endemic regions. *Eur J Radiol* 2012;81:3518-3523.
62. Mac Manus MP, Hicks RJ, Matthews JP, Wirth A, Rischin D, Ball DL. Metabolic (FDG-PET) response after radical radiotherapy/chemoradiotherapy for non-small cell lung cancer correlates with pattern of failure. *Lung Cancer* 2005;49:95-108.
63. Lopez Guerra JL, Gladish G, Komaki R, Gomez D, Zhuang Y, Liao Z. Large decreases in standardized uptake values after definitive radiation are associated with better survival of patients with locally advanced non-small cell lung cancer. *J Nucl Med* 2012;53:225-233.
64. Erasmus JJ, Patz Jr E. Positron emission tomography imaging in the thorax. *Clin Chest Med* 1999;20:715-724.
65. Velasquez ER, Aerts HJ, Oberije C, De Ruyscher D, Lampin P. Prediction of residual metabolic activity after treatment in NSCLC patients. *Acta Oncol* 2010;49:1033-1049.
66. Fleckenstein J, Hellwig D, Kremp S, Grgic A, Gröschel A, Kirsch CM, Nestle U, Rube C. F-18-FDG-PET confined radiotherapy of locally advanced NSCLC with concomitant chemotherapy: results of the PET-PLAN pilot trial. *Int J Radiat Oncol Biol Phys* 2011;81:283-289.
67. van Baardwijk A, Reymen B, Wanders S, Borger J, Ollers M, Dingemans AM, Bootsma G, Geraedts W, Pitz C, Lunde R, Peters F, Lambin P, De Ruyscher D. Mature results of a phase II trial on individualised accelerated radiotherapy based on normal tissue constraints in concurrent chemoradiation for stage III non-small cell lung cancer. *Eur J Cancer* 2012;48:2339-2346.
68. Chi A, Nguyen NP, Welsh JS, Tse W, Monga M, Oduntan O, Almubarak M, Rogers J, Remick SC, Gius D. Strategies of dose escalation in the treatment of locally advanced non-small cell lung cancer: image guidance and beyond. *Front Oncol* 2014;4:156.
69. Aupérin A, Le Pêchoux C, Rolland E, Curran WJ, Furuse K, Fournel P, Belderbos J, Clamon G, Ulutin HC, Paulus R, Yamanaka T, Bozonnat MC, Uitterhoeve A, Wang X, Stewart L, Arriagada R, Burdett S, Pignon JP. Meta-analysis of concomitant versus sequential radiochemotherapy in locally advanced non-small-cell lung cancer. *J Clin Oncol* 2010;28:2181-2190.
70. Shirai K, Nakagawa A, Abe T, Kawahara M, Saitoh J, Ohno T, Nakano T. Use of FDG-PET in radiation treatment planning for thoracic cancers. *Int J Mol Imaging* 2012;2012:609545.
71. Fischer BM, Mortensen J, Langer SW, Loft A, Berthelsen AK, Petersen BI, Daugaard G, Lassen U, Hansen HH. A prospective study of PET/CT in initial staging of small-cell lung cancer: comparison with CT, bone scintigraphy and bone marrow analysis. *Ann Oncol* 2007;18:338-345.
72. Bradley JD, Dehdashti F, Mintun MA, Govindan R, Trinkaus K, Siegel BA. Positron emission tomography in limited-stage small-cell lung cancer: a prospective study. *J Clin Oncol* 2004;22:3248-3254.
73. Niho S, Fujii H, Murakami K, Nagase S, Yoh K, Goto K, Ohmatsu H, Kubota K, Sekiguchi R, Nawano S, Saijo N, Nishiwaki Y. Detection of unsuspected distant metastases and/or regional nodes by FDG-PET in LD-SCLC scan in apparent limited-disease small-cell lung cancer. *Lung Cancer* 2007;57:328-333.
74. Arslan N, Tuncel M, Kuzhan O, Alagoz E, Budakoglu B, Ozet A, Ozguven MA. Evaluation of outcome prediction and disease extension by quantitative 2-deoxy-2-[18F] fluoro-D-glucose with positron emission tomography in patients with small cell lung cancer. *Ann Nucl Med* 2011;25:406-413.

75. Baas P, Belderbos JS, Senan S, Kwa HB, van Bochove A, van Tinteren H, Burgers JA, van Meerbeeck JP. Concurrent chemotherapy (carboplatin, paclitaxel, etoposide) and involved-field radiotherapy in limited stage small cell lung cancer: a Dutch multicenter phase II study. *Br J Cancer* 2006;94:625-630.
76. De Ruyscher D, Bremer RH, Koppe F, Wanders S, van Haren E, Hochstenbag M, Geeraedts W, Pitz C, Simons J, ten Velde G, Dohmen J, Snoep G, Boersma L, Verschueren T, van Baardwijk A, Dehing C, Pijls M, Minken A, Lambin P. Omission of elective node irradiation on basis of CT-scans in patients with limited disease small cell lung cancer: a phase II trial. *Radiother Oncol* 2006;80:307-312.
77. Videtic GM, Belderbos JS, Spring Kong FM, Kepka L, Martel MK, Jeremic B. Report from the International Atomic Energy Agency (IAEA) consultants' meeting on elective nodal irradiation in lung cancer: smallcell lung cancer (SCLC). *Int J Radiat Oncol Biol Phys* 2008;72:327-334.
78. van Loon J, De Ruyscher D, Wanders R, Boersma L, Simons J, Oellers M, Dingemans AM, Hochstenbag M, Bootsma G, Geraedts W, Pitz C, Teule J, Rhami A, Thimister W, Snoep G, Dehing-Oberije C, Lambin P. Selective nodal irradiation on basis of (18) FDG-PET scans in limited disease small-cell lung cancer: a prospective study. *Int J Radiat Oncol Biol Phys* 2010;77:329-336.
79. Shirvani SM, Komaki R, Heymach JV, Fossella FV, Chang JY. Positron emission tomography/computed tomography-guided intensity-modulated radiotherapy for limited stage small-cell lung cancer. *Int J Radiat Oncol Biol Phys* 2012;82:91-97.
80. van Loon J, Offermann C, Ollers M, van Elmpt W, Vegt E, Rahmy A, Dingemans AM, Lambin P, De Ruyscher D. Early CT and FDG-metabolic tumour volume changes show a significant correlation with survival in stage I-III small cell lung cancer: a hypothesis generating study. *Radiother Oncol* 2011;99:172-175.



Morphologic and Metabolic Comparison of Treatment Responsiveness with ¹⁸F-Fluorodeoxyglucose-Positron Emission Tomography/Computed Tomography According to Lung Cancer Type

Akciğer Kanseri Tipine Göre ¹⁸Florodeoksiglukoz-Pozitron Emisyon Tomografisi/Bilgisayarlı Tomografi ile Tedavi Yanıtının Morfolojik ve Metabolik Karşılaştırılması

Mehmet Fatih Börksüz¹, Taner Erselcan², Zekiye Hasbek³, Birsen Yücel⁴, Bülent Turgut³

¹Aksaray State Hospital, Clinic of Nuclear Medicine, Aksaray, Turkey

²Muğla Sıtkı Koçman University Faculty of Medicine, Department of Nuclear Medicine, Muğla, Turkey

³Cumhuriyet University Faculty of Medicine, Department of Nuclear Medicine, Sivas, Turkey

⁴Cumhuriyet University Faculty of Medicine, Department of Radiation Oncology, Sivas, Turkey

Abstract

Objective: The aim of the present study was to evaluate the response to treatment by histopathologic type in patients with lung cancer and under follow-up with ¹⁸F-fluoro-2-deoxy-glucose-positron emission tomography/computed tomography (¹⁸F-FDG PET/CT) imaging by using Response Evaluation Criteria in Solid Tumors (RECIST) and European Organisation for Research and Treatment of Cancer (EORTC) criteria that evaluate morphologic and metabolic parameters.

Methods: On two separate (pre- and post-treatment) ¹⁸F-FDG PET/CT images, the longest dimension of primary tumor as well as of secondary lesions were measured and sum of these two measurements was recorded as the total dimension in 40 patients. PET parameters such as standardized uptake value (SUV_{max}), metabolic volume and total lesion glycolysis (TLG) were also recorded for these target lesions on two separate ¹⁸F-FDG PET/CT images. The percent (%) change was calculated for all these parameters. Morphologic evaluation was based on RECIST 1.1 and the metabolic evaluation was based on EORTC.

Results: When evaluated before and after treatment, in spite of the statistically significant change ($p < 0.05$) in SUV_{max}, the change was not significant in TLG, in the longest total size and in the longest size ($p > 0.05$). In histopathologic typing, when we compare the post-treatment phase change with the treatment responses of RECIST 1.1 and EORTC criteria; for RECIST 1.1 in squamous cell lung cancer group, progression was observed in sixteen patients (57%), stability in seven patients (25%), partial response in five patients (18%); and for EORTC progression was detected in four patients (14%), stability in thirteen patients (47%), partial response in eleven patients (39%), in 12 of these patients an increase in stage (43%), in 4 of them a decrease in stage (14%), and in 12 of them stability in stage (43%) were determined. But in adenocancer patients ($n=7$), for RECIST 1.1, progression was determined in four patients (57%), stability in two patients (29%), partial response in one patient (14%); for EORTC, progression in one patient (14%), stability in four patients (57%), partial response in two patients (29%) were observed and in these patients, an increase in stage was detected in 3 of them (43%), while 4 of them remained stable. According to histopathologic diagnosis, between squamous cell cancer and adenocancer cases, no significant difference was determined in terms of SUV_{max} ($p > 0.05$). Post-treatment SUV_{max} was significantly different in primary tumor but was not significantly different in nodal involvement and metastatic lesions for squamous cell carcinoma patients as compared to the pre-treatment SUV_{max} measurements. Similarly, there was no significant difference between primary tumor and nodal involvement for adenocarcinoma patients.

Conclusion: Whether metabolic or morphologic changes are more accurate in evaluating treatment response in lung cancer remains unknown, and there is no gold standard diagnostic method on this issue yet. The most reliable results can only be

Address for Correspondence: Mehmet Fatih Börksüz MD, Aksaray State Hospital, Clinic of Nuclear Medicine, Aksaray, Turkey
Phone: +90 382 212 9100-1336 E-mail: mfborksuz@gmail.com **Received:** 16.02.2015 **Accepted:** 03.05.2016

achieved by survival curve parameters. However, we believe SUV_{max} seems to provide more easy and practical data for the evaluation of treatment response.

Keywords: Standardized uptake value, total lesion glycolysis, metabolic tumor volume, lung cancer, positron emission tomography/computed tomography, treatment response

Öz

Amaç: Bu çalışmadaki amaç ^{18}F -floro-2-deoksi-glikoz-positron emisyon tomografisi/bilgisayarlı tomografi (^{18}F -FDG PET/BT) ile takip edilen akciğer kanseri hastalarında histopatolojik hücre tipine göre tedavi yanıtını, morfolojik ve metabolik parametreleri dikkate alan Solid Tümörlerde Cevap Değerlendirme (RECIST) ve Avrupa Kanser Araştırma ve Tedavi Organizasyonu (EORTC) kriterleri ışığında değerlendirmektir.

Yöntem: Kırk hastanın çekilen iki ayrı (tedavi öncesi ve sonrası) ^{18}F -FDG PET/BT tetkikindeki primer tümörün ve eş zamanlı ikincil lezyonların en uzun boyutları ölçüldü ve bu ölçümler toplanarak 'toplam boyut' olarak kaydedildi. Hedef alınan bu lezyonların standart tutulum değeri (SUV_{maks}), metabolik tümör volümü ve toplam lezyon glikolizis (TLG) gibi PET parametreleri tedavi öncesi ve sonrası iki ayrı ^{18}F -FDG PET/BT tetkikinde kaydedildi. Bu verilerin tedavi öncesine göre yüzde (%) değişimi her hasta için ayrı ayrı hesaplandı. Morfolojik değerlendirme RECIST 1.1, metabolik değerlendirme ise EORTC kriterlerine göre yapıldı.

Bulgular: Tedavi öncesi ve sonrası değerlendirildiğinde, SUV_{maks} 'taki istatistiksel olarak anlamlı ($p<0,05$) değişime karşın, en uzun boyut, en uzun toplam boyut ve TLG'deki değişim anlamlı değildi ($p>0,05$). Histopatolojik tiplendirmede, RECIST 1.1 ve EORTC kriterlerine göre tedavi yanıtlarını tedavi sonrası evre değişimi ile karşılaştırdığımızda; RECIST 1.1'e göre skuamöz hücreli akciğer kanseri grubunda on altı hastada progresyon (%57), yedi hastada stabilite (%25), beş hastada parsiyel cevap (%18), EORTC'a göre dört hastada progresyon (%14), on üç hastada stabilite (%47), on bir hastada parsiyel cevap (%39) izlenirken, bu hastaların on ikisinde evrede artış (%43), dördünde evrede azalma (%14) ve on ikisinde evrede stabilite (%43) saptandı. Adenokanserli hasta grubunda ($n=7$) ise RECIST 1.1'e göre dört hastada progresyon (%57), iki hastada stabilite (%29), bir hastada parsiyel cevap (%14); EORTC'a göre bir hastada progresyon (%14), dört hastada stabilite (%57), iki hastada parsiyel cevap (%29) izlenirken, bu hastaların üçünde evrede artış (%43), dördünde ise evrede stabilite saptandı. Histopatolojik tanıya göre skuamöz hücreli kanser ve adenokanser olguları arasında SUV_{maks} değerlerinde anlamlı farklılık saptanmadı ($p>0,05$). Skuamöz hücreli kanserde primer tümörde tedavi sonrası SUV_{maks} değişimi anlamlı iken, nodal tutulumda ve metastatik lezyondaki değişimde ise anlamlı farklılık saptanmadı. Benzer şekilde, adenokanser hastalarında da primer tümörde ve nodal tutulumda anlamlı farklılık saptanmadı.

Sonuç: Akciğer kanserinde tedavi yanıt değerlendirmede metabolik ve morfolojik değişikliklerden hangisinin daha doğru sonuç verdiği kesin olarak bilinmiyor olup bu konuda altın standart bir tanı yöntemi de henüz yoktur. En doğru sonuçlar ancak yaşam eğrisi parametreleri ile gösterilebilir. Ancak, SUV ölçümünün tedavi yanıtını takipte daha kolay ve pratik bilgi verdiğini düşünüyoruz.

Anahtar kelimeler: Standart tutulum değeri, toplam lezyon glikolizis, metabolik tümör hacmi, akciğer kanseri, positron emisyon tomografisi/bilgisayarlı tomografi, tedavi yanıtı

Introduction

Lung cancer is the most common cancer in men and the fifth cancer in women, with 53300 new male cases per year (1). The majority of lung cancer is non-small cell lung cancer (NSCLC) tumors which consist of subtypes such as adenocarcinoma, squamous cell carcinoma, large cell carcinoma and carcinoid tumor (2). ^{18}F -fluoro-2-deoxy-glucose positron emission tomography/computed tomography (^{18}F -FDG PET/CT) is widely used throughout the world in lung cancer for primary diagnosis, staging, restaging, evaluation of treatment response and radiotherapy (RT) planning (3). The maximum standardized uptake value (SUV_{max}) is widely recognized as an adequate imaging biomarker for the prognosis of lung cancer (4). A SUV of >2.5 is considered as evidence of malignancy in solitary lung nodules. However, lesions smaller than twice the resolution of imaging systems usually yield underestimated SUV values (5). Moreover, SUV may be lower than 2.5 in

bronchoalveolar carcinoma involving no other histological component (6). Parameters such as SUV_{max} have been used for diagnosis and evaluation of treatment effectiveness in lung cancer. In addition, metabolic parameters such as metabolic tumor volume (MTV) and total lesion glycolysis (TLG) can also be estimated by ^{18}F -FDG PET/CT that have been considered as prognostic factors in patients with NSCLC, independent of tumor-node-metastasis stage (7). MTV represents the three-dimensional total volume within the region of interest drawn around the lesion. The highest SUV (SUV_{max}) and the average SUV (SUV_{mean}) measured within this volume can be estimated. TLG value for the lesion, which is directly related to these two measurements, is calculated as follows: "TLG=MTVx SUV_{mean} " (8). The Response Evaluation Criteria in Solid Tumors (RECIST) criteria are being used for the morphologic evaluation of the response to treatment in lung cancer, while the metabolic response is being evaluated by the European Organization for Research and Treatment of Cancer (EORTC) criteria.

Since the introduction of ^{18}F -FDG PET/CT in routine clinical practice, studies on the Positron Emission Tomography Response Criteria in Solid Tumors (PERCIST), which is the criteria of tumor response as related to ^{18}F -FDG-PET, are being conducted. PERCIST suggests using lean body mass-normalized value instead of SUV (the activity concentration in tumor/injected dose/patient weight). The aim of the present study was to assess treatment response according to histological types in lung cancer patients by using RECIST and EORTC criteria, which evaluate morphologic and metabolic parameters.

Materials and Methods

A total of forty patients (38 males, two females, median age=63.3±6 years; range=46-73) who underwent PET/CT were included in the study. In the initial assessment, there was a mixed population in whom primary staging had been done and the treatment had been given. ^{18}F -FDG PET/CT was performed to assess treatment response following chemotherapy or chemoradiotherapy. PET imaging was performed using a combined PET/CT scanner (Discovery 600 PET/CT GE Medical Systems, USA). Each patient fasted for at least 6 h before imaging. After ensuring that blood glucose was <150 mg/dl, approximately 370 MBq ^{18}F -FDG were administered i.v. 1 h before image acquisition. Attenuation correction of PET images with the CT data was performed. The CT scan was performed first. Right after CT data acquisition, a standard PET imaging protocol was taken from the cranium to the mid-thigh with an acquisition time of 3 min/bed in 3-dimensional mode. CT and PET images were matched and fused into transaxial, coronal and sagittal images. The data were transferred via the Digital Imaging and Communications in Medicine protocol to a processing Workstation (AW Volumeshare 5 GE Medical Systems S.C.S, France). The visual and semi-quantitative analyses were then performed. The longest dimension of the primary tumor on two separate ^{18}F -FDG PET/CT images were measured in the mediastinum window on CT. Moreover, "total size" was calculated by summing the longest dimensions of the two lesions with maximum size or of any five lesions in an organ (lung). For the lymph nodes, the short axis measurement was also included in this measurement. Two separate ^{18}F -FDG PET/CT images obtained in the pre-treatment and post-treatment periods were assessed and the SUV_{max} , SUV_{mean} and MTV of the target lesions were recorded. The percent change in the longest size of the primary tumor and total size as well as in SUV_{max} , SUV_{mean} and TLG was calculated for each patient in comparison to the pre-treatment values. Morphologic assessment was made according to RECIST 1.1 criteria by considering the percent change in the total longest dimension of the target lesions in the post-treatment period. Metabolic assessment was made according to EORTC criteria by calculating the percent change in SUV_{max} of the primary tumor in the post-treatment period.

Statistical Analysis

Data were analyzed by using SPSS version 14.0 and expressed as mean±standard deviation. The pre-treatment and post-treatment dimensions measured on CT, and SUV_{max} and TLG values on PET were compared by the paired T-test. Among the histopathologic diagnosis of the patients, the two major groups of patients with a diagnosis of squamous cell carcinoma (n=28/40) or adenocarcinoma (n=7/40) were compared in terms of SUV_{max} values by using Kruskal Wallis analysis. Moreover, the percent change in post-treatment longest dimension, SUV_{max} and TLG (increased or decreased) were compared by using chi-square (Fisher) test. Significance level was set at $p<0.05$.

Results

Of the forty patients included in the study, 2 were female (5.0%) and 38 were male (95.0%) with a mean age of 63.3±6 years (range, 46-73 years). In terms of histopathologic diagnosis, 28 patients had squamous cell lung carcinoma (70%), seven had adenocarcinoma (17.5%), four had small cell cancer (10%) and one had pleomorphic cell lung cancer (2.5%) (Table 1). Mean follow-up time was 23.1±12.6 weeks (range, 10-67 weeks). The treatment methods were separate RT+chemotherapy (CT) sessions in two patients, chemoradiotherapy in three patients and only CT in the remaining 35 patients. Nine patients had distant metastatic lesions in addition to the primary lesion and lymph node involvement, and the metastasis was measurable in seven of these patients. According to the histopathologic diagnosis, pre-treatment SUV_{max} was 16.1±6.9 (n=28) vs. 20.4±14.1 (n=7) in patients with squamous cell carcinoma and adenocarcinoma, respectively ($p>0.05$). Post-treatment change in SUV_{max} was found to be statistically significant in patients with squamous cell carcinoma. However, there was no statistical difference in the FDG uptake change for patients with lymph node involvement or metastatic

Table 1. Demographic and clinico-histopathologic characteristics

Characteristics	n (%)
Age (years)	
Mean age at diagnosis (years) (range)	63.3±6.3 years, range 46-73 years
Sex	
Female	2 (5%)
Male	38 (95%)
Pathological classification	
Squamous cell carcinoma	28 (70.5%)
Adenocarcinoma	7 (17.5%)
Small cell carcinoma	4 (10%)
Pleomorphic cell carcinoma	1 (2.5%)

lesions. Similarly, there was no significant difference in primary tumor and nodal involvement in the comparison of adenocarcinoma patients. Pre- and post-treatment longest dimension, SUV_{max} and TLG of the primary tumor were compared in twenty-eight patients with a histopathologic diagnosis of squamous cell carcinoma who constitute the majority of the patients in order to assess treatment response. Mean SUV_{max} was significantly different between pre- and post-treatment measurements ($p < 0.05$), with no difference in terms of longest dimension, total dimension and mean TLG ($p > 0.05$). The pre- and post-treatment longest dimension, SUV_{max} and TLG were also compared in adenocarcinoma patients. Patients with adenocarcinoma ($n=7$) had no significant difference in these parameters

measured before and after the treatment ($p > 0.05$) (Table 2). Table 3 represents the pre-treatment and post-treatment SUV_{max} change in the primary tumor, lymph node and metastatic lesions stratified by histopathologic diagnosis. When the response to treatment was compared in patients with squamous cell cancer according to RECIST 1.1 and EORTC criteria by post-treatment stage change, RECIST 1.1 revealed progression in sixteen patients (57%), stability in seven (25%) and partial response in five (18%); while EORTC revealed progression in four (14%), stability in thirteen (47%) and partial response in eleven (39%) patients (Table 4). Of these patients, twelve (43%) showed increased stage, 4 (14%) had decreased stage with the remaining 12 (43%) at a stable stage. In patients with

Table 2. Pre-treatment and post-treatment highest standardized uptake value change in the primary tumor, lymph node and metastatic lesions according to histopathologic diagnosis

	Pre-treatment SUV_{max}	Post-treatment SUV_{max}	p
Squamous cell carcinoma, primary tumor (n=28)	16.1±6.9	13.1±7.8	<0.05*
Squamous cell carcinoma, nodal involvement (n=9)	16.3±7.4	12.1±9.1	>0.05
Squamous cell carcinoma, distant metastatic lesions (n=6)	16.1±5.7	10.9±8.8	>0.05
Adenocarcinoma, primary tumor (n=7)	20.4±14.1	13.5±6.7	>0.05
Adenocarcinoma, nodal involvement (n=4)	16.1±3.9	8.1±4.3	>0.05
Small cell carcinoma, primary tumor (n=4)	15.5± 4.2	9.8±3.5	>0.05
Pleomorphic cell carcinoma, primary tumor (n=1)	5.1	9.9	-

SUV_{max} : Highest standardized uptake value

Table 3. The number of cases with change in size and metabolic parameters according to histological type and the percent change (%)

(Primary tumor)	Squamous cell carcinoma (n=28)		Adenocarcinoma (n=7)		Small cell carcinoma (n=2)		Pleomorphic adenoma (n=1)	
	Number of cases	Percentage (%)	Number of cases	Percentage (%)	Number of cases	Percentage (%)	Number of cases	Percentage (%)
Decrease in the longest dimension	18	(18/28) 64%	2	(2/7) 28%	2	(2/4) 50%	0	0/1 0%
Increase in the longest dimension	10	(10/28) 36%	5	(5/7) 71%	2	(2/4) 50%	1	1/1 100%
Decrease in SUV_{max}	20	(20/28) 71%	4	(4/7) 57%	2	(2/4) 50%	0	0/1 0%
Increase in SUV_{max}	8	(8/28) 29%	3	(3/7) 43%	2	(2/4) 50%	1	1/1 100%
Decrease in TLG	18	(18/28) 64%	5	(3/7) 43%	2	(2/4) 50%	0	0/1 0%
Increase in TLG	10	(10/28) 36%	2	(4/7) 57%	2	(2/4) 50%	1	1/1 100%

SUV_{max} : Highest standardized uptake value, TLG: Total lesion glycolysis

Table 4. The treatment responses of squamous cell cancer patients according to Response Evaluation Criteria in Solid Tumors 1.1 and European Organisation for Research and Treatment of Cancer criteria

	RECIST 1.1	EORTC
Progression	16 (57%)	4 (14%)
Partial response	7 (25%)	13 (47%)
Stability	5 (18%)	11 (39%)

RECIST: Response Evaluation Criteria in Solid Tumors, EORTC: European Organisation for Research and Treatment of Cancer

adenocarcinoma (n=7), RECIST 1.1 revealed progression in four (57%), stability in two (29%), and partial response in one (14%) patient; while EORTC showed progression in one (14%), stability in four (57%), and partial response in two (29%) patients. Of these patients, 3 (43%) showed increased stage and the remaining 4 had a stable stage. Data on change in size and metabolic parameters and rates (%) according to histopathologic type of primary tumor are presented in Table 2. In our study, PET/CT and CT data of four patients diagnosed with small cell lung cancer before and after treatment were compared and the following conclusion was reached: Although the average SUV_{max} decreased, two patients showed metastatic progression and upstaging. And one patient with the diagnosis of stage 4 pleomorphic Ca according to pre-treatment PET/CT, showed an increase in size and TLG at post-treatment PET/CT.

Discussion

^{18}F -FDG PET/CT is used for the diagnosis and staging of lung cancer as well as for the assessment of response to treatment. In the present study, we investigated the association between the morphologic features (dimension) and metabolic criteria for assessment of response to treatment (SUV and TLG). One of the first studies by Kubota et al. (9) assessing the metabolic and morphologic comparison of response to treatment in patients with lung cancer was carried out with radiopharmaceutical ^{11}C L-methionine, which is a marker for protein synthesis and cell proliferation. Change in dimension has been assessed by CT and the change in nodal uptake has been measured by PET not using a hybrid device. The outcome has been divided into 3 groups of early progression, late local recurrence and no local recurrence. Methionine uptake was decreased by 72% and 65% in the groups of late local recurrence and no local recurrence at PET imaging obtained 2 weeks after RT, while it was found to decrease by 22% in the group of early progression. The authors have concluded that PET imaging was more beneficial in predicting local recurrence and progression as compared to CT imaging. Kubota et al. (9) have carried out PET and CT imaging methods on separate devices. In contrast to these studies, we used an integrated PET/CT device. Although there was no significant change in the longest dimension of the primary tumor and in total target dimension and TLG of the primary tumor, the SUV_{max} showed a statistically significant change after the treatment in patients with squamous cell carcinoma as well as in the whole group. Another study by Patz et al. (10) assessing the response to treatment only with PET imaging included 113 patients treated with chemotherapy, RT, surgery or a combination of these modalities. The authors have evaluated the examinations performed within an average of 8 months after the treatment, and have found that the PET imaging was negative in 13 vs. 100 positive patients. In our study,

two of the forty patients died in the last evaluation time. For this reason, in the present study, we did not perform a survival analysis. Another study has evaluated the patients treated with only chemotherapy and has aimed to predict the final outcome on PET imaging obtained after the first course of chemotherapy. In that study carried out on seven patients by Weber et al. (11), median survival time was 151 days in patients with more than 20% decrease in FDG SUV vs. 54 days in those without. The authors have also suggested a close relationship between assessment criteria for response to treatment and metabolic response in solid tumors. Cerfolio et al. (12) have evaluated 56 patients with NSCLC by ^{18}F -FDG-PET within 1 month after neoadjuvant chemotherapy or combined RT before surgery. The authors have found a correlation between the change in SUV_{max} and percent rate of non-living cell number (%) during the resection. It was reported that the overall pathological response could be predicted with 96% accuracy when an 80% decrease in SUV_{max} was considered as the threshold value.

Pöttgen et al. (13), on the other hand, have performed resection to patients in whom PET images were obtained about 63 days after 3 courses of induction chemotherapy and 84 days after combined RT. There was an average of 67% decrease in SUV_{max} in patients treated with induction chemotherapy, with no or less than 10% living cancer cells in the resection. Moreover, patients having more than 10% living cancer cells had a mean decrease of 34% in SUV_{max} . In the present study, in the post-treatment evaluations, 22 patients had an average decrease of 25.4 ± 15.8 mm in the longest dimension of the primary tumor while the remaining eighteen patients had an average increase of 30.6 ± 28.6 mm in the longest dimension of the primary tumor. When the target lesions were also included in these measurements according to the RECIST 1.1 criteria, 22 patients had an average decrease of 24.8 ± 16.1 mm and eighteen patients had an average increase of 39.2 ± 44 mm. According to the RECIST 1.1 criteria, when the new lesion formation and the increase in unmeasurable lesions were also included in these measurements, eight patients had partial response, 22 had progressive disease and 10 had a stable disease. In the evaluations by using the SUV_{max} values based on EORTC criteria, SUV_{max} decreased by $38.9 \pm 25.6\%$ in twenty-seven patients. In the remaining thirteen patients, there was an increase by $23 \pm 17.8\%$. Overall, sixteen patients had partial response, 19 had a stable disease and 5 had a progressive disease. Use of the changes in post-treatment longest dimension and SUV_{max} for the evaluation of response to treatment yields different results. In the present study, patients were evaluated according to the metabolic and morphologic features separately and the response to treatment differed with the use of RECIST 1.1 and EORTC criteria. With today's technology, there is no gold standard diagnostic method to be used to determine which one is more accurate in evaluating the

response to treatment. It is also not possible to evaluate all suspicious lesions with histopathologic methods. Therefore, response to treatment should be evaluated by comparisons with survival curves. However, FDG uptake is associated with living cancer cells and SUV increases with the increasing FDG uptake. Therefore, FDG uptake may be useful in the differentiation of tumor tissue, fibrosis and necrosis for which anatomical boundaries are not always distinguishable. Ordu et al. (14) reported in their study that, in advanced NSCLC patients, in evaluation of response to chemotherapy and in determination of overall survival, the metabolic response with PERCIST may be an early predictive factor in comparison with morphologic response. Our study showed that although there was no significant change in the longest total dimension, the change in post-treatment SUV_{max} was significant whether only the longest dimension of the primary tumor or of target lesions were taken into account. There were seven patients who met the criteria of longest total dimension for the evaluation of metastatic disease ($n=7/9$). The longest total dimension in metastatic disease did not differ significantly between pre- and post-treatment periods. However, average SUV_{max} in metastatic lesions and nodal involvement differed significantly between pre- and post-treatment periods. As in the primary tumor, the response of metastatic lesions was also different between pre- and post-treatment periods in terms of dimension (morphologic feature) and SUV_{max} (metabolic feature). Overall, dimension criteria tended to be negative for the patient (unresponsiveness to treatment). Treatment response criteria should be standardized in a way that can be easily used in clinical practice for the patient examination reports. However, response criteria usually are not specified in the imaging methods for cancer patients (both in CT and PET/CT). This may result in difficulty for daily clinical practice. Moreover, although lymph nodes are included in RECIST 1.1, it is not always possible to determine the post-treatment changes in lymph nodes that are close to each other (and in conglomerated nodes). After the treatment period, a lymph node may have a decrease in size while the size of the next lymph node might have been increased. Because these nodes do not have clear borders, it is quite difficult to evaluate the treatment response in lymph nodes. In addition, RECIST 1.1 basically considers the tumor and the lymph node size. However, recent targeted anticancer drugs inhibit the growth of cells without killing the tumor cells. Thus, responders may display morphologic changes such as necrosis, cavitation, and hemorrhage in tumor without change in size (15). In this context, a more practical and easily used method, the metabolic criteria can be preferred.

Conclusion

In this study on lung cancer patients, there was no significant difference between squamous cell and adenocarcinoma group in terms of primary tumor SUV_{max} rates. There was no significant difference between pre- and

post-treatment measurements in the longest dimension of primary tumor and in the total longest dimension selected as a target lesion. There was a significant SUV_{max} change after the treatment as compared to that of prior to the treatment. In the determination of treatment response, it is not known exactly yet whether metabolic or morphologic changes as evaluated by RECIST 1.1 and EORTC is more accurate in determining treatment response is yet unknown. Unfortunately, we could not comment on this issue because we had a limited number of patients and follow-up period. At the same time, we think that SUV rates can be preferred for treatment response evaluation due to its easier applicability in clinical practice.

Ethics

Ethics Committee Approval: The study were approved by the Cumhuriyet University of Local Ethics Committee, Informed Consent: Consent form was filled out by all participants.

Peer-review: Externally peer-reviewed.

Authorship Contributions

Surgical and Medical Practices: Mehmet Fatih Börksüz, Taner Erselcan, Concept: Mehmet Fatih Börksüz, Taner Erselcan, Design: Mehmet Fatih Börksüz, Taner Erselcan, Data Collection or Processing: Mehmet Fatih Börksüz, Taner Erselcan, Birsen Yücel, Analysis or Interpretation: Mehmet Fatih Börksüz, Taner Erselcan, Zekiye Hasbek, Bülent Turgut, Literature Search: Mehmet Fatih Börksüz, Taner Erselcan, Zekiye Hasbek, Writing: Mehmet Fatih Börksüz, Taner Erselcan, Zekiye Hasbek.

Conflict of Interest: No conflict of interest was declared by the authors.

Financial Disclosure: The authors declared that this study has received no financial support.

References

1. Sağlık Bakanlığı Türkiye Halk Sağlığı Kurumu Kanser Daire Başkanlığı'nın 2008 yılına ait kanser veri istatistikleri. www.kanser.gov.tr/dairefaaliyetleri/kanser-istatistikleri (15.10.2013).
2. Minguet J, Smith KH, Bramlage P. Targeted therapies for treatment of non-small cell lung cancer - recent advances and future perspectives. *Int J Cancer* 2016;138:2549-2561.
3. Mettler FA, Guiberteau MJ. 18F-FDG PET/CT Neoplasm Imaging. In: Mettler FA, Guiberteau MJ (eds). *Essentials of Nuclear Medicine Imaging*. Philadelphia, Elsevier Inc, 2012 361-395.
4. Ito R, Iwano S, Kishimoto M, Ito S, Kato K, Naganawa S. Correlation between FDG-PET/CT findings and solid type non small cell cancer prognostic factors: are there differences between adenocarcinoma and squamous cell carcinoma? *Ann Nucl Med*. 2015;doi:10.1007/s12149-015-1025-z.
5. Hagge RJ, Coleman RE. Positron emission tomography: lung cancer. *Semin Roentgenol* 2002;37:110-117.
6. Peller PJ, Lowe VJ, Tuncali Çağlar M. Akciğer Kanseri. içinde: Wahl RL (ed). *PET ve PET/BT Prensipler ve Klinik Uygulamalar*. Rotatıp Kitabevi, 2011:248-259.

7. Zhang C, Liao C, Penney BC, Appelbaum DE, Simon CA, Pu Y. Relationship between overall survival of patients with non-small cell lung cancer and whole-body metabolic tumor burden seen on postsurgical fluorodeoxyglucose PET images. *Radiology* 2015;275:862-869.
8. Hatt M, Visvikis D, Pradier O, Cheze-le Rest C. Baseline 18F-FDG PET image-derived parameters for therapy response prediction in oesophageal cancer. *Eur J Nucl Med Mol Imaging* 2011;38:1595-1606.
9. Kubota K, Yamada S, Ishiwata K, Ito M, Fujiwara T, Fukuda H, Tada M, Ido T. Evaluation of the treatment response of lung cancer with positron emission tomography and L-[methyl-11C] methionine: a preliminary study. *Eur J Nucl Med* 1993;20:495-501.
10. Patz EF Jr, Connolly J, Herndon J. Prognostic value of thoracic FDG-PET imaging after treatment for non-small cell lung cancer. *AJR Am J Roentgenol* 2000;174:769-774.
11. Weber WA, Petersen V, Schmidt B, Tyndale-Hines L, Link T, Peschel C, Schwaiger M. Positron emission tomography in non-small cell lung cancer; prediction of response to chemotherapy by quantitative assessment of glucose use. *J Clin Oncol* 2003;21:2651-2657.
12. Cerfolio RJ, Bryant AS, Winokur TS, Ohja B, Bartolucci AA. Repeat FDG-PET after neoadjuvant therapy is a predictor of pathologic response in patients with non-small cell lung cancer. *Ann Thorac Surg* 2004;78:1903-1909.
13. Pöttgen C, Levegrün S, Theegarten D, Marnitz S, Grehl S, Pink R, Eberhardt W, Stamatis G, Gauler T, Antoch G, Bockisch A, Stuschke M. Value of 18F-fluoro-2-deoxy-D-glucose-positron emission tomography/computed tomography in nonsmall-cell lung cancer for prediction of pathologic response and times to relapse after neoadjuvant chemoradiotherapy. *Clin Cancer Res* 2006;12:97-106.
14. Ordu C, Selcuk NA, Akosman C, Eren OO, Altunok EC, Toklu T, Oyan B. Comparison of metabolic and anatomic response to chemotherapy based on PERCIST and RECIST in patients with advanced stage non-small cell lung cancer. *Asian Pac J Cancer Prev* 2015;16:321-326.
15. Yaghmai V, Miller FH, Rezaei P, Benson AB, Salem R. Response to treatment series: part 2, tumor response assessment—using new and conventional criteria. *AJR Am J Roentgenol* 2011;197:18-27.



Evaluation of Silent Myocardial Ischemia with Single-Photon Emission Computed Tomography/Computed Tomography in Asymptomatic Subjects with Diabetes and Pre-Diabetes

Asemptomatik Diyabetik ve Pre-Diyabetik Hastalarda Miyokardiyal Sessiz İskeminin Tek Foton Emisyon Bilgisayarlı Tomografi/Bilgisayarlı Tomografi ile Değerlendirilmesi

Elif Özdemir¹, Şefika Burçak Polat², Nilüfer Yıldırım¹, Şeyda Türkölmez³, Reyhan Ersoy⁴, Tahir Dumaz⁵, Telat Keleş⁵, Engin Bozkurt⁵, Bekir Çakır⁴

¹Atatürk Training and Research Hospital, Clinic of Nuclear Medicine, Ankara, Turkey

²Atatürk Training and Research Hospital, Clinic of Endocrinology and Metabolism, Ankara, Turkey

³Yıldırım Beyazıt University Faculty of Medicine, Department of Nuclear Medicine, Ankara, Turkey

⁴Yıldırım Beyazıt University Faculty of Medicine, Department of Endocrinology and Metabolism, Ankara, Turkey

⁵Yıldırım Beyazıt University Faculty of Medicine, Department of Cardiology, Ankara, Turkey

Abstract

Objective: The aim of this study was to disclose the prevalence of myocardial ischemia, as detected by adenosine stress myocardial perfusion imaging (MPI) with hybrid single-photon emission computed tomography/computed tomography (SPECT/CT), in asymptomatic diabetic and pre-diabetic patients and to find out whether ischemia predicted the occurrence of adverse cardiac/cerebrovascular events (ACCE) at follow-up.

Methods: Forty-three diabetic and thirty-five pre-diabetic asymptomatic patients without any history of coronary artery disease, underwent MPI and were followed-up for a 12.8±2.2 (8-19) months for the occurrence of ACCE. Baseline variables that would predict the presence of ischemia and the value of ischemia on MPI for predicting the occurrence of ACCE at follow-up were evaluated by logistic regression analysis.

Results: Ischemia was detected in ten (23.3%) of the diabetic and in four (11.4%) of the pre-diabetic patients. The presence of diabetes was the only independent predictor of myocardial ischemia [odds ratio (OR): 12.31, 95% confidence interval (CI): 1.83-82.66; p<0.01]. During 12.8±2.2 (8-19) months of follow-up, ACCE was observed in five out of 78 (6.4%) patients. Patients with ischemia were significantly more likely to have ACCE during follow-up as compared to those with normal MPI scans (event rates: 21.4% vs. 3.1%, OR: 8.455 95% CI: 1.264-56.562, p=0.038).

Conclusion: Myocardial ischemia as detected by adenosine stress SPECT/CT in a population of asymptomatic patients with diabetes mellitus or pre-diabetes appeared to predict the occurrence of ACCE at follow-up.

Keywords: Type 2 diabetes mellitus, pre-diabetes, silent myocardial ischemia, single-photon emission computed tomography/computed tomography

Öz

Amaç: Bu çalışmanın amacı asemptomatik diyabetik ve pre-diyabetik hastalarda stres miyokardiyal perfüzyon tek foton emisyon bilgisayarlı tomografi/bilgisayarlı tomografi miyokard perfüzyon sintigrafisi (MPS) ile miyokardiyal iskemi prevalansını belirlemek ve iskemi bulgularının takipte istenmeyen kardiyak ve serebrovasküler olayları öngörüp görmediğini saptamaktır.

Address for Correspondence: Elif Özdemir MD, Atatürk Training and Research Hospital, Clinic of Nuclear Medicine, Ankara, Turkey
Phone: +90 532 684 18 80 E-mail: ecingi@yahoo.com **Received:** 03.03.2015 **Accepted:** 09.02.2016

Yöntem: Daha önce bilinen koroner arter hastalığı olmayan 43 diyabetik ve 35 pre-diyabetik asemptomatik hastaya MPS yapılarak, hastalar istenmeyen kardiyak/serebrovasküler olaylar açısından ortalama 12,8±2,2 (8-19) ay takip edildi. İskemiye öngören bazal değişkenler ve MPS'nin takipte istenmeyen kardiyovasküler olayları öngörmedeki değeri lojistik regresyon modeli ile değerlendirildi.

Bulgular: Diyabetik hastaların onunda (%23,3) ve pre-diyabetik hastaların dördünde (%11,4) MPS ile iskemi saptandı. Miyokardiyal iskemi açısından tek bağımsız risk faktörü diabetes mellitus varlığı idi (odds ratio (OR): 12,31, %95 güven aralığı (GA): 1,83-82,66; p<0,01). Ortalama 12,8±2,2 (8-19) aylık takip süresi boyunca yetmiş sekiz hastanın beşinde (%6,4) istenmeyen kardiyovasküler olay gelişti. Sintigrafide iskemi bulgusu olanların takibinde kardiyovasküler olay gelişme riski, normal MPS bulguları olanlara göre belirgin olarak yüksekti (olay oranı: %21,4 ile %3,1, OR: 8,455 %95 GA: 1,264-56,562, p=0,038).

Sonuç: Adenozin stres SPECT/CT ile saptanan iskeminin asemptomatik diyabetik ve pre-diyabetik hastalarda takipte gelişecek olan kardiyovasküler olayları öngördüğü söylenebilir.

Anahtar kelimeler: Tip 2 diyabet, prediyabet, sessiz iskemi, tek foton emisyon bilgisayarlı tomografi/bilgisayarlı tomografi

Introduction

Type 2 diabetes mellitus (DM) is associated with an increased risk of coronary artery disease (CAD) and has long been considered a CAD equivalent (1,2). CAD is usually silent in diabetics, and the reported prevalence of silent myocardial ischemia ranges between 6-57% (3,4). This wide range is probably due to differences in patient population and in sensitivity rates of various imaging modalities used in these studies to detect ischemia. Intermediate states of abnormal glucose regulation that exist between normal glucose homeostasis and diabetes are defined as pre-diabetes and include impaired glucose tolerance (IGT), impaired fasting glucose (IFG) or both. Patients with IFG or IGT have a relatively high risk of developing overt diabetes in the future, and CAD risk has been reported to increase in pre-diabetics before glucose levels reach diabetic thresholds (5). Cardio-metabolic derangements occur long before the diagnosis of diabetes and contribute to the 2-fold increased risk of cardiovascular disease seen in IGT and the 4-fold increased CAD risk seen in diabetes (1). According to the American College of Cardiology (ACC) practice guidelines, stress myocardial perfusion imaging (MPI) may be considered for advanced cardiovascular risk assessment in asymptomatic adults with diabetes (class IIb, LoE=C) (6). A similar level of recommendation (class IIb) has been put forward by the European Society of Cardiology for screening selected high-risk patients with DM for the presence of silent myocardial ischemia (7). Quantitative MPI with single-photon emission tomography (SPECT) is a powerful diagnostic modality being used for risk stratification and determination of prognosis in CAD. Recently developed hybrid SPECT/computed tomography (CT) systems were reported to reduce false positive results of myocardial perfusion scintigraphy by eliminating soft tissue attenuation problems and improve the accuracy of MPI (8). In this prospective study, we aimed to disclose the prevalence of silent ischemia, as detected by adenosine stress MPI with hybrid SPECT/CT, in asymptomatic diabetic and pre-diabetic patients and to find out whether ischemia on MPI predicts the occurrence of adverse cardiac/cerebrovascular events (ACCE) at follow-

up. We also tried to evaluate the factors that could predict the occurrence of ischemia in this patient subset.

Materials and Methods

We enrolled 35 pre-diabetic and forty-three diabetic patients (mean age=55.6±8.5 years, 35 females) without any history of CAD. The diagnosis of DM and pre-diabetes were made according to American Diabetes Association (ADA) criteria (9). Diabetes diagnosis was based on three fasting blood glucose levels ≥ 126 mg/dL. Subjects who had fasting plasma glucose levels between 100-125 mg/dL were subjected to 75 gr oral glucose tolerance test (OGTT) where, after an overnight fasting, subjects were given a load of 75 g glucose in 300 mL water. Blood samples for glucose measurements were drawn before the loading and at 120 minutes thereafter. Categories of glucose tolerance were defined according to 2013 ADA criteria (9). IFG was defined as fasting plasma glucose between 100-125 mg/dL and 120 min plasma glucose level < 140 mg/dL, whereas IGT was defined as 120 min plasma glucose between 140-199 mg/dL during OGTT. The 120 min glucose level ≥ 200 mg/dL on 75 gr OGTT were designated as DM. Patients who had either IFG or IGT or both were classified as pre-diabetes. The study was approved by the Hospital Ethical Committee, and informed consent was obtained from all participants before the study procedures.

Exclusion criteria were defined as follows;

- 1- History of CAD [previous myocardial infarction (MI), percutaneous coronary intervention (PCI) or coronary bypass graft surgery (CABG)],
- 2- Electrocardiogram (ECG) findings suggestive of Q wave-MI, ischemic ST-segment or T-wave changes, or complete left bundle branch block,
- 3- Typical angina pectoris,
- 4- Absolute contraindication for adenosine stress testing,
- 5- Segmental wall motion abnormality (WMA) or left ventricular hypertrophy on transthoracic echocardiography,
- 6- Comorbid conditions that might influence plasma

glucose levels such as Cushing syndrome, acromegaly, pheochromocytoma,

7- Use of drugs that may affect plasma glucose levels such as corticosteroids, neuroleptics, antiviral agents, beta agonists, interferon, diazoxide.

After a detailed medical history and a thorough physical examination, a 12-lead ECG and a trans-thoracic echocardiogram were recorded for each patient. Age at onset of diabetes, duration of diabetes and recently used medications were recorded. Major cardiovascular risk factors including smoking, dyslipidemia, hypertension, and family history of CAD were also recorded. Hypertension was defined as systolic blood pressure ≥ 140 mmHg, diastolic blood pressure ≥ 90 mmHg, or any treatment with an antihypertensive drug. Microalbuminuria was evaluated on 24-hour urine samples in all patients. The fundoscopic examination was applied to patients with DM.

Laboratory testing: Venous blood samples were drawn in the fasting state using vacutainer tubes. Plasma glucose, HbA_{1c}, triglycerides, total and high-density lipoproteins (HDL) and cholesterol concentrations were measured by enzymatic assays (Roche Diagnostics GmbH, Mannheim, Germany). Albumin measurement in 24-hour urine samples was made by immunoradioturbidimetric method (Aeroset, Abbott), and levels ≥ 30 mg/day were defined as 'microalbuminuria'.

Myocardial perfusion imaging with SPECT/CT: All patients underwent same-day rest/stress technetium-99m methoxy-isobutyl-isonitrile (^{99m}Tc-MIBI) gated-SPECT MPI by adenosine stress with hybrid SPECT/CT system (Infinia, GE Healthcare). Pharmacologic stress with adenosine was chosen as the stress modality of choice to standardize the stress level and eliminate potential confounding that could arise from different levels of maximum achievable stress due to varying levels of exercise capacity in different patients. For adenosine stress test, patients were asked to refrain from consuming caffeinated beverages after midnight prior to testing. In the morning 296-370 MBq ^{99m}Tc-MIBI was injected intravenously at rest and imaging was performed 60 min after injection. Three or four hours after resting acquisition, stress protocol was started. One hundred forty μ g/kg per minute adenosine (adenosine-LM, Abfenfarma) was infused intravenously over 4-6 min. ^{99m}Tc-MIBI (of 888-1110 MBq) was administered 3 minutes after the beginning of adenosine infusion. After the radiotracer injection, adenosine infusion was continued for another 1-2 minutes. ECG was monitored continuously and blood pressure and heart rate were obtained at 1-min intervals. Stress images were acquired 30-45 minutes after radiotracer injection. The SPECT MPI acquisition was performed on a dual-head camera (Infinia, GE Healthcare) with a low-energy, high-resolution collimator; a 20% symmetric window at 140 keV; a 64x64 matrix; and an elliptic orbit with step-and-shoot acquisition at 3° intervals over a 180° arc (45° right anterior oblique to 45° left posterior oblique) with 30 steps

(60 views). Scan time was set to 20 s per frame for stressed and 25 s per frame for resting conditions. Gating included 16 frames per R-R cycle. For attenuation correction (AC), all patients underwent low-dose CT using a Hawkeye system (Infinia; GE Healthcare). Single-slice non-spiral CT (x-ray tube current, 2.5 mA; voltage, 140 kVp) with a slice thickness of 10 mm and a scan time of more than 5 min for a typical 13-cm field of view was obtained. After reconstruction and transfer to a Xeleris workstation (GE Healthcare), AC maps were generated. SPECT images were reconstructed into short and vertical and horizontal long axes using standard reconstruction-that is, filtered back projection-and iterative reconstruction with CT-AC. Visual interpretation of SPECT images was always performed side by side by 2 experienced nuclear medicine specialists. SPECT images were analyzed by using Emory Cardiac Toolbox software package. For semi-quantitative analysis, SPECT images were visually scored using a 20-segment model of the left ventricle and images with AC were evaluated visually and each segment was scored between 0 and 4. Zero was defined as normal perfusion, 1: equivocal, 2: moderate reduction, 3: severe reduction, and 4: lack of perfusion. Summed stress score (SSS) and summed rest scores were obtained by adding the scores of the 20 segments. The summed difference score (SDS) represents the difference between the stress and rest scores. In the semi-quantitative analysis done by using AC images, SSS >1 and SDS >1 were accepted as positive for ischemia (10). Wall motion, wall thickening and left ventricular ejection fraction (LVEF) were evaluated using Quantitative Gated SPECT; (Cedars-Sinai Medical Center) software package.

Patient follow-up: The patients were followed up for a mean of 12.8 \pm 2.2 (8-19) months for the occurrence of ACCE defined as the occurrence of either typical angina pectoris, MI, myocardial revascularization (PCI or CABG), stroke, cardiovascular or cerebrovascular death, new cardiac arrhythmia or congestive heart failure. Predictors of ischemia in the whole group and in those with DM were evaluated using multiple logistic regression analysis.

Statistical Analysis

Data analysis was performed by using SPSS for Windows, version 11.5 (SPSS Inc., Chicago, IL, United States). The distribution pattern of metric discrete and continuous variables was evaluated by Kolmogorov-Smirnov test. Metric discrete and continuous variables were shown as the mean \pm standard deviation (SD) or median (minimum-maximum), where applicable. The mean value differences between groups were compared by Student's t-test. Mann-Whitney U test was applied for comparisons of the median values. Nominal data were analyzed by Pearson's chi-square or Fisher's exact test, where appropriate. The predictors of ischemia on MPI were evaluated by Multiple Logistic Regression Analyses. Any variable found to be significant on univariate testing (p-value <0.25) was subjected to testing in the multivariate

model. Odds ratios and 95% confidence intervals for each independent variable were also calculated. A p value less than 0.05 was considered statistically significant.

Results

We enrolled 43 diabetics and 35 pre-diabetic subjects. DM had been present for a median of 7 years in the diabetic group. Among the pre-diabetics, 20 had IFG, 6 had IGT and 9 had both. The demographic properties, risk factors and medications that were being used at study entry are shown in Table 1. The two groups (diabetics and pre-diabetics) were similar with regard to age, gender and body mass index. On the other hand, the diabetics were more likely to be hypertensive (50% vs. 11.4%, $p=0.001$), had higher serum triglyceride levels (170 vs. 130 mg/dl, $p=0.002$), and were on lipid-lowering therapy more frequently (16.3% vs. 2.9%,

$p=0.06$) as compared to pre-diabetics. Otherwise, the two groups looked similar. Diabetic retinopathy was present in 23.3% of the diabetic population. Microalbuminuria was evident in 14% of the diabetics, and none of the pre-diabetic patients.

SPECT findings: By using 20 segment model, attenuation corrected images, SSS and SDS scores, 4 out of 35 (11.4%) in the pre-diabetics and 10 out of 43 (23.3%) in the diabetic group were found to have ischemia on SPECT/CT MPI (Table 2) (Figure 1). Among the four pre-diabetics with ischemia on MPI, 1 had IFG and 3 had IGT.

Hypo-perfusion involving more than 5% of the left ventricle was detected only in two diabetic patients. Although no patient had WMA on echocardiography at study entry, we detected segmental WMA (all hypokinesia) on post-stress gated images in five diabetic patients on MPI. No patient in the pre-diabetic group had WMA on MPI. The

Table 1. Characteristics of the study population (n=78)

	Prediabetes (n=35)	Diabetes mellitus (n=43)	p
Age (years)	54.1±10.4	56.8±6.3	0.188
Female/male	16/19	19/24	
BMI (kg/m ²)	29.8±5.4	27.9±3.1	0.097
Duration of disease (years)	6 (1-9)	7 (1-20)	
FPG (mg/dl)	105.5±8.9	163.9±55.7	<0.001
HbA _{1c} (%)	5.6±0.5	7.1±1.2	<0.001
Total cholesterol (mg/dl)	203.9±40	192.6±39.9	0.240
LDL cholesterol (mg/dl)	117.3±39.8	110.3±33.5	0.424
HDL cholesterol (mg/dl)	52.2±12.1	48.9±12.8	0.133
Triglycerides (mg/dl)	130±71.6	150±75.5	0.002
Hypertension	4 (11.4%)	21 (50%)	0.001
Smoking	8 (22.8%)	11 (25.5%)	0.640
Family history of CAD	9 (25.7%)	10 (23.2%)	0.686
Retinopathy	-	10 (23.3%)	
Microalbuminuria	-	6 (14%)	
Diabetes Treatment			
None	26 (74.3%)	3 (7%)	
Diet only	1 (2.9%)	1 (2.3%)	
Oral agent	8 (22.9)	21 (48.8%)	<0.001
Insulin	-	18 (41.9%)	
Aspirin	2 (5.7%)	8 (19%)	0.101
Statins	1 (2.9%)	7 (16.3%)	0.068
IGT	6 (17.1%)		
IFG	20 (57.1)		
IGT+IFG	9 (25.7%)		

BMI: Body mass index, FPG: Fasting plasma glucose, LDL: Low density lipoprotein, HDL: High density lipoprotein, CAD: Coronary artery disease, IGT: Impaired glucose tolerance, IFG: Impaired fasting glucose

mean LVEF by gated SPECT was $72\pm 7.3\%$ in the pre-diabetic and $70\pm 7.7\%$ in the diabetic group. High SSS and/or SDS scores before AC turned to normal values after AC in 25 patients (31.6%) in the whole group. Table 3 shows the univariate analysis results of all possible predictors of ischemia in the whole group. Those variables found to be significant ($p < 0.25$) on univariate testing were subjected to multivariate analysis, where the presence of DM was found to be the only independent predictor of an abnormal MPI result [odds ratio (OR): 12, 31, 95% confidence interval (CI): 1.83-82.66; $p < 0.01$]. No significant correlation was evident between ischemia on MPI and age, sex, hypertension, microalbuminuria, family history of CAD, smoking, aspirin use, and fasting blood

glucose. In the diabetic group, ischemia on MPI was not correlated with hypertension, smoking, family history of CAD, retinopathy, microalbuminuria, treatment modality for DM (oral antidiabetics, insulin, diet), and disease duration. Multivariate analysis revealed a small but a significant correlation between total cholesterol levels and ischemia (OR: 1.035, 95% CI: 1.0005-1.071, $p = 0.047$).

Follow up: During 12.8 ± 2.2 (8-19) months of patient follow-up, we observed ACCE in two (5.7%) pre-diabetic and three (7%) diabetic patients (Table 2). One diabetic patient developed MI and underwent PCI with stenting. This patient had positive scintigraphic findings and his SSS was 8. Four other patients (two diabetics, two pre-diabetic) developed typical angina pectoris and were

Table 2. Myocardial perfusion imaging findings and adverse cardiac/cerebrovascular event rates

	Prediabetes (n=35)	Diabetes mellitus (n=43)	p
Myocardial ischemia	4 (11.4%)	10 (23.3%)	0.290
Gated SPECT-WMA	-	5 (11.6%)	
LVEF	72 ± 7.3	70 ± 7.7	0.392
ACCE	2 (5.7%)	3 (7%)	1.000

SPECT: Single-photon emission computed tomography, WMA: Wall motion abnormalities, LVEF: Left ventricular ejection fraction, ACCE: Adverse cardiac/cerebrovascular event

Table 3. Univariate analysis of the variables predictive of ischemia on myocardial perfusion imaging

Variables	Ischemia (-) (n=64)	Ischemia (+) (n=14)	P	Odds ratio (95% CI)
Age (years)	55.4 ± 8.2	56.4 ± 9.7	0.685	1.015 (0.946-1.089)
Gender				
Male	37 (57.8%)	6 (42.9%)	-	1.000
Female	27 (42.2%)	8 (57.1%)	0.31	2.252 (0.565-8.876)
Groups				
Prediabetes	31 (48.4%)	4 (28.6%)	-	1.000
Diabetes	33 (51.6%)	10 (71.4%)	0.176	2.348 (0.667-8.270)
Smoking	3 (4.7%)	0 (0.0%)	1.000	-
Family history of CAD	16 (25.0%)	3 (21.4%)	1.000	0.818 (0.202-3.306)
FPG (mg/dl)	115 (80-291)	128 (102-334)	0.528	1.002 (0.991-1.013)
HbA _{1c} (%)	6.3 (4.5-10.8)	5.6 (5.0-10.0)	0.175	0.779 (0.449-1.352)
Total cholesterol (mg/dl)	194.7 ± 37.4	213.6 ± 46.4	0.106	1.012 (0.997-1.027)
LDL cholesterol (mg/dl)	110.8 ± 35.4	126.3 ± 40.0	0.152	1.012 (0.995-1.029)
HDL cholesterol (mg/dl)	49.1 ± 12.5	53.3 ± 11.9	0.252	1.027 (0.981-1.076)
Triglycerides (mg/dl)	145.5 ± 70.6 (57-382)	148 ± 71.1 (74-377)	0.720	1.003 (0.995-1.011)
Aspirin	8 (12.7%)	2 (14.3%)	1.000	1.146 (0.216-6.090)
Hypertension	21 (32.8%)	4 (28.6%)	1.000	0.819 (0.230-2.921)
Dyslipidemia	22 (34.4%)	7 (50.0%)	0.273	1.909 (0.594-6.137)
Two or more CAD risk factors	21 (32.8%)	5 (35.7%)	1.000	1.138 (0.339-3.820)

CI: Confidence interval, CAD: Coronary artery disease, LDL: Low density lipoprotein, HDL: High density lipoprotein, FPG: Fasting plasma glucose

started on anti-anginal therapy. No patient died because of a cardiovascular or cerebrovascular event during follow-up. Three of the five patients who developed ACCE on follow-up had ischemia on MPI. Patients who had ischemia on MPI were significantly more likely to have ACCE during follow-up as compared to those who had totally normal MPI scans (event rates: 21.4% vs. 3.1%, OR: 8.455 95% CI: 1.264-56.562, $p=0.038$).

Discussion

The major findings of this study are;

1- By using adenosine stress MPI with gated SPECT/CT, myocardial ischemia was detected in 23.3% and 11.4% of asymptomatic diabetic and pre-diabetic subjects, respectively,

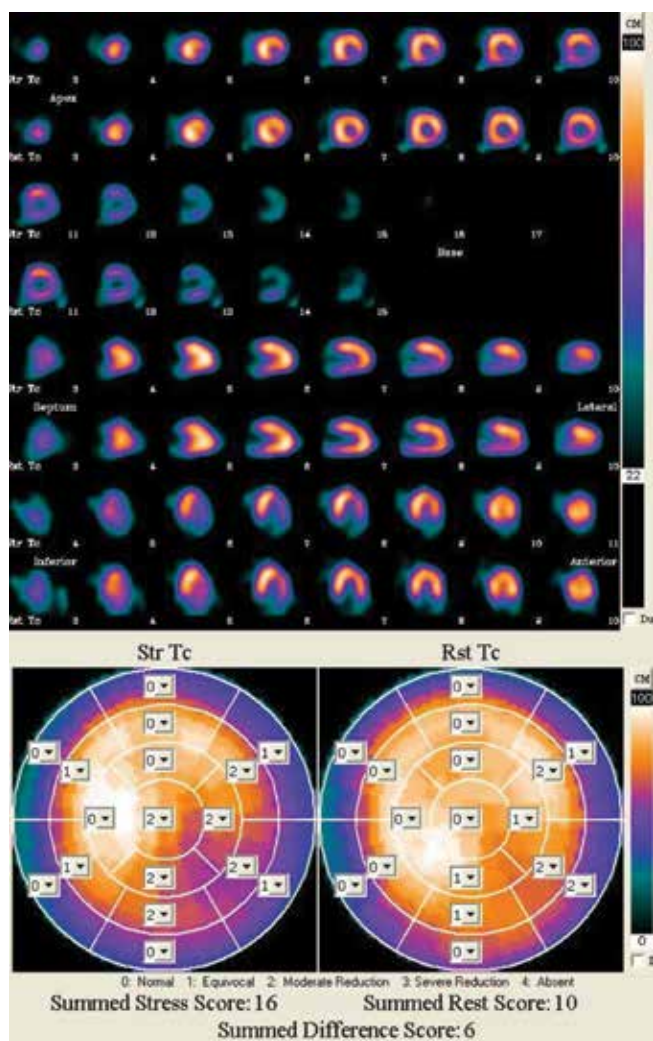


Figure 1. Stress and rest myocardial perfusion single-photon emission computed tomography images of a diabetic patient revealed reversible ischemia in the inferolateral wall

2- Although the population size and the event numbers are too small to draw any firm conclusions, subjects with ischemia on MPI were significantly more likely to experience ACCE as compared to those with normal scans.

The presence of silent ischemia has been evaluated in diabetic patients utilizing different methods of ischemia detection. In studies using nuclear imaging modalities, perfusion abnormalities were detected in 6-57% of asymptomatic patients with DM (4,11,12,13,14,15,16). In the present study, we evaluated completely asymptomatic patients with diabetes and pre-diabetes without clinically documented CAD. The prevalence of silent ischemia in our study is close to that reported in the Detection of Ischemia in Asymptomatic Diabetics (DIAD) trial (22%), one of the largest trials on asymptomatic ischemia in diabetic patients. Population-based studies report an increased rate of macrovascular complications and mortality in pre-diabetes; and fasting plasma glucose, postprandial plasma glucose and HbA_{1c} are related with increased mortality independent of obesity, hypertension and lipid profile (17,18). Nasr and Sliem (19) reported that pre-diabetics have myocardial defects, which represent a pattern of cardiovascular risk. In our study, the prevalence of hypertension, hypertriglyceridemia and use of statins were more common in the diabetic group as compared to pre-diabetics. Wall motion abnormalities and MPI abnormalities were more frequent in the diabetic group as compared to pre-diabetics but the differences did not reach statistical significance. Our small study population and an even smaller number of pre-diabetics preclude any meaningful discussion on the relative importance of pre-diabetes as opposed to diabetes with regard to the occurrence of asymptomatic ischemia.

Routine screening for silent ischemia in asymptomatic diabetic patients has been a matter of debate for a long time. Guidelines recommend routine screening only for high-risk patients. Janand-Delenne et al. (15) found a positive correlation between silent myocardial ischemia and DM duration, renal status and other classical CAD risk factors except family history. They recommend screening for male patients in whom the duration of DM is 10 years or even less when more than one cardiovascular risk factor is present. In a recent study by Giovacchini et al., (20) microalbuminuria was the only predictor of silent ischemia in diabetes. Gokcel et al. (12) reported a positive correlation between silent ischemia and retinopathy, male sex, hypertension and low HDL-cholesterol levels in patients with DM. In our patient population, which included both diabetics and pre-diabetics, the presence of DM was the only independent predictor of the occurrence of silent ischemia. In the diabetic group, only total cholesterol, neither microalbuminuria nor retinopathy, were found to be significant predictors of ischemia. Our small study sample may have obscured any such possible association, nevertheless it should be kept in mind that diabetic

complications do not have to follow a particular sequence. Our findings seem to be in line with those of Peix et al., (21) who showed that the presence of DM was the only predictor of abnormal myocardial perfusion and that total cholesterol/HDL ratio greater than 4 was correlated with perfusion abnormalities. In the DIAD study, where 522 diabetic patients were evaluated with adenosine MPI, an abnormal stress test result was not significantly associated with demographic characteristics, traditional cardiac risk factors, or laboratory variables (4). Anand et al. (22) also screened 510 asymptomatic diabetic patients and did not show any correlation with conventional risk factors and myocardial perfusion abnormalities. In that study, Coronary Artery Calcium (CAC) score was the only predictor of myocardial perfusion abnormality. In light of these findings, they recommended a strategy of initial CAC imaging followed by selective myocardial perfusion scintigraphy (MPS), which has the advantage of combining the high sensitivity rate of CAC imaging with the specificity of MPS for predicting angiographic stenosis.

MPI is a well-established method for the evaluation of CAD and has a high diagnostic accuracy (23,24,25). In our study, we used SPECT/CT for MPI and AC was made with low dose CT and left ventricular function was evaluated in each patient with gated SPECT. The American Society of Nuclear Cardiology and the Society of Nuclear Medicine concluded in their joint position statement that incorporation of AC in addition to ECG gating with MPI would improve image quality, interpretive certainty, and diagnostic accuracy (26). It was shown previously in several studies that AC increased the diagnostic accuracy and contributed to better risk stratification, possibly via decreasing the rate of false positive results (10,27,28,29). In the semi-quantitative analysis, no cut-off values of SSS, SDS and SRS have been established for CT-AC. In a limited number of studies, the cardiac event rate was significantly higher in patients with CT-based AC-SSS between 1-3 compared to the ones with non-AC-SSS between 1-3 (10,29). In our study, we considered SSS or SDS greater than 1 as positive. AC made a great contribution to our study since twenty-five patients (31.6%) with SSS >4 or /and SDS >2 scores in non-attenuation corrected images turned out to have a score of '0' when AC was performed. We believe that the reduction of false positive results on MPI by using AC may prevent unnecessary diagnostic and therapeutic interventions in this patient subset. MPI has been shown to predict the occurrence of adverse cardiac events in asymptomatic diabetic patients (11,12). In a recent study, Kakaletsis et al. (30) used stress MPI in asymptomatic diabetic patients to predict the occurrence of cardiac events at follow-up. They did not use CT for AC and reported that ischemia on MPI was associated with an OR of 3.8 for cardiac event prediction. The OR increased to 7.7 when only extensive ischemia on MPI was taken into account. We observed a significantly higher rate of ACCE (OR: 8.455 95% CI: 1.264-56.562, p=0.038) at follow-up

in diabetic and pre-diabetic patients with ischemia on MPI as opposed to those without. The OR that we have found in our study seems to be higher than those reported in the literature. The high rate of cardiac adverse events at follow-up in our study seems to be contradictory to the rate reported in the landmark DIAD trial (6.4% over a mean of 12 months versus 2.9% over 4.8 years, respectively) (4). This discrepancy deserves an explanation and the most likely sources are the small sample size and the simplistic clinical definition of cardiac events in our study. Four out of five cardiac events on follow-up were angina necessitating the institution of anti-anginal therapy. Still, hard end-points like MI appeared to have similar frequencies (1.28% versus 1.3% respectively) in the 2 studies. We believe that when performed by highly accurate methods like the one used in our trial (MPI with gated SPECT/CT), ischemia detection in this patient population may be useful in accurate prediction of the likelihood of ACCE on follow-up, and thus, guide patient selection for more advanced evaluation with respect to CAD. Adenosine SPECT/CT as an imaging modality is a promising tool to detect silent ischemia in diabetic and non-diabetic patients. Whether such a strategy of screening for ischemia in this population will yield clinical improvement still remains to be proven by further studies.

There are some limitations in our study;

- 1- No control group was included due to ethical reasons,
- 2- The small population size precluded any meaningful discussion of IGT and IFG groups, even diabetics and pre-diabetics separately,
- 3- The follow-up interval for cardiac events was rather short.

Conclusion

In conclusion, although the population size and the event numbers are too small to draw any firm conclusions, subjects with ischemia on MPI were significantly more likely to experience ACCE as compared to those with normal scans.

Ethics

Ethics Committee Approval: The study was approved by the Ankara Atatürk Training and Research Hospital Local Ethics Committee, Informed Consent: Consent form was filled out by all participants.

Peer-review: Externally peer-reviewed.

Authorship Contributions

Medical Practices: Elif Özdemir, Şefika Burçak Polat, Nilüfer Yıldırım, Reyhan Ersoy, Tahir Durmaz, Telat Keleş, Concept: Elif Özdemir, Şeyda Türkölmez, Reyhan Ersoy, Bekir Çakır, Engin Bozkurt, Design: Elif Özdemir, Şefika Burçak Polat, Nilüfer Yıldırım, Data Collection or Processing: Elif Özdemir, Şefika Burçak Polat, Nilüfer Yıldırım, Reyhan Ersoy, Tahir

Durmaz, Telat Keleş, Analysis or Interpretation: Elif Özdemir, Şefika Burçak Polat, Reyhan Ersoy, Şeyda Türkölmez, Tahir Durmaz, Literature Search: Elif Özdemir, Şefika Burçak Polat, Nilüfer Yıldırım Writing: Elif Özdemir, Şefika Burçak Polat, Nilüfer Yıldırım, Reyhan Ersoy, Tahir Durmaz, Telat Keleş, Engin Bozkurt, Şeyda Türkölmez, Bekir Çakır.

Conflict of Interest: No conflict of interest was declared by the authors.

Financial Disclosure: The authors declared that this study has received no financial support.

References

- Stolar M. Addressing cardiovascular risk in patients with type 2 diabetes: Focus on primary care. *Am J Med Sci* 2011;341:132-140.
- Wilson PW. Diabetes mellitus and coronary heart disease. *Endocrinol Metab Clin North Am* 2001;30:857-881.
- Xanthos T, Ekmektzoglou KA, Papadimitriou L. Reviewing myocardial silent ischemia: Specific patient subgroups. *Int J Cardiol* 2008;124:139-148.
- Wackers FJ, Young LH, Inzucchi SE, Chyun DA, Davey JA, Barrett EJ, Taillefer R, Wittlin SD, Heller GV, Filipchuk N, Engel S, Ratner RE, Iskandrian AE; Detection of Ischemia in Asymptomatic Diabetics Investigators. Detection of silent myocardial ischemia in asymptomatic diabetic subjects: The DIAD study. *Diabetes Care* 2004;27:1954-1961.
- Marini MA, Succurro E, Castaldo E, Cufone S, Arturi F, Sciacqua A, Lauro R, Hribal ML, Perticone F, Sesti G. Cardiometabolic risk profiles and carotid atherosclerosis in individuals with prediabetes identified by fasting glucose, postchallenge glucose, and hemoglobin A1c criteria. *Diabetes Care* 2012;35:1144-1149.
- Greenland P, Alpert JS, Beller GA, Benjamin EJ, Budoff MJ, Fayad ZA, Foster E, Hlatky MA, Hodgson JM, Kushner FG, Lauer MS, Shaw LJ, Smith SC Jr, Taylor AJ, Weintraub WS, Wenger NK, Jacobs AK, Smith SC Jr, Anderson JL, Albert N, Buller CE, Creager MA, Ettinger SM, Guyton RA, Halperin JL, Hochman JS, Kushner FG, Nishimura R, Ohman EM, Page RL, Stevenson WG, Tarkington LG, Yancy CW; American College of Cardiology Foundation; American Heart Association. 2010 ACCF/AHA guideline for assessment of cardiovascular risk in asymptomatic adults: A report of the American College of Cardiology Foundation/American Heart Association Task Force on Practice Guidelines. *J Am Coll Cardiol* 2010;56:50-103.
- Authors/Task Force Members, Rydén L, Grant PJ, Anker SD, Berne C, Cosentino G, Danchin N, Deaton C, Escaned J, Hammes HP, Huikuri H, Marre M, Marx N, Mellbin L, Ostergren J, Patrono C, Seferovic P, Uva MS, Taskinen MR, Tendera M, Tuomilehto J, Valensi P, Zamorano JL; ESC Committee for Practice Guidelines (CPG), Zamorano JL, Achenbach S, Baumgartner H, Bax JJ, Bueno H, Dean V, Deaton C, Erol C, Fagard R, Ferrari R, Hasdai D, Hoes AW, Kirchhof P, Knuuti J, Kolh P, Lancellotti P, Linhart A, Nihoyannopoulos P, Piepoli MF, Ponikowski P, Sirnes PA, Tamargo JL, Tendera M, Torbicki A, Wijns W, Windecker S; Document Reviewers, De Backer G, Sirnes PA, Ezquerro EA, Avogaro A, Badimon L, Baranova E, Baumgartner H, Betteridge J, Ceriello A, Fagard R, Funck-Brentano C, Gulba DC, Hasdai D, Hoes AW, Kjekshus JK, Knuuti J, Kolh P, Lev E, Mueller C, Neyses L, Nilsson PM, Perk J, Ponikowski P, Reiner Z, Sattar N, Schächinger V, Scheen A, Schirmer H, Strömberg A, Sudzhaeva S, Tamargo JL, Viigimaa M, Vlachopoulos C, Xuereb RG. ESC Guidelines on diabetes, pre-diabetes, and cardiovascular diseases developed in collaboration with the EASD: The Task Force on diabetes, pre-diabetes, and cardiovascular diseases of the European Society of Cardiology (ESC) and developed in collaboration with the European Association for the Study of Diabetes (EASD). *Eur Heart J* 2013;34:3035-3087.
- Garcia EV. SPECT attenuation correction: An essential tool to realize nuclear cardiology's manifest destiny. *J Nucl Cardiol* 2007;14:16-24.
- American Diabetes Association. Standards of medical care in diabetes 2013. *Diabetes Care* 2013;36(Suppl 1):11-66.
- Baghdasarian SB, Noble GL, Ahlberg AW, Katten D, Heller GV. Risk stratification with attenuation corrected stress Tc-99m sestamibi SPECT myocardial perfusion imaging in the absence of ECG-gating due to arrhythmias. *J Nucl Cardiol* 2009;16:533-539.
- De Lorenzo A, Lima RS, Siqueira-Filho AG, Pantoja MR. Prevalence and prognostic value of perfusion defects detected by stress technetium-99m sestamibi myocardial perfusion single-photon emission computed tomography in asymptomatic patients with diabetes mellitus and no known coronary artery disease. *Am J Cardiol* 2002;90:827-832.
- Gokcel A, Aydin M, Yalcin F, Yapar AF, Ertorer ME, Ozsahin AK, Muderrisoglu H, Aktas A, Guvener N, Akbaba M. Silent coronary artery disease in patients with type 2 diabetes mellitus. *Acta Diabetol* 2003;40:176-180.
- Scholte AJ, Schuijf JD, Kharagjitsingh AV, Dibbets-Schneider P, Stokkel MP, van der Wall EE, Bax JJ. Prevalence and predictors of an abnormal stress myocardial perfusion study in asymptomatic patients with type 2 diabetes mellitus. *Eur J Nucl Med Mol Imaging* 2009;36:567-575.
- Faglia E, Favales F, Calia P, Paleari F, Segalini G, Gamba PL, Rocca A, Musacchio N, Mastropasqua A, Testori G, Rampini P, Moratti F, Braga A, Morabito A; Milan Study on Atherosclerosis and Diabetes (Mi SAD). Cardiac events in 735 type 2 diabetic patients who underwent screening for unknown asymptomatic coronary heart disease: 5-year follow-up report from the Milan Study on Atherosclerosis and Diabetes (MiSAD). *Diabetes Care* 2002;25:2032-2036.
- Janand-Delenne B, Savin B, Habib G, Bory M, Vague P, Lassmann-Vague V. Silent myocardial ischemia in patients with diabetes: Who to screen. *Diabetes Care* 1999;22:1396-1400.
- Miller TD, Rajagopalan N, Hodge DO, Frye RL, Gibbons RJ. Yield of stress single-photon emission computed tomography in asymptomatic patients with diabetes. *Am Heart J* 2004;147:890-896.
- Shaw JE, Hodge AM, De Courten M, Chitson P, Zimmet PZ. Isolated post-challenge hyperglycaemia confirmed as a risk factor for mortality. *Diabetologia* 1999;42:1050-1054.
- Nakamura Y, Saitoh S, Takagi S, Ohnishi H, Chiba Y, Kato N, Akasaka H, Miura T, Tsuchihashi K, Shimamoto K. Impact of abnormal glucose tolerance, hypertension and other risk factors on coronary artery disease. *Circ J* 2007;71:20-25.
- Nasr G, Sliem H. Silent myocardial ischemia in prediabetics in relation to insulin resistance. *J Cardiovasc Dis Res* 2010;3:116-121.
- Giovacchini G, Cappagli M, Carro S, Borini S, Montepagani A, Leoncini R, Mazzotta G, Sambuceti G, Mariani G, Volterrani D, Zellweger MJ, Ciarmiello A. Microalbuminuria predicts silent myocardial ischaemia in type 2 diabetes patients. *Eur J Nucl Med Mol Imaging* 2013;40:548-557.
- Peix A, Cabrera LO, Heres F, Rodríguez L, Valdés A, Valiente J, García R, Licea M, Mendoza V, Gárciga F, Rodríguez Y, Carrillo R, Mena E, Fernández Y, Montero M, Dondi M. Interrelationship between myocardial perfusion imaging, coronary calcium score, and endothelial function in asymptomatic diabetics and controls. *J Nucl Cardiol* 2011;18:398-406.
- Anand DV, Lim E, Hopkins D, Corder R, Shaw LJ, Sharp P, Lipkin D, Lahiri A. Risk stratification in uncomplicated type 2 diabetes: Prospective evaluation of the combined use of coronary artery calcium imaging and selective myocardial perfusion scintigraphy. *Eur Heart J* 2006;27:713-721.
- Gimelli A, Rossi G, Landi P, Marzullo P, Iervasi G, L'abbate A, Rovai D. Stress/rest myocardial perfusion abnormalities by gated SPECT: Still the best predictor of cardiac events in stable ischemic heart disease. *J Nucl Med* 2009; 50:546-53.
- Galassi AR, Azzarelli S, Tomaselli A, Giosofatto R, Ragusa A, Musumeci S, Tamburino C, Giuffrida G. Incremental prognostic value of technetium-99m-tetrofosmin exercise myocardial perfusion imaging for predicting outcomes in patients with suspected or known coronary artery disease. *Am J Cardiol* 2001;88:101-106.
- Wiersma JJ, Verberne HJ, ten Holt WL, Radder IM, Dijkman LM, van Eck-Smit BL, Trip MD, Tijssen JG, Piek JJ. Prognostic value

- of myocardial perfusion scintigraphy in type 2 diabetic patients with mild, stable angina pectoris. *J Nucl Cardiol* 2009;16:524-532.
26. Heller GV, Links J, Bateman TM, Ziffer JA, Ficaró E, Cohen MC, Hendel RC. American Society of Nuclear Cardiology and Society of Nuclear Medicine joint position statement: Attenuation correction of myocardial perfusion SPECT scintigraphy. *J Nucl Cardiol* 2004;11:229-230.
 27. Links JM, DePuey EG, Taillefer R, Becker LC. Attenuation correction and gating synergistically improve the diagnostic accuracy of myocardial perfusion SPECT. *J Nucl Cardiol* 2002;9:183-187.
 28. Masood Y, Liu YH, Depuey G, Taillefer R, Araujo LI, Allen S, Delbeke D, Anstett F, Peretz A, Zito MJ, Tsatkin V, Wackers FJ. Clinical validation of SPECT attenuation correction using x-ray computed tomography-derived attenuation maps: Multicenter clinical trial with angiographic correlation. *J Nucl Cardiol* 2005;12:676-686.
 29. Pazhenkottil AP, Ghadri JR, Nkoulou RN, Wolfrum M, Buechel RR, Küest SM, Husmann L, Herzog BA, Gaemperli O, Kaufmann PA. Improved outcome prediction by SPECT myocardial perfusion imaging after CT attenuation correction. *J Nucl Med* 2011;52:196-200.
 30. Kakaletsis N, Moravidis E, Iliadis F, Hilidis I, Gotzamani-Psarrakou A, Didangelos T. The prognostic efficacy of myocardial perfusion imaging in optimally treated diabetic patients with no manifestations of coronary artery disease. *Nucl Med Commun* 2013;34:885-892.



Is Very High Thyroid Stimulating Hormone Level Required in Differentiated Thyroid Cancer for Ablation Success?

Diferansiye Tiroid Kanserlerinde Ablasyon Başarısı için Tiroid Simüle Edici Hormon Seviyesinin Çok Yüksek Olması Gerekli midir?

Zekiye Hasbek, Bülent Turgut

Cumhuriyet University Faculty of Medicine, Department of Nuclear Medicine, Sivas, Turkey

Abstract

Objective: Remnant ablation with radioactive iodine (I-131) is a successful form of treatment that aims to destroy the remaining residual tissue and/or metastatic tissue after total thyroidectomy in differentiated thyroid cancer (DTC) patients. High level of thyroid stimulating hormone (TSH) (≥ 30 mIU/L) is recommended for success of ablation treatment. In this retrospective study, our aim was to investigate whether the TSH levels at the time of ablation effect the success of radioactive iodine remnant ablation.

Methods: Patients who were diagnosed with DTC, treated with bilateral total/near total thyroidectomy and who were referred for I-131 remnant ablation were included in this study. Patients with undetectable TSH-stimulated serum thyroglobulin (Tg) level, normal physical examination, negative results on whole body scan with I-131, and no evidence of neck lymph node metastasis on ultrasound were defined as disease-free. The correlation between TSH level at the time of ablation and ablation success was assessed.

Results: Two hundred sixty one consecutive patients were included in the present study. Mean TSH level was 19.47 ± 6 mIU/L in the 34 patients with TSH < 30 mIU/L, while mean TSH level was 73.65 ± 27 mIU/L in the 227 patients with TSH ≥ 30 mIU/L during I-131 remnant ablation. Ablation was unsuccessful in only one patient with TSH < 30 mIU/L who had lung metastasis. Ablation was unsuccessful in 5.1% of patients with TSH ≥ 30 mIU/L. The effect of TSH level was not significant on ablation success ($p=0.472$).

Conclusion: In conclusion, we think that a high TSH serum level alone is not a factor for the success of ablation. Age, presence of metastasis, extent of residual thyroid mass should also be considered. Especially, in the presence of metastatic tissue, obtaining adequate increase in TSH level is not always possible. The success of ablation at lower levels of TSH elevations may be sufficient for patients, and long-term hypothyroidism may not be required.

Keywords: Thyroid cancer, thyroid stimulating hormone level, radioiodine therapy

Öz

Amaç: Diferansiye tiroid kanser (DTK), hastalarında total tiroidektomi sonrası radyoaktif iyot (I-131) ile remnant ablasyon kalan rezidü doku ve/veya metastatik dokunun yok edilmesi amacıyla kullanılan başarılı bir tedavi yöntemidir. Başarılı ablasyon tedavisi için yüksek tiroid simüle edici hormon (TSH) (≥ 30 mIU/L) seviyesi önerilmektedir. Bu retrospektif çalışmada ablasyon sırasındaki TSH düzeyinin radyoaktif iyot remnant ablasyonun başarısı üzerine etkisinin araştırılması amaçlandı.

Yöntem: Bu çalışmaya DTK tanısı olan, bilateral total/totale yakın tiroidektomi ile tedavi edilen ve I-131 ile remnant ablasyon için yönlendirilmiş hastalar dahil edildi. Detekte edilemeyen stimüle-TSH serum tiroglobulin düzeyi, normal fizik muayene, I-131 ile tüm vücut tarama sonuçları negatif ve ultrasonda boyun lenf nodu metastazı bulgusu olmayan hastalar hastaliksız olarak kabul edildi. Ablasyon başarısı ile ablasyon sırasındaki TSH düzeyi arasındaki ilişki değerlendirildi.

Bulgular: Mevcut çalışmaya ardışık 261 hasta dahil edildi. I-131 ile remnant ablasyon sırasında TSH düzeyi < 30 mIU/L olan 34 hastada ortalama TSH düzeyi $19,47 \pm 6$ mIU/L, TSH düzeyi ≥ 30 mIU/L olan 227 hastada ortalama TSH düzeyi $73,65 \pm 27$

Address for Correspondence: Zekiye Hasbek MD, Cumhuriyet University Faculty of Medicine, Department of Nuclear Medicine, Sivas, Turkey
Phone: +90 346 258 02 53 E-mail: hasbekz@yahoo.com **Received:** 04.03.2015 **Accepted:** 03.05.2016

mIU/L idi. TSH <30 mIU/L olan bu hastaların yalnızca birinde ablasyon başarısızdı ve bu hastada akciğer metastazı vardı. TSH düzeyi ≥ 30 mIU/L olan hastaların ise %5,1'inde ablasyon başarısızdı. TSH düzeyinin ablasyon başarısına etkisi anlamlı değildi ($p=0,472$).

Sonuç: Sonuç olarak, biz ablasyon başarısı için yalnızca yüksek serum TSH seviyesinin yeterli bir faktör olmayacağını düşünüyoruz. Yaş, metastaz varlığı, rezidü tiroid dokusunun büyüklüğü de dikkate alınması gereken faktörlerdir. Özellikle metastatik doku varlığında TSH seviyesini yeterli derecede yükseltmek mümkün olmaz. Ablasyon başarısında hastalarda daha düşük düzeyde TSH yükseklikleri yeterli olup, uzun süre hipotiroid dönemde kalınması gerekli olmayabilir.

Anahtar kelimeler: Tiroid kanseri, tiroid simüle edici hormon, radyoyot tedavi

Introduction

Thyroid cancer is the most common endocrine tumor, most of which are papillary thyroid carcinomas. Multidisciplinary treatment of differentiated thyroid cancer (DTC) patients consists of total thyroidectomy followed by radioactive iodine remnant ablation (RRA) and thyroid stimulating hormone (TSH) suppression treatment. RRA is a successful form of treatment that aims to destroy the remaining residual tissue and/or metastatic tissue after surgical treatment in patients with DTC (1). Elevated levels of serum thyroglobulin (Tg) (>2 ng/mL) is a specific indicator with high sensitivity, which indicates presence of residual thyroid tissue, metastatic focus or recurrence (2). Obtaining elevated levels of TSH (thyroid stimulating hormone) (≥ 30 mIU/L) is recommended for successful ablation (3). High serum TSH concentration enhances I-131 uptake by cancer cells. However, it is not known whether higher TSH levels produce a better rate of remnant ablation or cancer cure. In this retrospective study, our aim was to investigate whether TSH levels during ablation influenced the success of RRA. The secondary aim was to investigate the effect of Tg level at the time of ablation and other clinic and demographic patient related data on ablation success.

Materials and Methods

Patients who were diagnosed with DTC, treated with bilateral total/near total thyroidectomy and who were referred for RRA were included in this retrospective study. Exclusion criteria were patients receiving I-131 treatment in another hospital, patients who were not imaged with whole body scan (WBS) within 8-12th months after ablation, and patients with positive Tg antibodies (TgAb). Activity ranging between 100 to 250 mCi (mean 114 ± 22 mCi) of I-131 were administered orally. The standard therapeutic dose was applied (for ablation therapy: 100 mCi, for lymph node metastasis: 150 mCi, for lung metastasis: 200 mCi, for lung metastasis reablation: 250 mCi). RRA was given to patients who had a TSH level under 30 despite sufficient levothyroxine (LT4) thyroid hormone withdrawal (THW) time (minimum 4 weeks), due to suspicion of metastatic disease. Patients were divided into 2 groups as <30 mIU/L and ≥ 30 mIU/L according to serum TSH level. Serum TSH, serum Tg and serum TgAb levels were recorded before

RRA in all patients after adequate THW for 4-5 weeks. We also recommended a low-iodine diet 10 day before RRA for all patients. The initial clinical follow-up evaluation was performed at the 2nd and 6th months after RRA in all patients. Clinical follow-up included; physical examination, neck ultrasound, and serum Tg, TgAb, TSH, freeT4 measurements. Diagnostic Whole Body Scan (DxWBS) with approximately 185 MBq of I-131, neck ultrasound and chest X-ray, or if required neck and/or chest computed tomography examinations were performed, and serum Tg, TgAb and TSH levels were measured 8-12 months after RRA. Diagnostic WBS was performed 24 and 48 hours after administration of diagnostic dose I-131. TSH-stimulated serum Tg level measurements were obtained at the time of DxWBS performed 8-12 months after ablation in all patients. For stimulated TSH level, the LT4 preparation was stopped 4 weeks before I-131 administration, or recombinant TSH was administered (0.9 mg) by intramuscular injections on two successive days with the I-131 being given on the third day during DxWBS. Scintigraphic images were obtained with the use of a single-headed gamma camera (Toshiba GCA-7100A) that was equipped with a "high-energy parallel hole" collimator and interfaced to a dedicated computer. For image acquisition, a peak energy setting at 364 keV with a 20% window was used. The scan speed was 7 cm/min for all WBS. WBS with anterior and posterior views was acquired, and local static images were obtained. Patients with undetectable thyroid-stimulating hormone-stimulated serum Tg concentrations, normal physical examination, negative results on WBS, and no evidence of neck lymph node metastases on ultrasound were defined as disease-free. The correlation between TSH level at the time of ablation and the success of ablation was evaluated.

Statistical Analysis

SPSS 14.0 software was used for statistical analysis. Descriptive quantitative data are expressed as mean values and standard deviation, and qualitative data are expressed as percentages. Correlations between serum TSH and serum Tg levels were examined by the Spearman's rank correlation test. It was assumed that the observed differences were statistically significant at the $p \leq 0.05$ levels. Two-independent samples t-test was used to assess the relationship between success of ablation and levels of serum Tg and serum TSH. We also evaluated the

relationship between gender, type of tumor, the number of lesions, age, tumor size, lymph node metastasis at the time of diagnosis and success of ablation.

Results

Two hundred sixty one consecutive patients were included in the present study. There was 222 (85.1%) female and 39 (14.9%) male patients with a mean age of 45.96 ± 12 years (range; 16-80 years). Hundred and twenty three patients (47.1%) were under the age of 45 and 138 patients (52.9%) were over 45. Thyroid carcinomas were classified as papillary in 205 (78.5%) patients, as follicular in 34 (13%), as thyroid tumors of uncertain malignant potential 15 (5.7%), as poorly differentiated in 4 (1.5%), as aggressive histology (tall cell and insular variant) in 2 (0.8%), and as anaplastic cancer in 1 (0.4%). Mean serum TSH level was 19.47 ± 6 mIU/L in 34 patients with serum TSH level <30 mIU/L, and mean serum TSH level was 73.65 ± 27 mIU/L in 227 patients with serum TSH level ≥ 30 mIU/L at the time of RRA. In 20.6% of patients with serum TSH level <30 mIU/L, serum Tg level was <2 ng/mL and in 79.4%, serum Tg level was ≥ 2 ng/mL at the time of RRA. However, in 37.4% of patients with ≥ 30 mIU/L serum TSH level, serum Tg level was <2 ng/mL and in 62.6% serum Tg level was ≥ 2 ng/mL ($p=0.054$) (Table 1). Mean serum Tg level was 43.1 ng/mL (range: 0.10-914 ng/mL) in 34 patients with serum TSH level <30 mIU/L, mean serum Tg level was 19.69 ng/mL (range: 0.08-458 ng/mL) in 227 patients with serum TSH level ≥ 30 mIU/L ($p=0.003$). Postoperative stimulated serum Tg levels at the time of ablation therapy were ≤ 2 ng/mL in 90 patients (34.5%), 2-10 ng/mL in 81 patients (31%) and ≥ 10 ng/mL in 90 patients (34.5%). Mean stimulated serum Tg level was 7.15 ng/mL (range: 0.10-1000 ng/mL) and mean stimulated-TSH level was 86.11 mIU/mL (range:

12.4-226.5 mIU/mL) at the time of DxWBS. There was a negative correlation between serum TSH level and Tg levels ($p=0.007$, $r=-0.167$). Patients with radioactive iodine accumulation outside the thyroid bed (the cervical area or in other areas of the body) or in the thyroid bed region, and with high serum TSH levels (>10 ng/mL or 2-10 ng/mL) were considered as unsuccessful ablation at the time of DxWBS. If there was no significant pathologic radioactive iodine accumulation or minimal local accumulation in the thyroid bed region and if the serum TSH level was low (<2 ng/mL), this was regarded as successful ablation at the time of DxWBS. When all patients were considered, ablation was not successful in 12 patients after the first RRA. Findings of those patients are presented in Table 2. Serum TSH levels were <30 mIU/L in 34 patients (13%) at the time of RRA. Ablation was unsuccessful in only one patient with serum TSH level <30 mIU/L. This patient had lung metastasis, and the serum Tg level was 914 ng/mL at the time of RRA. Reablation was also unsuccessful in the same patient although the serum TSH level was >100 mIU/L at the time of treatment. Ablation was unsuccessful in 5.1% of patients with serum TSH level ≥ 30 mIU/L. The effect of serum TSH level was not significant on ablation success ($p=0.472$). There was no significant difference in terms of mean

Table 1. Comparison of serum thyroid stimulating hormone and thyroglobulin level

TSH level	Tg level	
	<2 ng/mL	≥ 2 ng/mL
<30 mIU/L	7 (20.6%)	27 (79.4%)
≥ 30 mIU/L	85 (37.4%)	142 (62.6%)

TSH: Thyroid stimulating hormone, Tg: Thyroglobulin

Table 2. Clinicopathologic findings of 12 patients in whom ablation was unsuccessful after the first radioiodine remnant ablation

Patient	Age/sex	TSH level	Histopathology	Tumor size	Clinical finding
1-F.O.	63/F	<30 mIU/L	Papillary cancer (Poorly differentiated)	55 mm	Lung+lymph node metastasis
2-H.D.	67/M	≥ 30 mIU/L	Papillary cancer (Classic variant)	35 mm	Bone metastasis
3-F.K.	57/F	≥ 30 mIU/L	Papillary cancer (Classic variant)	40 mm	Lymph node metastasis
4-A.O.M.	55/M	≥ 30 mIU/L	Papillary cancer (Classic variant)	30 mm	Lymph node metastasis
5-D.S.	47/F	≥ 30 mIU/L	Papillary cancer (Follicular variant)	25 mm	Bone metastasis
6-N.K.	53/F	≥ 30 mIU/L	Papillary cancer (Classic variant)	20 mm	Lymph node metastasis
7-K.A.	52/M	≥ 30 mIU/L	Papillary cancer (Follicular variant)	45 mm	Bone metastasis
8-Z.E.	72/F	≥ 30 mIU/L	Papillary cancer (Follicular variant)	15 mm	Lymph node metastasis
9-S.B.	53/F	≥ 30 mIU/L	Papillary cancer (Oncocytic variant)	90 mm	Lung+lymph node metastasis
10-M.K.	72/M	≥ 30 mIU/L	Papillary cancer (Oncocytic variant)	25 mm	Lung+lymph node metastasis
11-H.K.	50/F	≥ 30 mIU/L	Papillary cancer (Classic variant)	25 mm	Metastasis absent/residue tissue exist
12-M.G.	51/F	≥ 30 mIU/L	Papillary cancer (Classic variant)	15 mm	Lymph node metastasis

TSH: Thyroid stimulating hormone, F: Female, M: Male

serum TSH levels in patients with and without successful ablation ($p=0.472$). However, a significant difference was determined in mean serum Tg values ($p=0.001$) (Table 3). One patient had a serum TSH level <30 mIU/L at the time of both RRA administration and DxWBS obtained 10 months later. No residual tissue or metastatic foci was detected at the latest DxWBS performed. Serum Tg level was <0.20 ng/mL both at the time of low dose scanning scintigraphy and during follow-ups. No abnormal finding was detected clinically and radiologically. Gender, type of tumor, the number of lesions (multifocal or single) were not found to be significantly associated with RRA outcome ($p=0.086$, $p=0.848$, $p=0.524$, respectively). Tumor size and lymph node metastasis at the time of diagnosis were found to be significantly associated with RRA ($p=0.002$, $p=0.0001$, respectively). Also, age at the time of diagnosis was significantly associated with RRA ($p=0.0001$). While ablation was successful in all patients younger than 45 years, ablation was unsuccessful in 8.7% of patients older than 45 years.

Discussion

RRA is a safe and effective method which has been used for a long time in the treatment of DTC patients with total thyroidectomy. There are no controlled studies that assess the adequate level of endogenous TSH for optimal ablation therapy. However, when treating a patient with radioactive iodine, it is important to stimulate iodine uptake by elevating serum TSH levels prior to radioactive iodine administration. The recommended TSH level is ≥ 30 mIU/L (1). Because, the clearance of radioactive iodine is approximately 50% greater in euthyroid patients than in hypothyroid patients (4), a high serum TSH concentration enhances I-131 uptake by cancer cells. TSH stimulates the production and release of thyroid hormones as well as stimulating Tg production (5). Prolonged hypothyroidism is undesirable both due to hypothyroidism symptoms and the risk of stimulating tumor growth. Tg is a significant tumor marker for DTC patients. Prior to I-131 therapy, LT4 replacement must be discontinued for approximately 4-5 weeks to achieve an adequate TSH level, or TSH can be stimulated by recombinant human TSH (rhTSH) without discontinuing thyroid hormone therapy. A higher level of TSH can be obtained with rhTSH application as compared to THW protocol (6). Nevertheless, rhTSH is not yet recommended as the standard therapeutic for the purpose

of RRA in metastatic thyroid cancer. TSH stimulated Tg measurement is compulsory to achieve sufficient clinical sensitivity for the detection of persistent and/or recurrent disease for current clinical guidelines. There are studies in the literature analyzing both the required period for ensuring adequate TSH levels and the optimal TSH level in order to reach a sufficient Tg level. Sánchez et al. (7) showed that TSH increases to >30 mIU/L in 90% of patients 3 weeks after discontinuing LT4 suppressive therapy. Luna et al. (8) also claimed that discontinuation of thyroxine treatment for four weeks was not required. According to them, a fourteen day period was adequate in most patients, and 21 days were sufficient in almost all. Similarly, Serhal et al. (5) stated that discontinuing thyroid hormone preparations for 2-3 weeks provided adequate iodine uptake. Goldman et al. (9) reported that in patients using LT3, withdrawal for 2 weeks produced the same effect as 4 week drug interruption even in metastatic patients. Valle et al. (10) determined that TSH cutoff of ≥ 30 mIU/L was inadequate to detect patients with thyroid-stimulating hormone-stimulated serum Tg ≥ 2 ng/mL, while TSH $>80-100$ mIU/L was a better cut off. However, there is still no consensus on the TSH value to obtain the highest Tg level. Low serum Tg level at the time of ablation has a negative predictive value for the absence of residual disease, and the risk of persistent disease increases with stimulated Tg levels (11). Postoperative stimulated Tg level is primarily related to surgeon success, and the presence of refractory disease or normal thyroid remnant. Absence of residual thyroid tissue is extremely rare even after successful total thyroidectomy applied by experienced surgeons. In patients with total thyroidectomy followed by I-131 ablation for DTC, the baseline stimulated-Tg level is a good predictor of successful ablation (12). In the literature, some studies have reported that the serum Tg/serum TSH ratio was an important predictor of ablation success that correlated well with patient outcomes. Moreover, they suggested that this rate and similar laboratory parameters might be considered while determining risk stratifications of DTC patients (13,14). Although a high TSH level (≥ 30 mIU /L) is recommended for ablation success in all textbooks, to the best of our knowledge there is only one study that assesses the correlation between ablation success and low TSH level (<30 mIU/L) in the literature. Vrachimis et al. (15), reported in their study on 1.873 patients without distant metastases that endogenous TSH levels at the

Table 3. Comparison of serum thyroid stimulating hormone and thyroglobulin levels at the time of ablation according to ablation success

Success of ablation	n (%)	Mean TSH level (mIU/L)	Mean Tg level (ng/mL)
Successful ablation	249 (95.4%)	66.45 \pm 31	15.45 \pm 39
Unsuccessful ablation	12 (4.6%)	69.49 \pm 28	174.01 \pm 28

TSH: Thyroid stimulating hormone, Tg: Thyroglobulin

time of I-131 ablation were not correlated with ablation success rates, recurrence free survival or DTC related mortality. TSH level was <30 mIU/L in 275 of patients in that study. It is known that, TSH elevation is slow or minimal in the presence of large residual tissue after total thyroidectomy, or in the presence of metastatic disease. If Tg level is low (<2 ng/mL) then TSH levels are known to rise easily. A high Tg level indicates presence of large residual tissue or metastasis. Therefore, the adequate TSH levels may not be reached especially in metastatic patients and in patients with large residual tissue even if the T4 preparation is discontinued for longer periods. Besides, if patients have malignant struma ovarii or hypopituitarism, TSH level will not elevate (16). Sawicka-Gutaj et al. (17) reported that the preablative TSH level in DTC patients with pyramidal lobe was statistically lower than the control group. However, TSH level was not different between DTC patients with and without pyramidal lobe 1 year after RRA. Moreover, although high TSH levels with recombinant TSH can be obtained quickly there are doubts about sufficient iodine uptake. Due to the retrospective nature of our study, weekly TSH levels were unfortunately not measured. In this study, patients for whom thyroid hormone preparations were discontinued for 4-5 weeks and were treated even though having TSH levels <30 mIU/L at the day of RRA were evaluated. In our study, the ablation was unsuccessful in one out of 34 patients with TSH level <30 mIU/L. But serum Tg level was 914 ng/mL despite the low TSH level. The treatment was unsuccessful although TSH level was >100 mIU/L during reablation in the same patient. Ablation was unsuccessful in 5.1% of patients with TSH \geq 30 mIU/L. TSH level did not show a significant effect on ablation success. Presence of I-131 uptake by tumor, younger age, well differentiated histopathologic subtype, and presence of metastases are predictive factors for tumor response to radioiodine treatment (1). Serum TSH level gradually decreases with age (18). In our study, all patients who had unsuccessful ablation were above the age of 45. Age may be one of the reasons for not obtaining a desired TSH level. Interestingly, Montesano et al. (19) have determined that higher TSH levels can be achieved after rhTSH application in patients with advanced age. Besides, when considered together with Tg levels, the reason for the low TSH level may be related to the presence of residual tissue and/or metastatic disease. In such situations, extension of hypothyroid period does not contribute in terms of iodine uptake. In our study, the ablation was not successful in almost all patients who had metastatic disease. In one of these patients, ablation was unsuccessful due to large residual tissue. The level of cell differentiation is as much important as the volume of residual tissue in iodine efficiency. Additionally, there is no significant evidence that rapid tumor growth is stimulated by a brief rise in TSH concentration (4). Individual iodine supply is also important. When all these factors are

considered in combination, it may be concluded that the TSH level may not necessarily point out RRA activity.

Conclusion

In conclusion, we think that a high serum TSH level is not enough for the success of ablation by itself. The success of ablation at lower levels of TSH elevations may be sufficient for patients and long-term hypothyroidism may not be required. Instead of assessing TSH or Tg level alone before RRA; age, presence of metastasis, extent of residual thyroid mass should also be considered. RRA may still be performed even if TSH remains low despite a sufficient period of THW.

Ethics

Ethical Approval: This study was retrospective. All procedures performed in studies involving human participants were in accordance with the ethical standards of the institutional research committee and with the 1964 Helsinki Declaration and its later amendments or comparable ethical standards. This article does not contain any studies with human participants performed by any of the authors.

Peer-review: Externally peer-reviewed.

Authorship Contributions

Surgical and Medical Practices: Zekiye Hasbek, Bülent Turgut, Concept: Zekiye Hasbek, Design: Zekiye Hasbek, Data Collection or Processing: Zekiye Hasbek, Analysis or Interpretation: Zekiye Hasbek, Bülent Turgut, Literature Search: Zekiye Hasbek, Writing: Zekiye Hasbek.

Conflict of Interest: No conflict of interest was declared by the authors.

Financial Disclosure: The authors declared that this study has received no financial support.

References

1. Haugen BR, Alexander EK, Bible KC, Doherty GM, Mandel SJ, Nikiforov YE, Pacini F, Randolph GW, Sawka AM, Schlumberger M, Schuff KG, Sherman SI, Sosa JA, Steward DL, Tuttle RM, Wartofsky L. 2015 American Thyroid Association management guidelines for adult patients with thyroid nodules and differentiated thyroid cancer: the American Thyroid Association guidelines task force on thyroid nodules and differentiated thyroid cancer. *Thyroid* 2016;26:1-133.
2. Kucukalić-Selimović E, Alagić J, Valjevac A, Valjevac A, Hadzović-Dzuvo A, Begić A, Beslić N. The value of serum thyroglobulin levels and whole body (I-131) scintigraphy in the follow-up of the thyroid cancer patients after thyroidectomy. *Coll Antropol* 2012;36(Suppl 2):67-71.
3. Amdur RJ, Mazzaferri EL. The Diagnosis And Imaging of Thyroid Cancer. In: Amdur RJ, Mazzaferri EL (eds). *Essentials Of Thyroid Cancer Management*. Springer Science Business Media, Inc, 2005:229-231.

4. Dietlein M, Moka D, Schicha H. Radioiodine Therapy for thyroid cancer. In: Biersack HJ, Grünwald F (eds). *Thyroid Cancer*. Springer Science Business Media, Inc, 2005:95-126.
5. Serhal DI, Nasrallah MP, Arafah BM. Rapid rise in serum thyrotropin concentrations after thyroidectomy or withdrawal of suppressive thyroxine therapy in preparation for radioactive iodine administration to patients with differentiated thyroid cancer. *J Clin Endocrinol Metab* 2004;89:3285-3289.
6. Rani D, Kaisar S, Awasare S, Kamaldeep, Abhyankar A, Basu S. Examining recombinant human TSH primed 131I therapy protocol in patients with metastatic differentiated thyroid carcinoma: comparison with the traditional thyroid hormone withdrawal protocol. *Eur J Nucl Med Mol Imaging* 2014;41:1767-1780.
7. Sánchez R, Espinosa-de-los-Monteros AL, Mendoza V, Brea E, Hernández I, Sosa E, Mercado M. Adequate thyroid-stimulating hormone levels after levothyroxine discontinuation in the follow-up of patients with well-differentiated thyroid carcinoma. *Arch Med Res* 2002;33:478-481.
8. Luna R, Penín M, Seoane I, Alvarez E, Palmeiro R, García-Mayor R. [Should thyroxine treatment be discontinued for four weeks before I(131) thyroid ablation?]. *Endocrinol Nutr* 2012;59:227-231.
9. Goldman JM, Line BR, Aamodt RL, Robbins J. Influence of triiodothyronine withdrawal time on 131I uptake postthyroidectomy for thyroid cancer. *J Clin Endocrinol Metab* 1980;50:734-739.
10. Valle LA, Gorodeski Baskin RL, Porter K, Sijos JA, Khawaja R, Ringel MD, Kloos RT. In thyroidectomized patients with thyroid cancer, a serum thyrotropin of 30 μ U/mL after thyroxine withdrawal is not always adequate for detecting an elevated stimulated serum thyroglobulin. *Thyroid* 2013;23:185-193.
11. Pacini F, Capezzone M, Elisei R, Ceccarelli C, Taddei D, Pinchera A. Diagnostic 131-iodine whole-body scan may be avoided in thyroid cancer patients who have undetectable stimulated serum Tg levels after initial treatment. *J Clin Endocrinol Metab* 2002;87:1499-501.
12. Fatima N, Zaman M, Ikram M, Akhtar J, Islam N, Masood Q, Zaman U, Zaman A. Baseline stimulated thyroglobulin level as a good predictor of successful ablation after adjuvant radioiodine treatment for differentiated thyroid cancers. *Asian Pac J Cancer Prev* 2014;15:6443-6447.
13. Zubair Hussain S, Zaman MU, Malik S, Ram N, Asghar A, Rabbani U, Aftab N, Islam N. Preablation stimulated thyroglobulin/TSH ratio as a predictor of successful I(131)remnant ablation in patients with differentiated thyroid cancer following total thyroidectomy. *J Thyroid Res* 2014;2014:610273.
14. Neshandar Asli I, Siahkali AS, Shafie B, Javadi H, Assadi M. Prognostic value of basal serum thyroglobulin levels, but not basal antithyroglobulin antibody (TgAb) levels, in patients with differentiated thyroid cancer. *Mol Imaging Radionucl Ther* 2014;23:54-59.
15. Vrachimis A, Riemann B, Mäder U, Reiners C, Verburg FA. Endogenous TSH levels at the time of 131I ablation do not influence ablation success, recurrence-free survival or differentiated thyroid cancer-related mortality. *Eur J Nucl Med Mol Imaging devamina* 2016;43:224-231
16. Gut P, Matysiak-Grześ M, Fischbach J, Klimowicz A, Gryczyńska M, Ruchala M. Lack of TSH stimulation in patients with differentiated thyroid cancer- possible causes. *Contemp Oncol (Pozn)* 2012;16:273-275.
17. Sawicka-Gutaj N, Klimowicz A, Sowinski J, Oleksa R, Gryczynska M, Wyszomirska A, Czarnywojtek A, Ruchala M. Pyramidal lobe decreases endogenous TSH stimulation without impact on radioiodine therapy outcome in patients with differentiated thyroid cancer. *Ann Endocrinol* 2014;75:141-147.
18. Hoogendoorn EH, Hermus AR, de Vegt F, Ross HA, Verbeek AL, Kiemeny LA, Swinkels DW, Sweep FC, den Heijer M. Thyroid function and prevalence of anti-thyroperoxidase antibodies in a population with borderline sufficient iodine intake: influences of age and sex. *Clin Chem* 2006;52:104-111.
19. Montesano T, Durante C, Attard M, Crocetti U, Meringolo D, Bruno R, Tumino S, Rubello D, Al-Nahhas A, Colandrea M, Maranghi M, Travascio L, Ronga G, Torlontano M. Age influences TSH serum levels after withdrawal of l-thyroxine or rhTSH stimulation in patients affected by differentiated thyroid cancer. *Biomed Pharmacother* 2007;61:468-471.



Recurrence Incidence in Differentiated Thyroid Cancers and the Importance of Diagnostic Iodine-131 Scintigraphy in Clinical Follow-up

Diferansiye Tiroit Karsinomunda Rekürrens Sıklığı ve Klinik İzlemde Tanısal İyot-131 Sintigrafisinin Önemi

Filiz Hatipoğlu¹, İnanç Karapolat¹, Özgür Ömür², Ayşegül Akgün², Ahmet Yanarates³, Kamil Kumanlioğlu²

¹Şifa University Faculty of Medicine, Department of Nuclear Medicine, İzmir, Turkey

²Ege University Faculty of Medicine, Department of Nuclear Medicine, İzmir, Turkey

³İzmir Dr. Suat Seren State Hospital, Clinic of Nuclear Medicine, İzmir, Turkey

Abstract

Objective: Differentiated thyroid cancers (DTC) are tumors with good prognosis. However, local recurrence or distant metastasis can be observed. In our study, we aimed to investigate the incidence of recurrence and the importance of diagnostic iodine-131 whole body scan (WBS) in clinical follow-up in patients with DTC.

Methods: The clinical data of 217 patients with DTC who were followed-up more than 3 years were reviewed retrospectively. The incidence of recurrence was investigated in a group of patients who had radioactive iodine (RAI) treatment and showed no sign of residual thyroid tissue or metastasis with diagnostic WBS that was performed at 6-12 months after therapy and had a thyroglobulin (Tg) level lower than 2 ng/dl.

Results: At the time of diagnosis, ten cases had thyroid capsule invasion, 25 cases had extra-thyroid soft tissue invasion, 11 patients showed lymph node metastasis and four patients had distant organ metastasis. One hundred forty-five patients had RAI treatment at ablation dose (75-100 mCi), whereas 35 patients had RAI treatment at metastasis dose (150-200 mCi). Thirty-seven patients with papillary microcarcinoma did not receive RAI treatment. In 12 (7.5%) of the 160 patients who were considered as "successful ablation", a recurrence was identified. Recurrence was detected by diagnostic WBS in all cases and stimulated Tg level was <2 ng/dL with the exception of the two cases who had distant metastasis.

Conclusion: Identification of pathological findings with WBS in patients who developed local recurrence in the absence of elevated Tg highlights the importance of diagnostic WBS in clinical follow-up.

Keywords: Differentiated thyroid cancer, recurrence, iodine-131 scintigraphy

Öz

Amaç: Diferansiye tiroit karsinomları (DTK) iyi prognoza sahip tümörlerdir. Ancak lokal rekürrens ve uzak metastaz izlenebilmektedir. Çalışmamızda DTK'lı olgularda rekürrens sıklığının ve tanısal iyot-131 (I-131) tüm vücut tarama sintigrafisinin klinik izlemdeki öneminin araştırılması amaçlandı.

Yöntem: İzlem süresi 3 yılın üzerinde olan iki yüz on yedi DTK'lı olgunun klinik verileri retrospektif olarak incelendi. Radyoiyot (RAI) tedavisi alan hastalardan tedavi sonrası 6. ay-1. yıl tanısal I-131 tarama sintigrafisinde rezidüel tiroit dokusu ve metastaza ait bulgu saptanmayan, tiroglobulin (Tg) düzeyi 2 ng/dl'nin altında olan grupta rekürrens sıklığı araştırıldı.

Bulgular: Tanı anında on olguda tiroit kapsülü, 25 olguda ekstratiroidal yumuşak doku invazyonu, 11 hastada lenf nodu metastazi ve dört hastada uzak metastaz mevcuttu. Yüz kırk beş olgu ablasyon dozunda (75-100 mCi), 35 olgu metastaz dozunda (150-200 mCi) RAI tedavisi almıştı. Papiller mikrokarsinom tanılı 37 hasta ise RAI tedavisi almamıştı. Tedavi başarısına karar verilen 160 hastanın 12'sinde rekürrens hastalık saptandı (7,5%). Olguların tümünde rekürrens I-131 tarama sintigrafisi

Address for Correspondence: Filiz Hatipoğlu MD, Şifa University Faculty of Medicine, Department of Nuclear Medicine, İzmir, Turkey
Phone: +90 533 378 53 37 E-mail: karagozfiliz@yahoo.com **Received:** 14.08.2015 **Accepted:** 11.01.2016

ile saptanmış olup uzak metastazı olan iki hasta dışında stimüle Tg değerleri <2 ng/dL idi.

Sonuç: Lokal rekürrens gelişen tüm olgularda stimüle Tg yüksekliği olmaksızın I-131 tarama sintigrafisi ile patolojik bulguların saptanması klinik izlemde tanısız I-131 taramanın önemini vurgulamaktadır.

Anahtar kelimeler: Diferansiyel tiroit karsinomu, rekürrens, iyot-131 sintigrafisi

Introduction

Differentiated thyroid cancers (DTC) is a group of tumors with slow growth potential (1); long survival and a good clinical outcome is common, even in a patient with metastasis, when they are adequately treated with effective therapeutic approaches such as surgery, radioactive iodine (RAI) and thyroid hormone suppression (2). The 10-year survival rate in these tumors with good prognosis is above 90%. Nevertheless, local-regional recurrence or distant metastasis, especially in the first year of diagnosis, can be observed in 20% and 5-10% of the cases, respectively (3). Even though indicators of treatable recurrences and detrimental progress usually manifest within the first 5-10 years, life-long follow-up is critical since late mortality and recurrence is not uncommon (4). Traditionally, patients are followed-up according to prognostic factors, serum thyroglobulin (Tg) level and ultrasound (US) findings, anti-Tg antibody (anti-T) measurements along with concurrent whole body scintigraphy with I-131 (I-131 WBS) following thyroid stimulating hormone (TSH) stimulation at 6-12 months after surgery and ablation (5). The cervical US, serum Tg, and I-131 WBS are powerful tools to detect recurrence. Additional information can be achieved by computed tomography (CT) and magnetic resonance imaging (MRI) (6). Although I-131 scanning has a very high specificity of 99-100%, the rate of I-131-positive recurrences is about 50-60% in papillary and 64-67% in follicular thyroid cancer. In patients with I-131 negative recurrence, in addition to conventional radiologic imaging modalities, F-18 fluorodeoxyglucose (FDG) positron emission tomography (PET) and somatostatin receptor scintigraphy may yield significant information in detecting recurrence and metastasis (7). The aim of this study was to calculate the incidence of recurrence and explore which diagnostic tool was more reliable in detecting recurrence in patients with DTC.

Materials and Methods

Patients

We retrospectively reviewed clinical data pertaining to 217 patients [35 males (16%) and 182 females (84%)] who presented to the Department of Nuclear Medicine, Faculty of Medicine, Ege University with post-surgery DTC between 1991 and 2006, and regularly attended follow-up control visits for a period of 3 to 22 years. Ablation was deemed successful in patients who received RAI therapy after

surgery, did not show any sign of residual thyroid tissue or metastasis on diagnostic I-131 WBS performed 6-12 months after RAI therapy, and had serum Tg level <2 ng/dL in the stimulated period. Recurrence was defined as detection of a tumor in the thyroid bed, cervical lymph nodes or in distant organs. When recurrence was identified, diagnostic I-131 WBS, serum Tg level, and US findings were assessed and compared, while all clinical data of the patients were reviewed. A detailed information was given to all patients before the procedure to be applied and all patients signed informed consent forms. Ethics committee approval was not received due to the retrospective design of the study.

Radioactive Iodine Treatment and Follow-Up Protocol

For RAI treatment, TSH stimulation was induced after all patients were instructed not to use thyroid hormone replacement after thyroid surgery or to stop using the medication at least 4 weeks before therapy if thyroid hormone replacement had already been started. Before RAI treatment, patients were given a low-iodine diet for at least 2 weeks and asked not to use any medication or radiographic contrast agent that would decrease radioiodine uptake. Once TSH level was above 30 μ U/mL, 75-100 mCi I-131 was given per-orally for ablation, 150-175 mCi for extra-thyroid soft tissue invasion and lymph node metastasis, and 175-200 mCi for distant metastasis. I-131 WBS was performed on day 10 after RAI treatment, and diagnostic I-131 WBS was carried out under TSH stimulation with concurrent serum Tg, anti-T and TSH measurements by immunoradiometric assay method at approximately 6, 12, 18, 60 (5 years), 120 (10 years) and 180 months (15 years). Prior to diagnostic I-131 WBS, all patients were given a low-iodine diet for 2 weeks and asked to refrain using any medication or radiographic contrast agent that would decrease radioiodine uptake. Patients stopped using L-thyroxine hormone 6 weeks before the scan and used T3 in the first 4 weeks instead. In the last 2 weeks, TSH stimulation was induced by terminating T3, rendering endogenous TSH level to exceed 30 μ U/mL. For diagnostic I-131 WBS, 5 mCi I-131 was given orally following TSH stimulation, and anterior and posterior projection images were acquired after 48 hours. The post-treatment and diagnostic I-131 scans were carried out using dual-head gamma camera (Infinia, General Electric Medical Systems) equipped with high-energy parallel-hole collimators. Patients were imaged in the supine position. A 10% energy window around the 364 keV energy peak of I-131 was used. In addition, annual US was carried out throughout

the follow-up period and patients were assessed by other imaging modalities when necessary.

Statistical Analysis

All statistical analyzes were carried out using "SPSS 13.0 for Windows" (SPSS, Inc., Chicago, IL., USA) statistical software. Descriptive statistics of the patients are presented as mean±standard deviation and/or median (minimum-maximum).

Results

The mean age of the 217 patients, 182 females (84%) and 35 males (16%), was 52.17±13.18 years, and the mean follow-up period was 6.26±3.0 years. All patients had either total or near-total thyroidectomy. Postoperative histopathologic examination showed follicular cancer in 32 (14.7%) and papillary cancer in 185 (85.3%) cases. The mean tumor diameter was 1.84±1.47 cm. At the time of diagnosis; 10 cases had thyroid capsule invasion (4.6%), 25 had extra-thyroid soft tissue invasion (11.5%), 11 had lymph node metastasis (5.1%), and 4 had distant metastasis (1.8%). One hundred forty-five cases (66.8%) received RAI therapy at ablation dose (75-100 mCi) while 35 cases (16.1%) had RAI therapy at metastasis dose (150-200 mCi). Thirty-seven cases (17.1%) diagnosed with papillary microcarcinoma with a tumor size smaller than 1 cm did not receive RAI therapy. Treatment was considered successful in 160 cases when diagnostic I-131 WBS performed at 6-12 month post-therapy did not show abnormal I-131 uptake in the thyroid bed or any other region, and the stimulated serum Tg level was lower than 2 ng/dl. During follow-up of these patients who were considered as "successful ablation", I-131 WBS revealed local recurrence in 10 and distant metastasis in two patients. Recurrence was detected at years 12 and 16 in patients who had distant metastasis, and within the first 5 years in the ten patients who had a local recurrence (earliest 3rd year). Of these 12 patients, nine were female (75%) and three were male (25%), with a mean age of 53.33±13.46 years and a mean tumor size of 1.62±0.83 cm at the time of diagnosis. Of these twelve patients, one patient (8.3%) was followed-up for follicular and 11 patients (91.7%) for papillary thyroid cancer. One patient had extra-thyroid soft tissue invasion, and two patients had thyroid capsule invasion. During the 6-12 months follow-up period of these patients, Anti T was negative and with the exception of the two patients who had distant metastasis the stimulated Tg was <2 ng/dl. The median value of stimulated Tg was 0.2 ng/dL (minimum 0.01 ng/dL and maximum 1.1 ng/dl). I-131 WBS identified a recurrence in all these patients (Figure 1). At year 16, stable nodules found in thoracic CT images of a patient who had high Tg level (56 ng/dl) and right-sided pathologic pulmonary uptake on I-131 WBS were not interpreted as recurrence, but F-18 FDG-PET scan performed in the same year reported metastasis to the right lung. In another patient, increased

activity in the right upper thoracic region was found on I-131 WBS at year 12 as a result of newly developed bone metastasis to the scapula (Figure 2). The bone metastasis was confirmed by MRI. Both cervical US and I-131 WBS

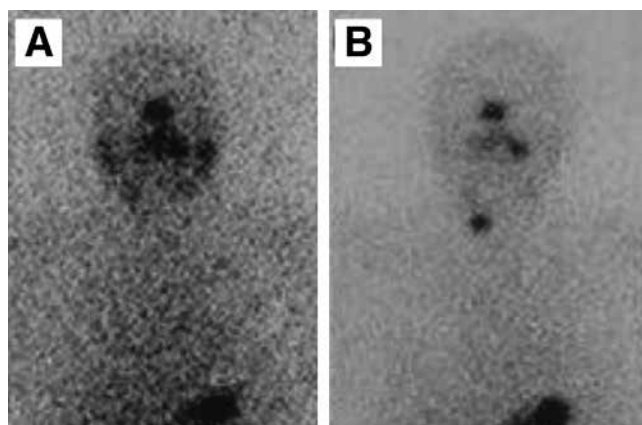


Figure 1. Depicted post-therapeutic and follow up I-131 whole-body scintigraphy images of a 41-year old female patient operated for papillary thyroid cancer and received 150 mCi radioactive iodine treatment. A) I-131 whole-body scintigraphy performed at 6 months post-radioactive iodine treatment showing no activity in the cervical region consistent with ablation, B) I-131 whole-body scintigraphy of the same patient performed 5 years after radioactive iodine treatment revealing increased focal activity in the right lobe of thyroid consistent with recurrent malignancy (stimulated serum thyroglobulin level of the patient during this period was 1.02 ng/dl)

Table 1. Clinical data in patients with differentiated thyroid cancers (n=217)

Clinical data	n=217
Age (year, mean±SD)	52.17±13.18
Gender (F/M)	182/35
Mean follow-up period (year, mean±SD)	6.26±3.0
Postoperative histopathologic examination (follicular/papillary, n, %)	32 (14.7)/185 (85.3)
Mean tumor diameter (cm, mean±SD)	1.84±1.47
Thyroid capsule invasion (n, %)	10 (4.6%)
Extra-thyroid soft tissue invasion (n, %)	25 (11.5%)
Lymph node metastasis (n, %)	11 (5.1%)
Distant metastasis (n, %)	4 (1.8%)
RAI therapy protocol (n, %)	
Ablation dose (75-100 mCi)	145 (66.8%)
Metastasis dose (150-200 mCi)	35 (16.1%)
Recurrence (n, %)	12 (7.5%)
Local recurrence	10
Distant metastasis	2

Descriptive statistics of the patients are presented as mean±standard deviation, DTC: Differentiated thyroid cancers, RAI: Radioactive iodine, SD: Standard deviation, F: Female, M: Male

revealed residual thyroid tissue in five patients with local recurrence, otherwise cervical US did not show any significant sign of recurrence while I-131 WBS revealed residual thyroid tissue in the other five patients with local recurrence. The frequency of recurrence in DTC patients was calculated as 7.5%. The clinical data of the patients with DTC are summarized in Table 1.

Discussion

DTC comprise more than 90% of all primary thyroid cancers. The ten-year survival rate in DTC is reported as 80-95% (8); this rate is determined as 57% even in patients with pulmonary metastasis (9). However, a persistent or recurrent disease can be found in 5-24% of patients despite slow-growth and good prognosis (8). In the present study, the frequency of recurrence was calculated as 7.5%. The frequency of recurrence in low-risk DTC patients in the literature is stated as 0.5-0.6% (10). In a study, the most common type of recurrence was regional recurrence (53%), followed by local (28%), distant (13%) and combined (6%) recurrences (11). In the present study, the number of patients with local recurrence was higher than those with distant metastasis.

In tumor node metastasis classification, the presence of a positive lymph node in a DTC patient aged 45 years and above is an independent risk factor for recurrence though it has been reported that mortality rate is not affected by this parameter. Numerous researchers argued that recurrence rate was related to the number and localization of positive lymph nodes (12,13). For instance, a positive lymph node in the lateral compartment is associated with a significantly higher recurrence rate and shorter recurrence time as compared to a node in the central compartment (14).

Even though lymph node metastasis was present in 5.1% of patients in our study group, none of the patients who developed recurrence had lymph node metastasis at the time of diagnosis. Due to the limited number of subjects in the research group, we were unable to compare the recurrence rates between patients with and without lymph node metastasis. Palme et al. (15) argued that male sex, advanced stage at diagnosis and extra-thyroid dissemination were independent determinants of DTC recurrence. Mazzaferri and Kloos (16) reported that the frequency of recurrence of papillary thyroid cancer was higher when patients were 20 years old or younger in comparison to 20-59-year-old patients. The effects of histologic type, tumor size, age and sex on persistent or recurrent disease in well-DTC have been investigated in a retrospective study covering the period 1979-2007. In contrast to previous studies, authors of this study argued that tumor size or sex was not a determinant of recurrence while age had a prognostic value in patients with radio-iodine treatment following total or near-total thyroidectomy (17). We were unable to establish whether a statistically significant difference existed between the patients who developed recurrence and the general group in terms of age, sex, tumor size, extra-thyroid involvement since the number of subjects was limited. However, the male/female ratio was higher in our patient group who developed recurrence.

Treatment of DTC includes total thyroidectomy, ablation with RAI, and suppression with L-thyroxine (18). Even after a successful initial treatment, the manifestation of clinical recurrence in as many as 20% of patients, and the disease-related mortality rate of 50-60% in patients with recurrence following curative treatment highlight the importance of life-long follow-up (19). I-131 WBS and serum Tg measurements with or without TSH stimulation

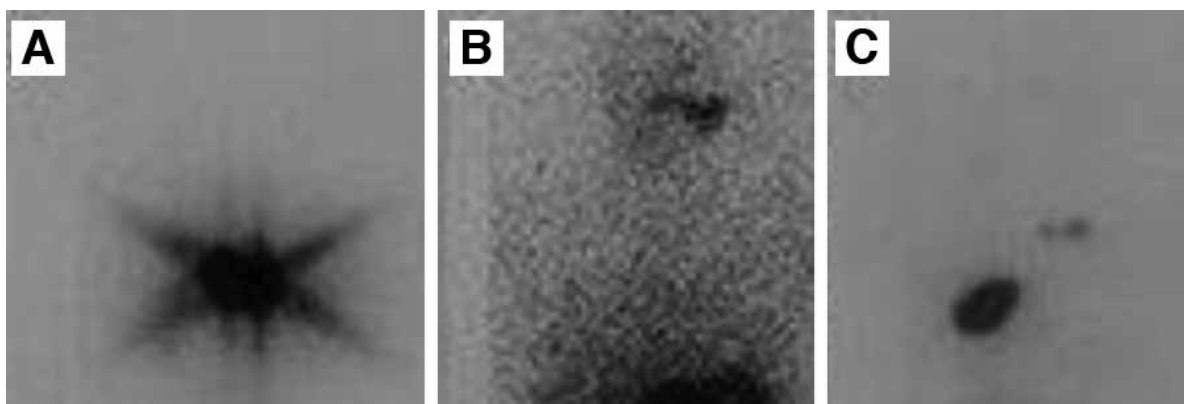


Figure 2. Shows post-therapeutic and follow up I-131 whole-body scintigraphy images of a 55-year old male patient operated for follicular thyroid cancer and received 100 mCi radioactive iodine treatment. A) I-131 whole-body scintigraphy performed 10 days after radioactive iodine therapy displayed high activity in the cervical region by residual tissue, B) I-131 whole-body scintigraphy of the same patient performed at 6 months after radioactive iodine therapy showed no activity consistent with ablation of residual tissue, C) I-131 whole-body scintigraphy of the same patient performed about 12 years after radioactive iodine treatment revealed increased focal activity in the thyroid bed consistent with recurrent malignancy, as well as intense uptake in the right upper thoracic region as a result of newly developed bone metastasis to the scapula (stimulated serum thyroglobulin level of the patient during this period was 187 ng/dl)

are the most commonly used methods to follow-up DTC patients after surgery and ablation treatment. Furthermore, at follow-up visits, US of the central compartment and regional lymph nodes along the cervical chain need to be carried out periodically, at postoperative 6 and 12 months and afterward, depending on the individual risk of recurrent disease (5). Tg is a glycoprotein specific to differentiated thyroid tissue. Stimulated serum Tg level ≥ 2.5 ng/dL after thyroidectomy and radioiodine ablation in anti-T negative patients indicates the persistence of thyroid tissue or recurrence (20). However, a recurrent and metastatic disease cannot be detected by serum Tg measurement alone in 10% of the cases (21). Another method to detect recurrent or metastatic disease is I-131 WBS (4). Metastatic or recurrent cancers can concentrate as much as 80% iodine. I-131 WBS enables detection of recurrence before clinical signs are evident (22). In the present study, with the exception of two patients with distant metastasis, stimulated Tg values of all patients who had recurrence were lower than 2 ng/dl, and recurrence was identified by I-131 WBS during standard follow-up evaluation. However, since the negative predictive value of undetected stimulated serum Tg measurement is 100%, some authors suggested that I-131 WBS did not yield further information in addition to Tg measured under stimulation in high-risk patients while some authors did not recommend I-131 WBS in low-risk patients at all (5,23). In routine practice, I-131 WBS is recommended in anti-T positive patients (23). I-131 WBS has a high specificity rate in demonstrating recurrences though a third of the patients with recurrence lose iodine avidity (24). In such patients, US is especially preferred to assess lateral and central cervical compartments. The sonographic examination is helpful in terms of local-regional recurrence observed in as many as 20% of patients with thyroid cancer. Studying a series of patients with recurrence in the thyroid bed, Frasoldati et al. (25) reported that US was more sensitive in detecting recurrence than serum Tg level and I-131 WBS. In this study, Tg level measurement after cessation of T4 by immunoradiometric assay, I-131 WBS, and US have been carried out in an attempt to compare their results with histologic findings of fine needle aspiration biopsy, and the sensitivity of US has been calculated as 94.1%. Even though cervical US is one of the preferred methods in patients suspected of having a local recurrence, small lymph nodes may be overlooked due to post-operative granulomatous tissue, resulting in an inaccurate diagnosis. Lending support to this view, in our study, cervical US did not reveal any pathologic signs in 5 of the patients with local recurrence, as detected by I-131 WBS. For recurrent tumors that lose their iodine avidity, MRI, with very high soft tissue contrast capability, can be used to depict deep cervical and mediastinal lymph nodes since US may be insufficient due to limitations in the mediastinum and bony structures. MRI cannot replace I-131 WBS, which is the standard procedure, but it has high specificity and

accuracy, especially in the mediastinum, in detecting nodal recurrence of tumors that lose their iodine avidity (26). In conclusion, it should be kept in mind that reactive changes that develop in the cervical region after thyroidectomy and RAI may hinder assessment and that the diagnostic method should be chosen according to the clinical condition of the patient. Even though the specificity of I-131 WBS is high, radioiodine positive recurrence rate is 50-60% in papillary and 64-67% in follicular thyroid cancer. In addition to MRI and cervical US, other imaging modalities such as abdominal US, bone scintigraphy, CT, and F-18 FDG PET should be employed in DTC patients with negative I-131 WBS and high serum Tg levels. F-18 FDG PET is capable of showing local recurrences as well as distant metastasis (27). Other nuclear medicine techniques that can be used to examine recurrence or metastatic focus in high-risk patients include WBS with Tl-201, Tc-99m sestamibi, and Tc-99m tetrofosmin, but the low spatial resolution associated with these techniques reduce detection of recurrence or metastasis by 25%. With a capacity of producing high-resolution images and depicting anatomic localization, F-18 FDG PET/CT stand at the forefront of these techniques. In a study on DTC patients with known or suspected recurrent disease, Middendorp and coworkers (7) examined the efficacies of F-18 FDG PET and Ga-68 DOTATOC under TSH suppression and I-131 WBS with TSH stimulation. They found that the performances of Ga-68 DOTATOC and F-18 FDG PET in radioiodine positive patients were comparable, while detection efficacy of F-18 FDG PET in radioiodine-negative patients was much higher. The authors concluded that their results needed to be supported by studies with larger series of patients and that, when recurrence is suspected, in the absence of a pathologic sign with I-131 WBS or F-18 FDG PET, Ga-68 DOTATOC PET could yield valuable information.

Conclusion

We conclude that in patients with suspicion of DTC recurrence I-131 WBS is an important imaging modality that should be used, but that it can be complemented by other imaging modalities depending on the clinical condition of the patient. Even though F-18-FDG PET/CT can be used in patients with high Tg but negative I-131 WBS, we recommend obtaining I-131 WBS in conjunction with F-18 FDG PET/CT to detect recurrence when foci with or without iodine avidity co-exist.

Ethics

Ethics Committee Approval: Ethic committee approval was not received due to a retrospective study.

Informed Consent: Consent form was filled out by all participants.

Peer-review: Externally peer-reviewed.

Authorship Contributions

Concept: Özgür Ömür, Kamil Kumanlioğlu, Design: Özgür Ömür, Ayşegül Akgün, İnanç Karapolat, Data Collection or Processing: Filiz Hatipoğlu, Ahmet Yanarates, Analysis or Interpretation: Filiz Hatipoğlu, Literature Search: Filiz Hatipoğlu, Writing: Filiz Hatipoğlu.

Conflict of Interest: No conflict of interest was declared by the authors.

Financial Disclosure: The authors declared that this study has received no financial support.

References

1. Sciuto R, Romano L, Rea S, Marandino F, Sperduti I, Maini L. Natural history and clinical outcome of differentiated thyroid carcinoma: A retrospective analysis of 1503 patients treated at a single institution. *Ann Oncol* 2009;20:1728-1735.
2. Sampson E, Brierley JD, Le LW, Rotstein L, Tsang RW. Clinical management and outcome of papillary and follicular (differentiated) thyroid cancer presenting with distant metastasis at diagnosis. *Cancer* 2007;110:1451-1456.
3. Stokkel MP, Duchateau CS, Dragoiescu C. The value of FDG PET in the follow-up of differentiated thyroid cancer: A review of the literature. *Q J Nucl Med Mol Imaging* 2006;50:78-87.
4. de Meer SG, Vriens MR, Zelissen PM, Rinkes IHB, de Keizer B. The role of routine diagnostic radioiodine whole-body scintigraphy in patients with high-risk differentiated thyroid cancer. *J Nucl Med* 2011;52:56-59.
5. American Thyroid Association (ATA) Guidelines Taskforce on Thyroid Nodules and Differentiated Thyroid Cancer, Cooper DS, Doherty GM, Haugen BR, Kloos RT, Lee SL, Mandel SJ, Mazzaferri EL, McIver B, Pacini F, Schlumberger M, Sherman SI, Steward DL, Tuttle RM. Revised American Thyroid Association management guidelines for patients with thyroid nodules and differentiated thyroid cancer. *Thyroid* 2009;19:1167-1214.
6. Bachelot A, Cailleux AF, Klain M, Baudin E, Ricard M, Bellon N, Caillou B, Travagli JP, Schlumberger M. Relationship between tumor burden and serum thyroglobulin level in patients with papillary and follicular thyroid carcinoma. *Thyroid* 2002;12:707-711.
7. Middendorp M, Selkinski I, Happel C, Kranert WT, Grünwald F. Comparison of positron emission tomography with (F18) FDG and (68)Ga DOTATOC in recurrent differentiated thyroid cancer: Preliminary data. *Q J Nucl Med Mol Imaging* 2010;54:76-83.
8. Schlumberger MJ. Papillary and follicular thyroid carcinoma. *N Engl J Med* 1998;338:297-306.
9. Schlumberger M, Tubiana M, De Vathaire F, Hill C, Gardet P, Travagli JP, Fragu P, Lumbroso J, Caillou B, Parmentier C. Long-term results of treatment of 283 patients with lung and bone metastases from differentiated thyroid carcinoma. *J Clin Endocrinol Metab* 1986;63:960-967.
10. Gerrard GE, Mason MT. The recurrence rate for low-risk differentiated thyroid cancer is extremely low (0.5% after more than 5 years of follow-up). *Clin Oncol (R Coll Radiol)* 2011;23:374-375.
11. Coburn M, Teates D, Wanebo HJ. Recurrent thyroid cancer. Role of surgery versus radioactive iodine (I-131). *Ann Surg* 1994;219:587-593.
12. Ito Y, Tomoda C, Urano T, Takamura Y, Miya A, Kobayashi K, Matsuzuka F, Kuma K, Miyauchi A. Ultrasonographically and anatomopathologically detectable node metastases in the lateral compartment as indicators of worse relapse-free survival in patients with papillary thyroid carcinoma. *World J Surg* 2005;29:917-920.
13. Ito Y, Fukushima M, Tomoda C, Inoue H, Kihara M, Higashiyama T, Urano T, Takamura Y, Miya A, Kobayashi K, Matsuzuka F, Miyauchi A. Prognosis of patients with papillary thyroid carcinoma having clinically apparent metastasis to the lateral compartment. *Endocr J* 2009;56:759-766.
14. de Meer SG, Dauwan M, de Keizer B, Valk GD, Rinkes IH, Vriens MR. Not the Number but the location of lymph nodes matters for recurrence rate and disease-free survival in patients with differentiated thyroid cancer. *World J Surg* 2012;36:1262-1267.
15. Palme CE, Waseem Z, Raza SN, Eski S, Walfish P, Freeman JL. Management and outcome of recurrent well-differentiated thyroid carcinoma. *Arch Otolaryngol Head Neck Surg* 2004;130:819-824.
16. Mazzaferri EL, Kloos RT. Clinical review 128: Current approaches to primary therapy for papillary and follicular thyroid cancer. *J Clin Endocrinol Metab* 2001;86:1447-1463.
17. Leung AM, Dave S, Lee SL, Campion FX, Garber JR, Pearce EN. Factors determining the persistence or recurrence of well-differentiated thyroid cancer treated by thyroidectomy and/or radioiodine in the Boston, Massachusetts area: A retrospective chart review. *Thyroid Res* 2011;4:9.
18. Cady B, Rossi R, Silverman M, Wool M. Further evidence of the validity of risk group definition in differentiated thyroid carcinoma. *Surgery* 1985;98:1171-1178.
19. Loh KC, Greenspan FS, Gee L, Miller TR, Yeo PP. Pathological tumor-node-metastasis (pTNM) staging of papillary and follicular thyroid carcinomas: A retrospective analysis of 700 patients. *J Clin Endocrinol Metab* 1997;82:3553-3562.
20. Zanotti-Fregonara P, Keller I, Calzada-Nocaudie M, Al-Nahhas A, Devaux JY, Grassetto G, Marzola MC, Rubello D, Hindié E. Increased serum thyroglobulin levels and negative imaging in thyroid cancer patients: Are there sources of benign secretion? A speculative short review. *Nucl Med Commun* 2010;31:1054-1058.
21. Bolk JH, Bussemaker JK, Nieuwenhuijzen Kruseman AC, De Vijlder JJ, Goslings BM. Thyroglobulin measurements in the follow-up of patients with differentiated thyroid carcinoma: Comparison with quantitative radioactive iodine uptake measurements and total body scans. *Neth J Med* 1985;28:340-346.
22. Coburn M, Teates D, Wanebo HJ. Recurrent thyroid cancer. Role of surgery versus radioactive iodine (I131). *Ann Surg* 1994;219:587-593.
23. Pacini F, Schlumberger M, Dralle H, Elisei R, Smit JW, Wiersinga W; European Thyroid Cancer Taskforce. European consensus for the management of patients with differentiated thyroid carcinoma of the follicular epithelium. *Eur J Endocrinol* 2006;154:787-803.
24. Schlumberger M, Pacini F. *Thyroid tumors*, 3rd ed. Paris, France: Editions Nucleon, 2006.
25. Frasoldati A, Pesenti M, Gallo M, Caroggio A, Salvo D, Valcavi R. Diagnosis of neck recurrences in patients with differentiated thyroid carcinoma. *Cancer* 2003;97:90-96.
26. Mihailovic J, Prvulovic M, Ivkovic M, Markoski B and Martinov D. MRI versus ¹³¹I whole-body scintigraphy for the detection of lymph node recurrences in differentiated thyroid carcinoma. *AJR Am J Roentgenol* 2010;195:1197-1203.
27. Feine U, Lietzenmayer R, Hanke JP, Held J, Wöhrle H, Müller Schuenberg W. 18FDG whole body PET in differentiated thyroid carcinoma: Flipflop in uptake patterns of 18FDG and 131I. *Nuklearmedizin* 1995;34:127-134.



Hypermetabolic Calcified Lymph Nodes on ¹⁸F-fluorodeoxyglucose-Positron Emission Tomography/Computed Tomography in a Case of Treated Ovarian Cancer Recurrence: Residual Disease or Benign Formation?

Tedavi Edilmiş Over Kanseri Nüksünde ¹⁸Florodeoksiglikoz-Pozitron Emisyon Tomografisi/ Bilgisayarlı Tomografi ile Saptanan Hipermetabolik Kalsifiye Lenf Nodları: Rezidüel Hastalık mı? Benign Oluşum mu?

Alexandra Nikaki¹, Athanasios Alexopoulos², Fani Vlachou¹, Vasiliki Filippi³, Ioannis Andreou³, Vasiliki Rapti², Konstantinos Gogos¹, Konstantinos Dalianis¹, Roxani Efthymiadou³, Vassilios Prassopoulos¹

¹SA Hygeia Hospital, Clinic of Nuclear Medicine and PET/CT, Athens, Greece

²SA Hygeia Hospital, Clinic of Pathology and Oncology, Athens, Greece

³SA Hygeia Hospital, Clinic of Radiology and PET/CT, Athens, Greece

Abstract

The contribution of positron emission tomography/computed tomography (PET/CT) with ¹⁸F-fluorodeoxyglucose (FDG) in evaluating ovarian cancer recurrence even after a prolonged disease-free interval, and in therapy response is well-described. Calcifications observed in CT, although usually attributed to benign conditions, may actually represent active disease. Such an example of calcified formations is psammoma bodies. We present a case of 56-y. o. patient with ovarian cancer relapse at the supraclavicular area 18 years after complete response and disease-free interval. The patient received chemotherapy and underwent ¹⁸F-FDG-PET/CT for the evaluation of treatment response. Both CT corrected and uncorrected PET images showed hypermetabolism in the massively calcified lymph nodes in the neck, mediastinum, axilla and abdomen, indicative of active residual disease.

Keywords: ¹⁸F-fluorodeoxyglucose, ovarian cancer, lymph nodes

Öz

¹⁸Florodeoksiglikoz-pozitron emisyon tomografisi/bilgisayarlı tomografinin (¹⁸F-FDG PET/BT) over kanserinde tedavi yanıtını ve uzun bir hastaliksız aradan sonra nüksü değerlendirmede katkısı ortaya konulmuştur. Genellikle benign durumlara atfedilmesine rağmen BT’de gözlenen kalsifikasyonları aslında aktif hastalık bulgusu olabilir. Buna benzer kalsifiye oluşumlara bir örnek psammoma cisimleridir. Biz 56 yaşında, tedaviye tam yanıt ve 18 yıllık hastaliksız sağkalım sonrası supraklaviküler alanda nüks ile saptanan bir nüks over kanseri hastasını sunduk. Hasta kemoterapi aldı ve tedaviye cevabın değerlendirilmesi için ¹⁸F-FDG-PET/BT uygulandı. Hem düzeltilmiş hem düzeltilmemiş PET-BT görüntülerinde aktif rezidüel hastalığın göstergesi olarak boyun, mediastinum, koltuk altı ve karında kitlesel kalsifiye lenf düğümlerinde hipermetabolizma saptandı.

Anahtar kelimeler: ¹⁸F-florodeoksiglikoz, over kanseri, lenf düğümleri

Address for Correspondence: Alexandra Nikaki MD, SA Hygeia Hospital, Clinic of Nuclear Medicine and PET/CT, Athens, Greece
Phone: +900302106867810 E-mail: anikaki@gmail.com **Received:** 26.03.2014 **Accepted:** 22.11.2014

Introduction

About 30-50/100.000 women per year are diagnosed with ovarian cancer and half of the deaths related to female genital system malignancies are attributed to ovarian cancer (1). The most common histologic type of ovarian cancer is epithelial, and the most common subtype of epithelial cancer is serous adenocarcinoma. More indolent forms also exist that are no longer considered as malignant (2). The presence of microcalcifications in the primary tumor and although less common, in metastatic lesions, have been described in the literature (3,4). In cases of serous papillary cancer, the calcifications can be related to psammoma bodies' deposits (3,4). Calcification deposits depicted at computed tomography (CT) are more often attributed to benign conditions. Moreover, calcifications in the already identified malignant lymph nodes are considered as response to chemo and/or radiotherapy (5,6,7). However, calcified lymph nodes, even in the presence of extensive calcification, may be active and should not be ignored (3). The role of fludeoxyglucose-positron emission tomography/computed tomography (FDG-PET/CT) in restaging, evaluating therapy response in ovarian cancer, as well as its impact on management decisions for the patients is well-described and has been reviewed (1,8). Attenuation uncorrected images should be reviewed in order to avoid misinterpretation of calcifications. This case presentation demonstrates the utility of FDG-PET/CT in the evaluation of residual disease in large calcified lymph nodes in a patient who underwent chemotherapy for recurrent serous adenocarcinoma of the ovaries, 18 years after the initial diagnosis.

Case Report

A 56 year-old woman had been treated 18 years ago for ovarian cancer. The patient underwent hysterectomy along with surgical removal of the fallopian tube and ovaries due to cancer of the right ovary. Histologic examination was consistent with well-differentiated serous papillary cystadenocarcinoma of the right ovary with scattered moderate differentiation, and metastatic invasion of the left ovary. Eighteen years later, the patient presented with a mass at the left supraclavicular space, corresponding to an enlarged lymph node. The fine needle aspiration biopsy (FNAB) of the enlarged supraclavicular lymph node revealed recurrence of the previously treated serous adenocarcinoma. Epithelial cells of cylindrical shape in papillary clusters, psammoma bodies and foamy histiocytes were observed. The patient underwent CT of the neck, thorax, upper and lower abdomen for evaluation of disease extent. Lymph nodes were detected at the neck, including the left supraclavicular area, the mediastinum, the left axilla, the right paraaortic region, the right common iliac and external iliac vessels, as well as the right retrocrural space. The lymph nodes were enlarged and displayed

large amount of calcifications, while some of them were completely replaced by calcium depositions (Figure 1). The patient underwent chemotherapy with Taxol and Cisplatin (every 21 days) for three cycles, and Taxol and Carboplatin for the remaining three cycles, and was referred for evaluation of response to treatment. The CT revealed size reduction in the lymph nodes with progression of calcification at the previously described sites, with a density reaching up to ~900 HU in the calcified lymph nodes (Figure 2). The patient was referred for PET/CT examination for investigation of residual disease at the described lymph nodes and evaluation of treatment response six weeks after the last chemotherapy session. 50 minutes after intravenous administration of 362 MBq ¹⁸F-FDG, the PET/CT examination was performed by a Siemens Biograph



Figure 1. Enlarged calcified lymph nodes at the neck and the left supraclavicular region (A), the left axilla (B), the mediastinum (B), the retrocrural space on the right (C) and the paraaortic area (D) (arrows)

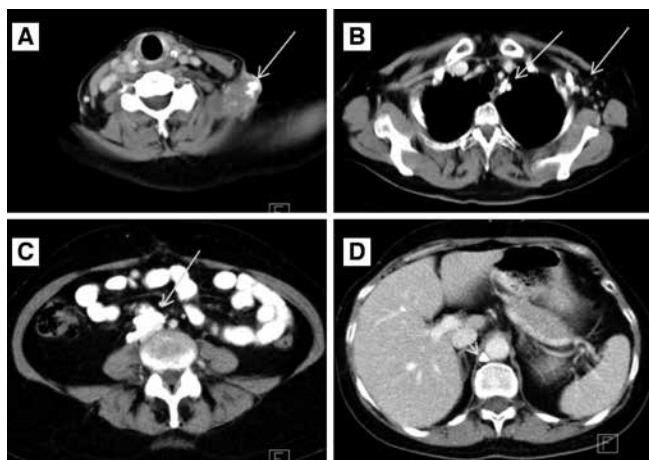


Figure 2. After 2 cycles of chemotherapy, the patient underwent computed tomography for evaluation of treatment response. Size reduction and presence of further calcification in the described lymph nodes were noted. Some of the lymph nodes were completely replaced by calcium depositions (A, B, C, D) (arrows)

LSO 16 sections device. Images were reconstructed at three levels, were corrected for attenuation and finally fused. Interpretation of PET/CT images was carried out by two experts (one nuclear medicine physician and one radiologist). Both corrected and uncorrected images were reviewed. Attenuation corrected FDG-PET/CT revealed hypermetabolism in all the described calcified lymph nodes, with a SUV_{max} ranging from 4.6 to 12.7, average SUV_{max} 8.78 (Figure 3). Uncorrected images also revealed active metabolic sites at all the described lymph nodes (Figure 4). The patient was referred for radiation treatment of the supraclavicular lymph node and was planned for close surveillance. On follow-up CT scans, additional calcifications were recognized in both the supraclavicular and the other lymph nodes. Follow-up fine needle aspiration of the still enlarged supraclavicular lymph node revealed metastasis from the known primary ovarian cancer, and the Magnetic Resonance Imaging revealed presence of another mass lesion of 5x3.5x3 cm size, which extended to the left axillary cavity. The patient underwent surgical removal of the supraclavicular lymph node and biopsy confirmed the diagnosis of metastasis and underlying multiple psammoma body deposits. After six months, the whole body CT revealed disease progression with multiple calcified lymph nodes as well as peritoneal implantation. A biopsy of the recently detected intra-tracheal mass confirmed the presence of new metastatic sites and moreover the presence of psammoma bodies. Based on the retrospective evaluation of patient's medical history, these calcifications were interpreted as psammoma bodies formations, which was also consistent with the more indolent course of the patient's disease.

Literature Review and Discussion

Although not the leading female genital cancer, half of the deaths related to female genital system malignancies are attributed to ovarian cancer (1,2). Risk factors associated with ovarian cancer include menstrual and hormonal exposure events, expression of oncogenes and tumor suppressor genes, gonadotropins and steroid hormones, growth factors, age, demographic and environmental factors (2,8). Necrosis is usually detected in more aggressive forms of serous ovarian carcinoma. Calcification in these regions can be related to either necrosis or hemorrhage (3), and therefore it can be mistaken for necrotic tissue. Evaluation of those lymph nodes by PET may reveal potential hypermetabolism, indicative of active disease rather than necrosis. A suspicion of recurrence is usually raised based on serum tumor marker CA-125 elevation, although any radiologic lesion may not be apparent at that given time. However, its accuracy of predicting cancer is quite limited, as in 36-73% of ovarian cancer cases the serum CA-125 levels remain within normal values (1). Relapse becomes less likely as disease-free interval increases, especially after 5-year disease-free surveillance (9). Our case presented with recurrence after an 18-year disease-free period. Excluding second-look laparotomy, CT is usually the initial imaging procedure once recurrence is suspected. CT is also the first imaging procedure performed for evaluation of therapy response. However, its diagnostic accuracy is limited both for the differentiation of residual fibrous tissue from active disease and for the evaluation of lymph nodes with benign characteristics, such as those with normal size (1). The role of FDG-PET/CT in re-staging, in assessing therapy response,

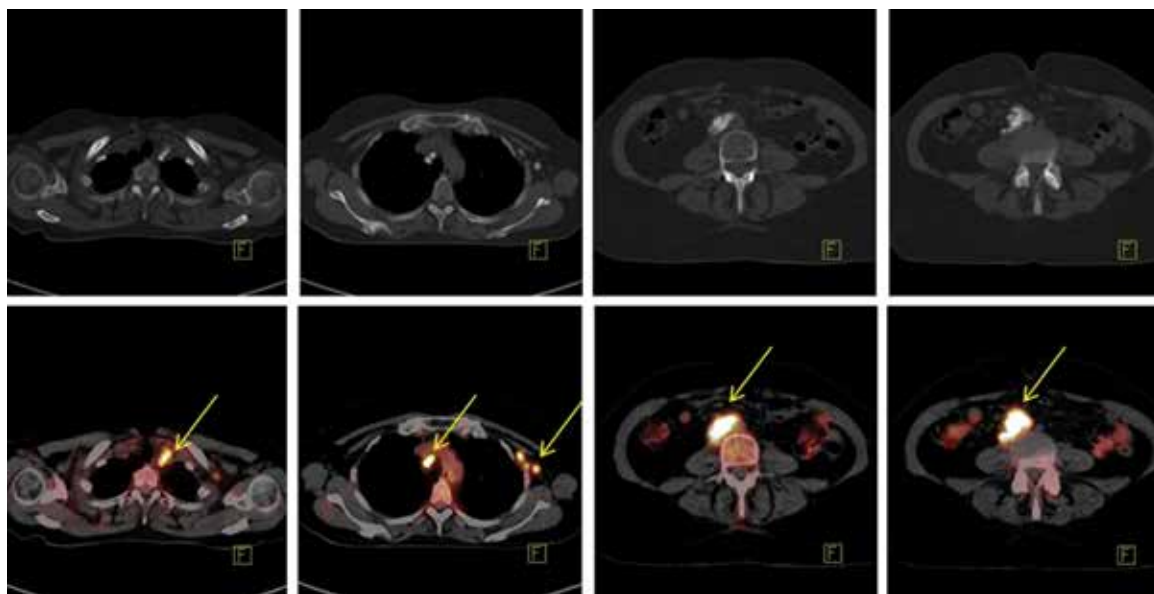


Figure 3. Calcified lymph nodes in the mediastinum and abdomen demonstrate high fludeoxyglucose uptake (arrows). Average $\text{SUV}_{\text{max}}=8.78$, highest $\text{SUV}_{\text{max}}=12.7$. Upper row: Calcifications as displayed by computed tomography (bone window). Lower row: Corresponding positron emission tomography/computed tomography images (soft tissue window)

as well as in altering the patient's management in suspicion of disease recurrence in ovarian cancer patients has been evaluated. The reported sensitivity, specificity, and accuracy rates in detecting suspected disease recurrence were reported as 74.2%, 90.9% and 82.6% for non-contrast enhanced CT (10). In another study, the accuracy of FDG-PET/CT for depicting recurrent tumor lesions according to anatomic localization was reported as 92% for the body, 96% for the chest, and 91% for the abdomen (11). Studies agree that PET/CT is more accurate than CT in detecting disease recurrence and reveal that it altered management decisions in over one third of patients (8,12). Lymph nodes with calcifications at CT are generally considered to be benign, with prior granulomatous disease being the most common etiology. It has been suggested that calcified mediastinal lymph nodes with high metabolic activity detected in NSCLC evaluation by PET/CT should not be necessarily considered as malignant, especially in countries where granulomatous diseases are endemic (5,13). Patterns of calcifications include amorphous, punctuate and linear types, and they can be detected either in the pre or post-therapy assessment, in primary and in metastatic lesions, either intra- or extra-abdominally (3,4,14,15). Calcification in ovaries is well described and is attributed to both neoplastic and non-neoplastic reasons (3,16). A few mechanisms have been proposed for the formation of calcifications such as hemorrhage, necrosis, mucinous degeneration, para-neoplastic syndrome and, most commonly in serous ovarian cancer, the formation of psammoma bodies. It is also suggested that tumor calcification in ovarian metastases is a dynamic process, independent of treatment effects, and therefore changes in calcification recognized on CT cannot be used as a marker of disease status (3). In our case, the calcified lymph nodes in the abdomen in the first pre-therapeutic CT examination

were interpreted as probably benign, and attention was only paid to the supraclavicular enlarged lymph node. The CT performed after treatment revealed reduction in lymph node size and increase of calcified deposits with alterations of their deposition pattern from punctuate to complete replacement, which were interpreted as response to therapy and raised the question whether these axillary, mediastinal and abdominal calcified lymph nodes were also malignant. A FDG-PET was performed in order to differentiate active and inactive lesions, which revealed hypermetabolic activity in all calcified lesions with an average SUV_{max} of 8.78, evidence of active tissue. However, the mechanism of FDG uptake in calcified lymph nodes containing psammomas is yet unclear. Calcification, as occurs with a metallic and opaque material, may cause false positive findings in FDG-PET/CT. Artifacts provoked by i.v. contrast agents, chemotherapy catheters, and other dense and opaque materials when using CT-based attenuation correction protocols have been described in the literature (5). On the other hand, such findings may obscure active nearby disease. In order to avoid misinterpretation, both CT corrected and uncorrected images were reviewed, and hypermetabolism was detected by both methods at all calcified sites. Increase in FDG uptake after treatment due to flare phenomenon, causing false positive results, has also been described after Tamoxifen or Bevacizumab therapy (17,18). To our knowledge, such an effect has not been described for lymph node calcifications. Furthermore, our patient was treated with Taxane and Platinum and PET/CT examination took place six weeks after the last chemotherapy treatment. Psammoma bodies are composed of lamellated calcified structures organized in a concentric manner, and can be detected both in neoplastic and non-neoplastic conditions (3,14,19,20). They are reported to be present in 15-30% of patients with ovarian serous cystadenocarcinoma (14). They are more common in primary tumors, and rare in metastatic lesions. The mechanism by which psammoma bodies are formed remains unclear. They are reported to result from dystrophic calcification, from calcium accumulation in degenerated or necrotic cells, or from collagen calcification. They are also likely to represent a biologic process which leads to degeneration of cancer cells, with consequent death and delay of tumor growth (14,19,21,22). This last proposition suggests that their formation is the cause of the indolent character they provide to neoplastic cells. More investigation is required to elucidate their exact nature, their formation mechanism, and whether they are the result or the cause of retardation of tumor growth in ovarian cancer. Although the exact mechanism of psammoma body formation is yet unclear, they are known to be associated with increased apoptotic cell death, BRAF mutation, and normal TP53 function, all of which are more profound in low-grade ovarian serous adenocarcinoma (22,23,24). FDG uptake can occur through inflammatory processes secondary to these mechanisms. However, cases of psammocarcinomas with a more aggressive course have

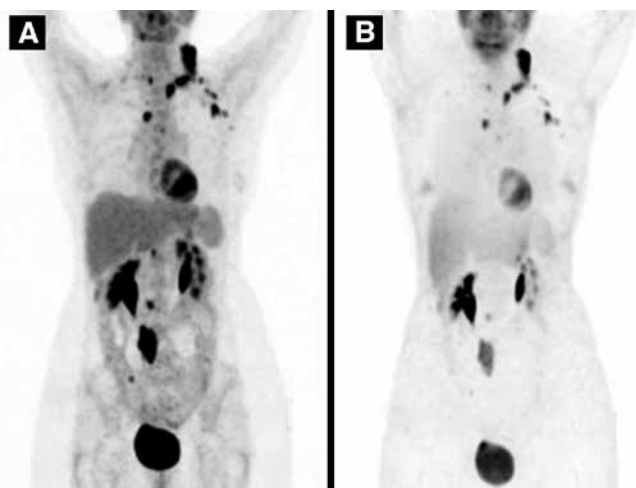


Figure 4. Both corrected (A) and uncorrected (B) images revealed high fludeoxyglucose uptake at the calcified lymph nodes, indicative of active disease

been described. Pyo et al. (25) demonstrated that psammoma deposits in papillary thyroid cancer are associated with multifocality and more extended disease. There are two distinct entities with regard to the deposition of psammomas in different carcinomas, carcinomas with psammoma bodies and psammocarcinomas. The latter arise from the ovaries or peritoneum, and certain criteria must be fulfilled in order to characterize a carcinoma with psammoma bodies as psammocarcinomas (22). Cases reported in the literature include primary psammocarcinomas of the ovary or peritoneum, or psammoma deposits in benign and malignant conditions such as serous adenocarcinoma of the ovaries, thyroid, meningioma, pancreas and calcifications in metastatic lesions (3,6,14,15,16,20,21,22,25,26). Our case displays the presence of psammoma bodies in metastatic lymph nodes diagnosed during ovarian cancer relapse after 18 years. Apart from CT imaging, calcified axillary lymph nodes due to psammoma body deposition have been described in other imaging modalities, such as mammography (27) and Tc-99m-methyl diphosphonate bone scan (15).

Conclusion

In conclusion, our case presentation has several remarkable characteristics. First, this case represents an ovarian serous carcinoma relapse after an 18-year disease-free interval. Second, it displays large calcified lymph nodes with increased density on CT images, which exhibit high FDG uptake in both attenuation corrected and uncorrected images, the last being evidence that increased FDG uptake is not an artifact. The formation of psammoma bodies could be suggested as a probable cause of calcification in this presented case. Similar to a previously described case, all sites of increased metabolic activity were considered as active tumor sites in the end.

Ethics

Informed Consent: All authors have filled in the informed consent.

Peer-review: External and Internal peer-reviewed.

Authorship Contributions

Surgical and Medical Practices: Vassilios Prassopoulos, Athanasios Alexopoulos, Roxani Efthymiadou, Fani Vlachou, Ioannis Andreou, Vassiliki Filippi, Vassiliki Rapti, Concept: Vassilios Prassopoulos, Athanasios Alexopoulos, Roxani Efthymiadou, Alexandra Nikaki, Design: Vassilios Prassopoulos, Athanasios Alexopoulos, Roxani Efthymiadou, Alexandra Nikaki, Data Collection or Processing: Vassilios Prassopoulos, Alexandra Nikaki, Athanasios Alexopoulos, Vassiliki Rapti, Analysis or Interpretation: Alexandra Nikaki, Athanasios Alexopoulos, Konstantinos Dalianis, Konstantinos Gogos, Literature

Search: Alexandra Nikaki, Athanasios Alexopoulos, Vassilios Prassopoulos, Roxani Efthymiadou, Fani Vlachou, Vassiliki Rapti, Writing: Alexandra Nikaki, Prassopoulos Vassilios, Athanasios Alexopoulos, Roxani Efthymiadou.

Conflict of Interest: No conflict of interest was declared by the authors.

Financial Disclosure: The authors declared that this study has received no financial support.

References

- Yen TC, Lai CH. Positron emission tomography in gynecologic cancer. *Semin Nucl Med* 2006;36:93-104.
- Cramer DW. The epidemiology of endometrial and ovarian cancer. *Hematol Oncol Clin North Am* 2012;26:1-12.
- Burkill GJ, Allen SD, A'hern RP, Gore ME, King DM. Significance of tumor calcification in ovarian carcinoma. *Br J of Radiol* 2009;82:640-644.
- Okada S, Ohaki Y, Inoue K, Kawamura T, Hayashi T, Kato T, Kumazaki T. Calcification in mucinous and serous cystic ovarian tumors. *J Nippon Med Sch* 2005;72:29-34.
- Mehta A, Mehta A, Laymon Ch, Blodgett T. Calcified Lymph Nodes Causing Clinically Relevant Attenuation Correction Artifacts on PET/CT Imaging. *J Radiol Case Rep* 2010;4:31-37.
- Grotenhuis BA, Wijnhoven BP, Hermans JJ, Biermann K, van Lanschot JJ. Fixed size of enlarged calcified lymph nodes in esophageal adenocarcinoma despite complete remission. *Case Rep Gastroenterol* 2009;3:182-186.
- Bluemke DA, Fishman EK, Kuhlman JE, Zinreich ES. Complications of radiation therapy: CT evaluation. *Radiographics* 1991;11:581-600.
- Lucignani G. FDG-PET in gynaecological cancers: recent observations. *Eur J Nucl Med Mol Imaging* 2008;35:2133-2139.
- Rubin SC, Randall TC, Armstrong KA, Chi DS, Hoskins WJ. Ten-year follow-up of ovarian cancer patients after second-look laparotomy with negative findings. *Obstet Gynecol* 1999;93:21-24.
- Kitajima K, Murakami K, Yamasaki E, Domeki Y, Kaji Y, Fukasawa I, Inaba N, Suganuma N, Sugimura K. Performance of integrated FDG-PET/contrast-enhanced CT in the diagnosis of recurrent ovarian cancer: comparison with integrated FDG-PET/non-contrast-enhanced CT and enhanced CT. *Eur J Nucl Med Mol Imaging* 2008;35:1439-1448.
- Sebastian S, Lee SI, Horowitz NS, Scott JA, Fischman AJ, Simeone JF, Fuller AF, Hahn PF. PET-CT vs. CT alone in ovarian cancer recurrence. *Abdomen Imaging* 2008;33:112-118.
- Soussan M, Wartski M, Chereil P, Fourme E, Goupil A, Le Stanc E, Callet N, Alexandre J, Pecking AP, Alberini JL. Impact of FDG PET-CT imaging on the decision making in the biologic suspicion of ovarian carcinoma recurrence. *Gynecol Oncol* 2008;108:160-165.
- Lee JW, Kim BS, Lee DS, Chung JK, Lee MC, Kim S, Kang WJ. ¹⁸F-FDG PET/CT in mediastinal lymph node staging of non-small-cell lung cancer in a tuberculosis-endemic country: consideration of lymph node calcification and distribution pattern to improve specificity. *Eur J Nucl Med Mol Imaging* 2009;36:1794-1802.
- Gontier E, Wartski M, Guinebretiere JM, Alberini JL. ¹⁸F-FDG PET/CT in a patient with lymph node metastasis from ovarian adenocarcinoma. *AJR Am J Roentgenol* 2006;187:285-289.
- Ozulker T, Ozulker F, Ozpacaci T. ^{99m}Tc-MDP and ¹⁸F-FDG uptake in calcified metastatic lesions from ovarian papillary serous adenocarcinoma. *Hell J Nucl Med* 2009;12:287-288.
- Pusiol T, Parolari AM, Pisciolli I, Morelli L, Del Nonno F, Licci S. Prevalence and significance of psammoma bodies in cervicovaginal smears in a cervical cancer screening program with emphasis on a case of primary bilateral ovarian psammocarcinoma. *Cytojournal* 2008;5:7.

17. Krupitskaya Y, Eslamy HK, Nguyen DD, Kumar A, Wakelee HA. Osteoblastic bone flare on F18-FDG PET in non-small cell lung cancer (NSCLC) patients receiving bevacizumab in addition to standard chemotherapy. *J Thorac Oncol* 2009;4:429-431.
18. Mortimer JE, Dehdashti F, Siegel BA, Trinkaus K, Katzenellenbogen JA, Welch MJ. Metabolic flare: indicator of hormone responsiveness in advanced breast cancer. *J Clin Oncol* 2001;19:2797-2803.
19. Das DK. Psammoma Body: a product of dystrophic calcification or of a biologically active process that aims at limiting the growth and spread of tumor? *Diagnostic Cytopathology* 2009;37:534-541.
20. Shih WJ, Wang AM, Domstad PA, Cho SR, DeLand FH. Intracranial meningioma with abnormal localization of bone-seeking radiopharmaceutical: correlation with gross and microscopic pathology. *Eur J Nucl Med* 1985;11:43-45.
21. Ohike N, Sato M, Kawahara M, Ohyama S, Morohoshi T. Ductal adenocarcinoma of pancreas with psammomatous calcification. Report of a case. *JOP* 2008;9:335-338.
22. Jain D, Akhila L, Kawatra V, Aggarwal P, Khurana N. Psammocarcinoma of ovary with serous custadenofibroma of contralateral ovary: a case report. *J Med Case Rep* 2009;3:9330.
23. Motohara T, Tashiro H, Miyahara Y, Sakaguchi I, Ohtake H, Katabuchi H. Long-term oncological outcomes of ovarian serous carcinomas with psammoma bodies: a novel insight into the molecular pathogenesis of ovarian epithelial carcinoma. *Cancer Sci* 2010;101:1550-1556.
24. Vang R, Shih leM, Kurman RJ. Ovarian low-grade and high-grade serous carcinoma: pathogenesis, clinicopathologic and molecular biologic features, and diagnostic problems. *Adv Anat Pathol* 2009;16:267-282.
25. Pyo JS, Kang G, Kim DH, Park C, Kim JH, Sohn JH. The Prognostic relevance of psammoma bodies and ultrasonographic intratumoral calcifications in papillary thyroid carcinoma. *World J Surg* 2013;37:2330-2335.
26. Zhen-Zhong D, Zheng N, Liu H, Liao DY, Ye XQ, Zhou QM, Jie, Li HH, Liu Q, Lu KM. Elevated CA125 in primary peritoneal serous psammocarcinoma: a case report and review of the literature. *BMJ Case Rep* 2009:2009.
27. Singer C, Blankstein E, Koenigsberg T, Mercado C, Pile-Spellman E, Smith SJ. Mammographic appearance of axillary lymph node calcification in patients with metastatic ovarian carcinoma. *AJR Am J Roentgenol* 2001;176:1437-1440.



Sentinel Lymph Node Detection by 3D Freehand Single-Photon Emission Computed Tomography in Early Stage Breast Cancer

Erken Evre Meme Kanserinde 3D Freehand Tek Foton Emisyon Bilgisayarlı Tomografi ile Sentinel Lenf Nodu Tespiti

Salih Sinan Gültekin^{1*}, Ahmet Oğuz Hasdemir², Serhat Tokgöz², Gülay Özgehan², Hakan Güzel², Cüneyt Yücesoy³, Emine Öztürk³, Ata Türker Ankök⁴

¹Dışkapı Yıldırım Beyazıt Training and Research Hospital, Clinic of Nuclear Medicine, Ankara, Turkey

²Dışkapı Yıldırım Beyazıt Training and Research Hospital, Clinic of Surgery, Ankara, Turkey

³Dışkapı Yıldırım Beyazıt Training and Research Hospital, Clinic of Radiology, Ankara, Turkey

⁴Dışkapı Yıldırım Beyazıt Training and Research Hospital, Clinic of Pathology, Ankara, Turkey

*Hacettepe University Kastamonu Faculty of Medicine, Department of Nuclear Medicine, Ankara, Turkey

Abstract

We herein present our first experience obtained by 3D freehand single-photon emission computed tomography (SPECT) (F-SPECT) guidance for sentinel lymph node detection (SLND) in two patients with early stage breast cancer. F-SPECT guidance was carried out using one-day protocol in one case and by the two-day protocol in the other one. SLND was performed successfully in both patients. Histopathologic evaluation showed that the excised nodes were tumor negative. Thus, patients underwent breast-conserving surgery alone.

Keywords: Breast cancer, sentinel lymph node biopsy, radionuclide tomography, single photon emission computed tomography, computer assisted three dimensional imaging, image guided surgery

Öz

Bu yazıda erken evre meme kanserli iki hastada sentinel lenf nodu tespiti (SLNT) için bilgisayarlı tek foton emisyonlu tomografisi (SPECT) 3D freehand SPECT (F-SPECT) rehberliği yoluyla edinilen ilk deneyimimizi sunuyoruz. F-SPECT rehberliği bu olguların birisinde tek gün protokolü diğerinde iki gün protokolü kullanılarak gerçekleştirildi. SLNT her iki hastada başarı ile gerçekleştirildi. Histopatolojik inceleme çıkarılan nodların tümör negatif olduğunu gösterdi. Hastalar bu sayede sadece meme koruyucu cerrahi geçirdiler.

Anahtar kelimeler: Meme kanseri, sentinel lenf nod biyopsisi, radyonüklid tomografi, bilgisayarlı tek foton emisyonlu tomografisi, bilgisayar destekli üç boyutlu görüntüleme, görüntü kılavuzluğunda cerrahi

Introduction

Breast surgery has evolved from radical mastectomy to minimally invasive procedures in time. Axillary node status is the main prognostic factor in the management of breast cancer patients. Nodal axillary involvement is shown in 10-30% of the cases with a T1 tumor, and in 45% of T2

tumors (1). Routine axillary lymph node dissection may cause additional risks such as lymphedema, persistent pain, and sensory impairment. Sentinel lymph node detection (SLND) allows information about the first nodal basin of lymphatic flow, and to decide whether axillary dissection by a minimally invasive approach is required or not. Currently, SLND is more favorable than routine axillary

Address for Correspondence: Salih Sinan Gültekin MD, Dışkapı Yıldırım Beyazıt Training and Research Hospital, Clinic of Nuclear Medicine, Ankara, Turkey
Phone: +90 533 761 49 91 E-mail: gultekinsinan@gmail.com **Received:** 23.11.2014 **Accepted:** 16.12.2014

Molecular Imaging and Radionuclide Therapy, published by Galenos Publishing.

node dissection in accordance with recent expert views (1,2,3). With the introduction of SLND concept, radio-guided surgery has become a popular technique in breast cancer patients (1,2,3). Preoperative lymphoscintigraphy and intraoperative detection methods (hand-held gamma probe or blue dye) with one-day or two-day protocols (4) have become widely used methods despite some limitations. Single photon emission computed tomography (SPECT)/computed tomography (CT) hybrid imaging could yield better results in certain cases (5). Today, research&development studies have recently focused on new imaging probes that contain an intraoperative counting probe integrated with a small-field-of-view gamma camera (5,6,7,8,9). In this paper, we present our first experiences for SLND in two early-stage breast cancer patients by using a three-dimensional (3D) freehand SPECT (F-SPECT) device (declipse SPECT®, SurgicEye, Munich, Germany).

Case Reports

Case 1

A 54-year-old postmenopausal woman was evaluated for a left-sided breast mass. A 14x11 mm mass located in the upper-middle part of the left breast with a breast imaging-reporting and data system (BI-RADS) 5 score was determined at breast ultrasound and mammography. The patient's cancer was staged as IA (T1N0M0). Preoperative lymphoscintigraphic images were obtained using a large field of view gamma camera (ECAM, Siemens, Illinois, USA) on anterior and oblique positions at 5, 30 and 60 min. following the periareolar-subdermal injection of ^{99m}Tc -labeled nano-colloid in a dose of 74 MBq/0.2 mL to the left breast. In the scintigraphic image, the two focal uptakes in nodal basin (Figure 1a) were considered as sentinel lymph nodes (SLNs). These foci were marked on skin in the left axillary region (Figure 1b). The patient

underwent 3D F-SPECT guided breast surgery with a two-day protocol. 24h after tracer injection, we scanned the breast and the axilla for a 2-4 min period in different directions (1 min each in the medial, dorsal and medial-dorsal directions) according to the procedure described by Wendler et al. (8). A sufficient count rate was determined by using a color code in green. The number and position of the sentinel nodes were observed on a computer screen and the completion of the surgical procedure was confirmed by repeat screenshots. 3D F-SPECT revealed two main radiotracer uptakes on the injection site (83%) and in the left level I axillary lymph nodes (17%) (Figure 1c). The lymphatic hot spot (mean count rate: 165 cps/s) was reached through a skin incision under the guidance of realtime 3D navigation definitions (Figure 2). After histological frozen section examination of the excised SLNs was reported as tumor negative, the procedure was completed with breast-conserving surgery with safe surgical margins (Figure 3). Final histopathology of the tumor revealed infiltrative ductal carcinoma.

Case 2

A 40-year-old premenopausal woman had a 21x15 mm mass in the upper-outer quadrant of her right breast compatible with BI-RADS 4c score on breast ultrasound and mammography. The patient was classified as Stage IIA (T2N0M0) breast cancer according to the imaging studies. A tru-cut biopsy was reported as infiltrative ductal carcinoma. Preoperative lymphoscintigraphy and F-SPECT guided surgery was performed using same radiotracer, injection and imaging techniques with the one-day protocol. Scintigraphic examination showed high nodal uptake in the right axillary region and this area was marked on the skin. 4 hours after radiotracer injection, breast surgery was started with the guidance of 3D F-SPECT imaging. The real-time image from 3D F-SPECT detected meaningful radiotracer uptakes in two hot spots on the injection site and the right



Figure 1. a) The lymphoscintigraphic image of the left breast on the left anterior oblique projection 30 min after radiotracer injection shows tracer accumulation in the injection site (long white arrow) and two adjacent axillary sentinel lymph nodes (short white arrow), b) The view of the operation theatre. Skin mark belonging to the sentinel lymph node is seen in the left axillary region, c) In the operating room, live video image shows two distinct radiotracer uptake foci in the injection site (rate: 83%, depth: 128 mm) and axillary region (rate: 17%, depth: 27 mm)

axilla. The hot spot which was located within the right level II axillary lymph nodes was accessed (mean count rate: 322 cps/s) and removed surgically. Frozen section evaluation revealed reactive lymph nodes that were tumor negative.

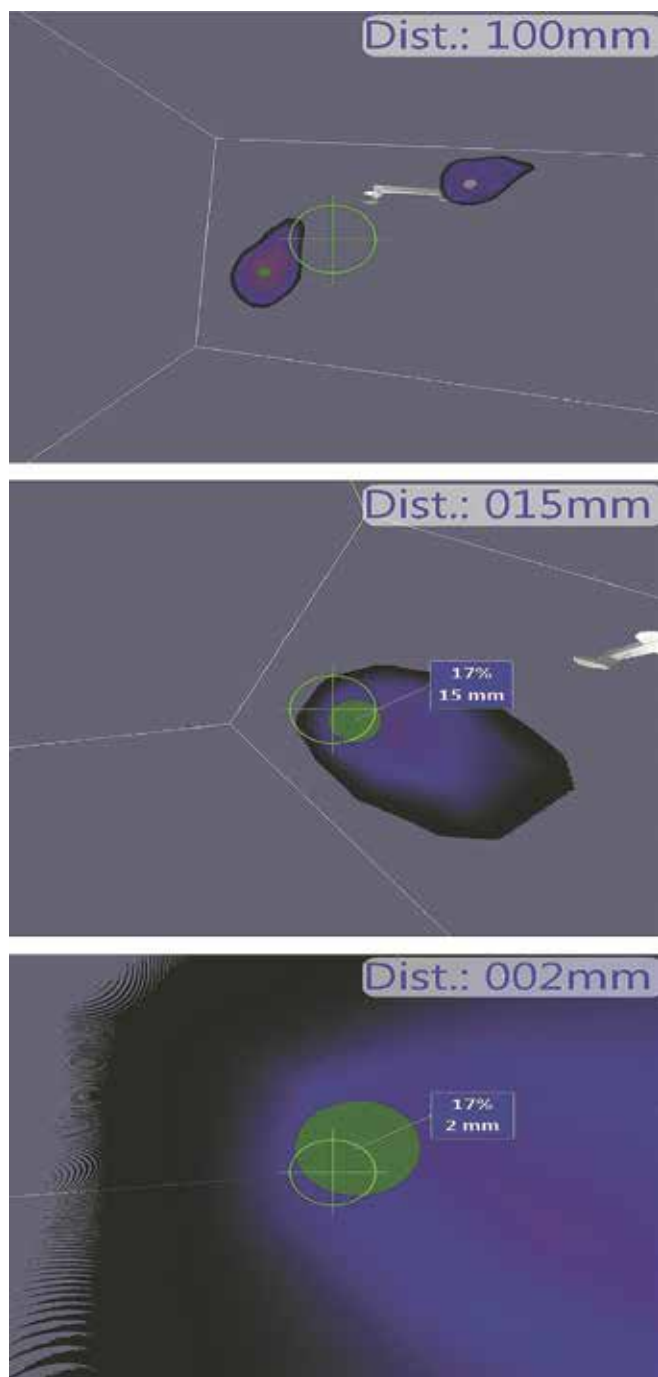


Figure 2. Three-dimensional navigation. The figure depicts the distance from the tip of the gamma navigation probe to the hot spot (respectively, top-down; 100 mm, 15 mm, 2 mm). Target sign defines the probe direction and optimal access path to the radioactive area

The surgeon completed the operation with breast-conserving surgery with safe surgical margins.

Literature Review and Discussion

Conventional nuclear medicine procedures have been reported to be useful for sentinel node detection (1,2). However, performance of the classical test for breast cancer showed a wide variation with a false-negative rate ranging from 0% to 29% as stated in a meta-analysis of 69 trials (10). The median false-negative rate was higher than 5% in all landmark studies with some inadequate results in special patient sub-groups (1,2,10,11). Therefore, researchers are trying to develop novel imaging tools and technology to improve these results. The introduction of portable gamma camera technology to clinical and experimental field enabled a rapid development. Mini gamma cameras, F-SPECT, and fluorescence imaging systems have been suggested for image-guided SLND. Mini gamma camera systems serve as a two-dimensional imaging modality. They were reported to contribute to the recognition of sentinel nodes settled in difficult anatomical areas or occult lesions (6,7). Others defended that these type of imaging systems had important limitations due to semi-flexibility, missing anatomical information, and undesirable effects such as shadowing and shine-through. Unlike the typical fixed gamma camera systems, 3D F-SPECT system is equipped with a hand-held gamma probe and an imaging camera that use a specialized software to provide a reconstructed 3D image of the sentinel node. The system provides additional in depth information and image fusion over a live video of the operation area, and allows both mobile data acquisition and real-time navigation tracking (8,9). The recent road map of intraoperative SLND was stated as real-time and 3D intraoperative imaging by two consecutive editorial comments (5,9). In the pivotal study (8), F-SPECT provided similar results when compared with SPECT/CT as a reference method. The accuracy, sensitivity, and positive predictive values were found to be 80%, 83% and 95% in the validation study, respectively. F-SPECT revealed at least one sentinel node in 87.5% of the patients. In the clinical study by Bluemel et al. (12), preoperative planar scintigraphy was used as the reference method while conventional intraoperative gamma probe was the standard alternative method. They (12) found that F-SPECT and conventional gamma probe had a detection rate of 92.3% (36/39) and 89.7% (35/39) in the evaluation on a per-patient basis and a detection rate of 92.7% (51/55) and 69.1% (38/55) in the evaluation on a per-lesion basis, respectively. There was a statistically significant difference ($p < 0.001$) between the two methods for sentinel node detection on a per-lesion basis. Finally, although the cost of buying a F-SPECT system was reported to be approximately £92,000, the real cost-effectiveness could not be evaluated because of its potential use in numerous surgical specialties (13). The success of SLND is closely related to selected protocols and parameters. Despite all efforts to achieve a standard SLND

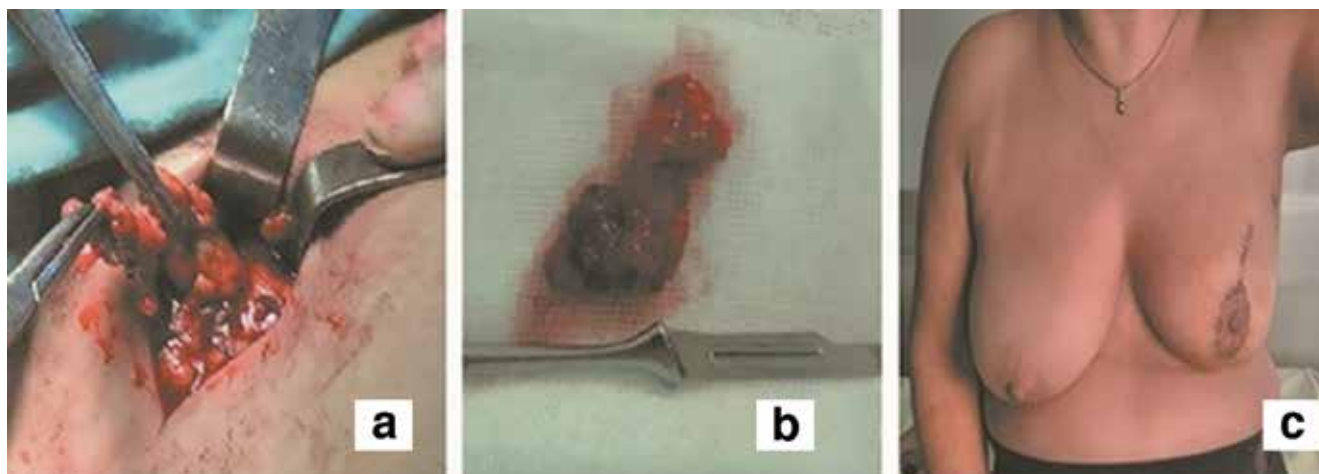


Figure 3. a) The figure shows axillary lymph node dissection during surgery, b) Surgical specimen belonging to the excised lymph nodes due to high radiotracer uptake (165 cps/s), c) The postoperative status of the left breast at tenth day after the surgery

protocol, there is still no consensus on the procedure of choice. The main limitations in creating a standard protocol are as follows: the diversity in imaging methods and in radioactive agents and injection types, rapid technological improvement, accessibility and pricing policies (1,2,4,10). ^{99m}Tc -sulfur colloid, ^{99m}Tc -nanocolloid, and ^{99m}Tc -antimony trisulfide have different particle sizes that may be a factor in SLN detection rates. However, as in our case, selection of the radiotracer is usually dependent on its local accessibility rather than other factors. Subareolar, periareolar or peritumoral injection techniques with deep (parenchymal or subcutaneous) or superficial (epidermal, subdermal or intradermal) administrations can be preferred (1,2). However, better results can be achieved with a superficial administration in subareolar or periareolar regions to visualize the axillary node, or with a deep administration in the peritumoral region to visualize the internal mammary node (14,15). In both of the major studies (8,12) the technique was based on the two-day protocol using different injection types and there was no comparison between different protocols.

Conclusion

In conclusion, the concept of SLND is currently one of the standard procedures for patients with breast cancer. Application of extensive axillary dissection for the identification and removal of a SLN can cause lymphedema both in the patient's arm and the conserved breast. The exact 3D definition is one of the new options to avoid the morbidity related to unnecessary lymphatic dissection. We tested this new method with two main protocols under stable conditions via usage of same radiotracer and injection technique and combined imaging method. In our cases, with the help of 3D F-SPECT system, we detected the SLN precisely with an error of only a few millimeters (Figure 2).

In our opinion, radio-guided breast surgery may be favorable because it allows lower postoperative morbidity with shorter operation time and a quite limited dissection area. We think that 3D F-SPECT technology is a promising method that could meet expectations. The simultaneous combination of SPECT and CT or optical images in the operative area may further increase the value of the current system. However, the number of articles published so far is small, and there is no comment about the impact of this method on morbidity in the literature. Further studies in the field of radio-guided surgery and intraoperative imaging seem to be required to reveal the exact potential of these methods to gain wide clinical acceptance.

Acknowledgment

We would like to thank "Nepha company" for the opportunity to use the freehand SPECT system.

Ethics

Informed Consent: Consent form was filled out by all participants.

Peer-review: Externally peer-reviewed.

Authorship Contributions

Surgical and Medical Practices: Ahmet Oğuz Hasdemir, Serhat Tokgöz, Gülay Özgehan, Hakan Güzel, *Concept:* Salih Sinan Gültekin, Ahmet Oğuz Hasdemir, *Design:* Salih Sinan Gültekin, Ahmet Oğuz Hasdemir, *Data Collection or Processing:* Salih Sinan Gültekin, Ahmet Oğuz Hasdemir, *Cüneyt Yücesoy, Emine Öztürk, Analysis or Interpretation:* Salih Sinan Gültekin, Ahmet Oğuz Hasdemir, *Literature Search:* Salih Sinan Gültekin, Ahmet Oğuz Hasdemir, *Ata Türker Arıkoç, Writing:* Salih Sinan Gültekin, Ahmet Oğuz Hasdemir.

Conflict of Interest: No conflict of interest was declared by the authors.

Financial Disclosure: The authors declared that this study has received no financial support.

References

- Vidal-Sicart S, Valdés Olmos R. Sentinel node mapping for breast cancer: current situation. *J Oncol* 2012;2012:361341.
- Boguševičius A, Čepulienė D. Quality of life after sentinel lymph node biopsy versus complete axillary lymph node dissection in early breast cancer: a 3-year follow-up study. *Medicina (Kaunas)* 2013;49:111-117.
- Cheng G, Kurita S, Torigian DA, Alavi A. Current status of sentinel lymph-node biopsy in patients with breast cancer. *Eur J Nucl Med Mol Imaging* 2011;38:562-575.
- Ali J, Alireza R, Mostafa M, Naser FM, Bahram M, Ramin S. Comparison between one day and two days protocols for sentinel node mapping of breast cancer patients. *Hell J Nucl Med* 2011;14:313-315.
- Olmos RA, Vidal-Sicart S, Nieweg OE. SPECT-CT and real-time intraoperative imaging: new tools for sentinel node localization and radioguided surgery? *Eur J Nucl Med Mol Imaging* 2009;36:1-5.
- Paredes P, Vidal-Sicart S, Zanón G, Roé N, Rubí S, Lafuente S, Pavía J, Pons F. Radioguided occult lesion localisation in breast cancer using an intraoperative portable gamma camera: first results. *Eur J Nucl Med Mol Imaging* 2008;35:230-235.
- Vidal-Sicart S, Paredes P, Zanón G, Pahisa J, Martínez-Román S, Caparrós X, Vilalta A, Rull R, Pons F. Added value of intraoperative real-time imaging in searches for difficult-to-locate sentinel nodes. *J Nucl Med* 2010;51:1219-1225.
- Wendler T, Herrmann K, Schnelzer A, Lasser T, Traub J, Kutter O, Ehlerding A, Scheidhauer K, Schuster T, Kiechle M, Schwaiger M, Navab N, Ziegler SI, Buck AK. First demonstration of 3-D lymphatic mapping in breast cancer using freehand SPECT. *Eur J Nucl Med Mol Imaging* 2010;37:1452-1461.
- Valdés Olmos RA, Vidal-Sicart S, Nieweg OE. Technological innovation in the sentinel node procedure: towards 3-D intraoperative imaging. *Eur J Nucl Med Mol Imaging* 2010;37:1449-1451.
- Kim T, Giuliano AE, Lyman GH. Lymphatic mapping and sentinel lymph node biopsy in early-stage breast carcinoma: a metaanalysis. *Cancer* 2006;106:4-16.
- Arican P, Peksoy I, Naldöken S, Bozkurt B. The effect of the excisional biopsy in the detection of the sentinel lymph node by lymphoscintigraphy and intraoperative gamma probe in breast cancer. *Mol Imaging Radionucl Ther* 2011;20:100-103.
- Bluemel C, Schnelzer A, Okur A, Ehlerding A, Paepke S, Scheidhauer K, Kiechle M. Freehand SPECT for image-guided sentinel lymph node biopsy in breast cancer. *Eur J Nucl Med Mol Imaging* 2013;40:1656-1661.
- Naji S, Tadros A, Traub J, Healy C. Case report: improving the speed and accuracy of melanoma sentinel node biopsy with 3D intraoperative imaging. *J Plast Reconstr Aesthet Surg* 2011;64:1712-1715.
- Mudun A, Sanli Y, Ozmen V, Turkmen C, Ozel S, Eroglu A, Igci A, Yavuz E, Tuzlali S, Muslumanoglu M, Cantez S. Comparison of different injection sites of radionuclide for sentinel lymph node detection in breast cancer: single institution experience. *Clin Nucl Med* 2008;33:262-267.
- Bauer TW, Spitz FR, Callans LS, Alavi A, Mick R, Weinstein SP, Bedrosian I, Fraker DL, Bauer TL, Czerniecki BJ. Subareolar and peritumoral injection identify similar sentinel nodes for breast cancer. *Ann Surg Oncol* 2002;9:169-176.



Kikuchi Disease with Generalized Lymph Node, Spleen and Subcutaneous Involvement Detected by Fluorine-18-Fluorodeoxyglucose Positron Emission Tomography/Computed Tomography

Flor-18-Florodeoksiglukoz Pozitron Emisyon Tomografisi/Bilgisayarlı Tomografi ile Saptanan Yaygın Lenf Nodu, Dalak ve Deri Altı Tutulumu Olan Kikuchi Hastalığı

Alshaima Alshammari¹, Evangelia Skoura², Nafisa Kazem¹, Rasha Ashkanani¹

¹Mubarak Al Kabeer Hospital, Clinic of Nuclear Medicine, Jabriya, Kuwait

²University College London Hospital, Clinic of Nuclear Medicine, London, United Kingdom

Abstract

Kikuchi-Fujimoto disease, known as Kikuchi disease, is a rare benign and self-limiting disorder that typically affects the regional cervical lymph nodes. Generalized lymphadenopathy and extranodal involvement are rare. We report a rare case of a 19-year-old female with a history of persistent fever, nausea, and debilitating malaise. Fluorine-18-fluorodeoxyglucose positron emission tomography/computed tomography (¹⁸F-FDG PET/CT) revealed multiple hypermetabolic generalized lymph nodes in the cervical, mediastinum, axillary, abdomen and pelvic regions with diffuse spleen, diffuse thyroid gland, and focal parotid involvement, bilaterally. In addition, subcutaneous lesions were noted in the left upper paraspinal and occipital regions. An excisional lymph node biopsy guided by ¹⁸F-FDG PET/CT revealed the patient's diagnosis as Kikuchi syndrome.

Keywords: Kikuchi-Fujimoto disease, histiocytic necrotizing lymphadenitis, fluorine-18-fluorodeoxyglucose

Öz

Kikuchi hastalığı olarak bilinen Kikuchi-Fujimoto hastalığı, genellikle bölgesel servikal lenf düğümlerini etkileyen, nadir görülen benign ve kendini sınırlayıcı bir hastalıktır. Yaygın lenfadenopati ve ektranodal tutulum nadirdir. Bu yazıda sürekli ateş, bulantı ve halsizlik şikayetleri olan 19 yaşında bir kadın hasta sunulmaktadır. Flor-18-florodeoksiglukoz pozitron emisyon tomografisi/bilgisayarlı tomografi (¹⁸F-FDG PET/BT) yaygın dalak, tiroid bezi ve fokal parotis katılımı ile bilateral servikal, mediastinal, aksiller, abdominal ve pelvik bölgelerde hipermetabolik multipl lenf nodları saptadı. Buna ek olarak, sol üst paraspinal ve oksipital bölgelerde subkutan lezyonlar mevcuttu. ¹⁸F-FDG PET/BT rehberliğinde yapılan eksizyonel lenf nodu biyopsisi ile Kikuchi sendromu tanısı kondu.

Anahtar kelimeler: Kikuchi-Fujimoto hastalığı, histiyositik nekrotizan lenfadenit, flor-18-florodeoksiglukoz

Introduction

Kikuchi-Fujimoto disease (KFD) also known as Kikuchi disease or histiocytic necrotizing lymphadenitis is a rare idiopathic and self-limiting disorder that typically affects the regional cervical lymph nodes (1). Generalized lymphadenopathy with involvement of mediastinal,

peritoneal, and retroperitoneal lymph nodes, and extra-nodal disease is a rare occurrence (2,3,4). Age at presentation is usually below 40 years with early reports showing female preponderance (female/male ratio, 4:1), while more recent data indicate that the actual male to female ratio is closer to 1:1 (5,6,7). Most cases have been reported from East Asia (8,9). In rare occasions,

Address for Correspondence: Alshaima Alshammari MD, Mubarak Al Kabeer Hospital, Clinic of Nuclear Medicine, Jabriya, Kuwait
Phone: (00965)99674017 E-mail: alshaima_97@hotmail.com **Received:** 19.01.2015 **Accepted:** 29.07.2015

the condition was reported in children (10). The exact pathogenesis is not completely understood, and viral and autoimmune pathogenesis have been speculated. Reports have suggested the combined immune response of T cells and histiocytes (particularly apoptotic CD8+ and CD123 plasmacytoid monocytes) against infectious agents, as a possible cause (11). An article suggested an association between *Mycobacterium szulgai* lymphadenitis and KFD based on coexisting characteristic histologic features of KFD in lymph nodes and a positive culture for *Mycobacterium szulgai* (12). It has also been linked to other autoimmune conditions regarding pathogenesis, like systemic lupus erythematosus (SLE), anti-phospholipid syndrome, polymyositis, systemic juvenile idiopathic arthritis, bilateral uveitis, arthritis and cutaneous necrotizing vasculitis (13). KFD almost always has a benign course and resolves in several weeks to months (14). Its treatment is largely supportive, mainly with anti-inflammatory and antimicrobial drugs; hence differentiating it from other more serious conditions is important to guide management (15,16,17).

Case Report

A previously healthy 19-years-old young woman presented with a history of persistent fever, nausea, debilitating malaise and bone pain. The patient had normal values of urea, creatinine, and serum electrolytes. She was investigated

for SLE, but her antinuclear factor, double-stranded DNA, and anti-neutrophil cytoplasmic antibody were all negative. Blood and urine cultures were unremarkable. Viral serology for hepatitis and Epstein-Barr virus and Mantoux test were also negative. The patient underwent imaging with fluorine-18-fluorodeoxyglucose positron emission tomography/computed tomography (^{18}F -FDG PET/CT) to investigate the cause of fever. ^{18}F -FDG PET/CT scan showed multiple hypermetabolic lymph nodes with generalized involvement: in the neck (Figure 1), mediastinum (Figure 2), axillary (Figure 2), abdomen and pelvic regions with diffuse spleen uptake (Figure 3). In addition, hypermetabolic subcutaneous lesions in the left upper para-spinal and occipital regions were noted (Figure 4). Standardized uptake value (SUV) maximum standardized value (SUV_{max}) of ^{18}F -FDG uptake in the affected lymph nodes and subcutaneous lesions was 6.3 ± 2.4 (mean \pm SD), with lymph node size ranging from 0.7-1.9 cm in the long-axis diameter. The spleen was not enlarged measuring 10.7 cm in cranio-caudal dimension with a SUV_{max} value of 5.8. An excisional cervical lymph node biopsy guided by ^{18}F -FDG PET/CT was performed. The histopathologic examination was consistent with the diagnosis of Kikuchi syndrome. Symptomatic treatment with antipyretics, non-steroidal anti-inflammatory drugs and low dose corticosteroids was administered. In the clinical follow-up after 3 months, she was symptom-free. No follow-up PET/CT study was performed.

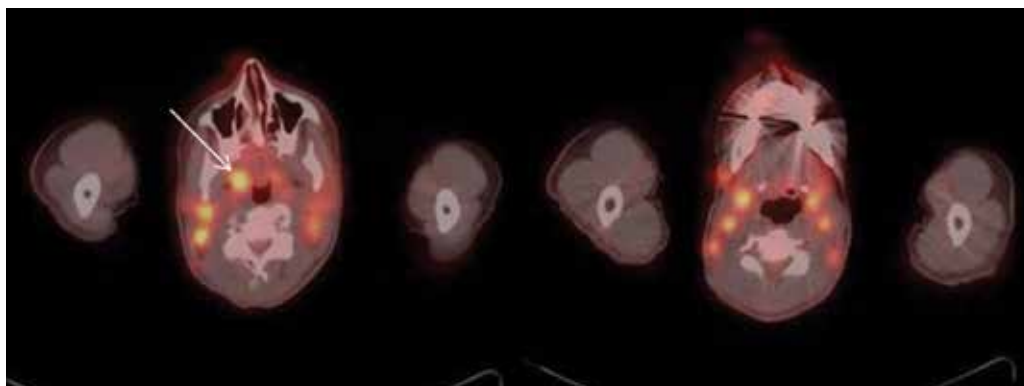


Figure 1. Increased fluorodeoxyglucose uptake in the deep cervical lymph nodes bilaterally, the largest and most avid node is noted in the right retropharyngeal region measuring 1.1x1.4 cm with SUV_{max} : 4.2 (arrow)

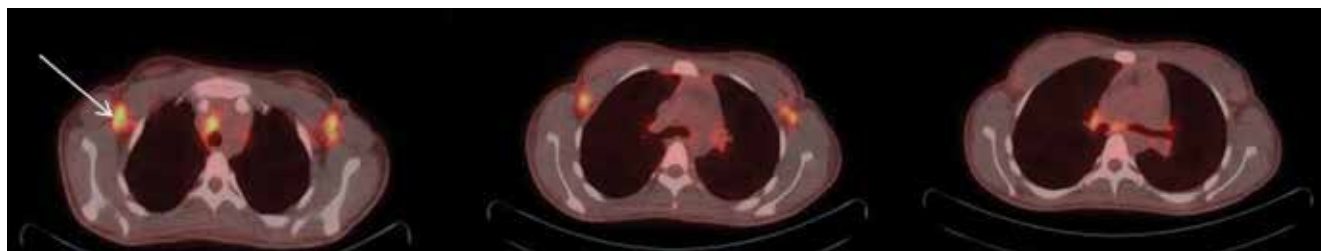


Figure 2. Increased fluorodeoxyglucose uptake in the pretracheal, subcarinal and right hilar lymph nodes and axillary lymph nodes bilaterally, most intense on the right axilla measuring 1.9x1.0 cm with SUV_{max} : 6.9 (arrow)

Literature Review and Discussion

KFD was first described in young Japanese females in 1972 (18). The patient's usual presentation is tender regional cervical lymphadenopathy, sometimes associated with mild-grade fever (1). Only a few patients develop generalized lymphadenopathy and hepatosplenomegaly as the initial manifestations of KFD and even fewer cases are reported to have bone marrow and cutaneous, usually facial, involvement (3). The differential diagnoses of the condition include tuberculosis, and SLE. It can also mimic more serious conditions such as non-Hodgkin lymphoma (NHL), plasmacytoid T-cell leukemia, Kawasaki disease, nodal colonization by acute myeloid leukemia, and even metastatic adenocarcinoma (19). Multiple pathogens have been reported in isolated case reports such as *Yersinia enterocolitica*, Brucellosis, *Bartonella henselae*, *Entamoeba histolytica*, *Mycobacterium szulgai*, and *Toxoplasma gondii*, however, the fact that most patients with KFD are unresponsive to antibiotics suggests that these microbiologic organisms were incidental findings (12,17). The results of a wide range of laboratory studies are usually either normal or non-specific, such as anemia and slightly raised erythrocyte sedimentation rate (11). Recognition of KFD is crucial, especially since it can be mistaken for malignant lymphoma. A patient who has been misdiagnosed as having large-cell lymphoma and has been subjected to a course of cytotoxic therapy before submitting histologic sections to an expert

pathologist has been previously reported (1). In fact, later studies suggested that up to 30% of patients with KFD have been reported to be initially misdiagnosed as malignant lymphoma and that some of them received unnecessary chemotherapy (20). KFD has been reported as one of the causes of prolonged fever of unknown origin (FUO). The utilization of ^{18}F -FDG PET/CT in numerous clinical centers for finding the cause of fever in the diagnostic work-up of FUO is increasing. In general, causes of fever include malignant, infectious and non-infectious diseases (21). In their review article on the value of ^{18}F -FDG PET and PET/CT in the diagnostic evaluation of patients with FUO, Meller et al. (22) found that FDG aided in reaching the final diagnosis with a frequency which varied between 25% and 69%. This article also demonstrated the wide range of possible causes of fever. In these studies, common causes of FUO detected by PET included various malignancies, several infectious diseases such as atypical pneumonia, spondylitis, tuberculosis, infected prostheses, and occult abscesses and non-infectious inflammatory diseases such as vasculitis, aortitis, and autoimmune diseases (22). PET imaging findings in KFD were first reported by Liao et al in 2003 (23). This was followed by multiple case reports and a few recent studies on ^{18}F -FDG PET/CT trying to find distinguishing features between KFD and malignant lymph nodes (20). Ito and his group studied seven patients with KFD and found that the SUV_{max} values of ^{18}F -FDG

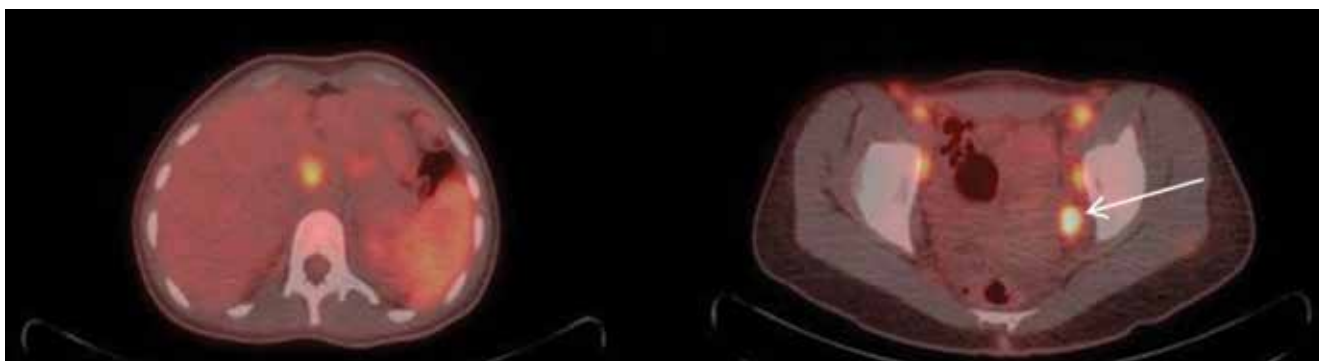


Figure 3. Increased fluorodeoxyglucose uptake in portocaval and external iliac chains bilaterally, most avid being the left external iliac lymph node measuring 1.7x1.5 with SUV_{max} : 7.5 (arrow), with associated diffuse splenic uptake

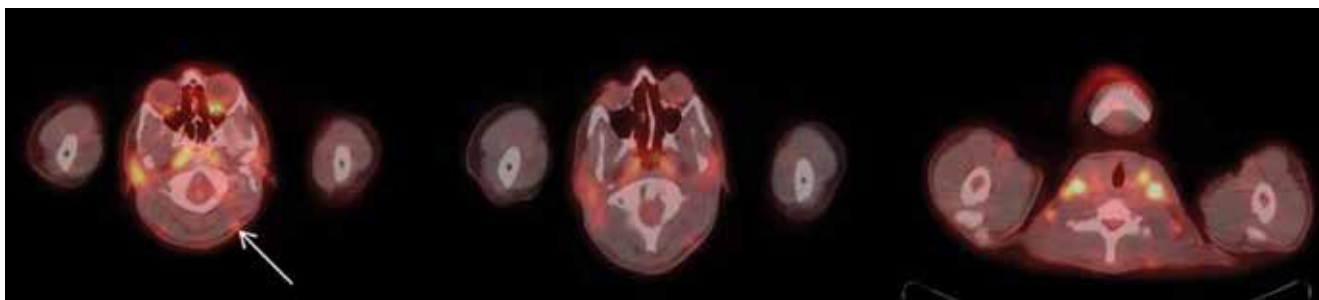


Figure 4. Subcutaneous mildly fluorodeoxyglucose avid lesions are seen in the occipital and upper para-spinal regions, SUV_{max} : 2.5 (arrow)

uptake in the affected lymph nodes were not beneficial for differentiating between benign and malignant tumors and that the values in the affected lymph nodes of patients with KFD were as high as the values found in malignancies (24). They suggested that the value of ^{18}F -FDG PET/CT is that it can aid in excluding the metastatic involvement of extra-nodal sites in malignant lymphoma and help guiding decisions regarding appropriate biopsy sites (24). Similarly, in another study comparing clinical manifestations and PET/CT findings between KFD and lymphoma patients, Kim and his colleagues (25) found that there were no significant differences in SUV_{max} values between KFD and malignant lymphoma. They also concluded that increased uptakes in extra-nodal organs, such as bone marrow, small bowel, thymus, kidney, orbit, and pleura was the only distinguishing factor between lymphoma and KFD, but that only KFD with nodal involvement was indistinguishable from lymphoma. Another study suggested that in cases with a generalized distribution of small to medium-sized lymph nodes in ^{18}F -FDG PET/CT with high ^{18}F -FDG uptake, KFD should be considered as part of differential diagnosis (26). In another article concerning the value of ^{18}F -FDG PET/CT in distinguishing KFD from NHL in patients with cervical lymphadenopathy, it was concluded that ^{18}F -FDG PET/CT can be useful for distinguishing this disease from NHLs by using SUV and partial volume corrected SUV (cor SUV) (27).

Conclusion

In conclusion, KFD is a rare, self-limited, and perhaps under-diagnosed condition. Recognition of this condition is crucial, especially because it can be mistaken for malignant lymphoma or adenocarcinoma. The awareness on this disease as a cause of fever and local lymphadenopathy, or rarely, as demonstrated in this case, generalized lymphadenopathy, might prevent misdiagnosis and inappropriate management. ^{18}F -FDG PET/CT imaging may suggest the diagnosis of KFD, may depict the distribution and size of the affected lymph nodes, and guide an optimal lymph node biopsy.

Ethics

Informed Consent: Consent form was filled out by all participants.

Peer-review: Externally peer-reviewed.

Authorship Contributions

Surgical and Medical Practices: Alshaima Alshammari, Evangelia Skoura, Nafisa Kazem, Rasha Ashkanani, Concept: Alshaima Alshammari, Evangelia Skoura, Design: Alshaima Alshammari, Evangelia Skoura, Data Collection or Processing: Alshaima Alshammari, Nafisa Kazem, Analysis or Interpretation: Alshaima Alshammari, Nafisa

Kazem, Literature Search: Alshaima Alshammari, Writing: Alshaima Alshammari.

Conflict of Interest: The authors declare that they have no conflicts of interest.

Financial Disclosure: The authors declared that this study has received no financial support.

References

1. Dorfman RF. Histiocytic necrotizing lymphadenitis of Kikuchi and Fujimoto. *Arch Pathol Lab Med* 1987;111:1026-1029.
2. Turner RR, Martin J, Dorfman RF. Necrotizing lymphadenitis: a study of 30 cases. *Am J Surg Pathol* 1983;7:115-123.
3. Kuo TT. Cutaneous manifestations of Kikuchi's histiocytic necrotizing lymphadenitis. *Am J Surg Pathol* 1990;14:872-876.
4. Sumiyoshi Y, Kikuchi M, Ohshima K, Masuda Y, Takeshita M, Okamura T. A case of histiocytic necrotizing lymphadenitis with bone marrow and skin involvement. *Virchows Arch A Pathol Anat Histopathol* 1992;420:275-279.
5. Tsang WY, Chan JK, Ng CS. Kikuchi's lymphadenitis: a morphologic analysis of 75 cases with special reference to unusual features. *Am J Surg Pathol* 1994;18:219-231.
6. Kuo T. Kikuchi's disease (histiocytic necrotizing lymphadenitis): a clinicopathologic study of 79 cases with an analysis of histologic subtypes, immunohistology, and DNA ploidy. *Am J Surg Pathol* 1995;19:798-809.
7. Yen A, Fearneyhough P, Raimer SS, Hudnall SD. EBV-associated Kikuchi's histiocytic necrotizing lymphadenitis with cutaneous manifestations. *J Am Acad Dermatol* 1997;36:342-346.
8. Ahmad M, Khan AB, Iqbal J. Histiocytic necrotizing lymphadenitis: a clinicopathological study. *J Pak Med Assoc* 1991;41:86-88.
9. Kutty MK, Anim JT, Sowayan S. Histiocytic necrotizing lymphadenitis (Kikuchi-Fujimoto disease) in Saudi Arabia. *Trop Geogr Med* 1991;43:68-75.
10. Kim CH, Hyun O J, Yoo IeR, Kim SH, Sohn HS, Chung SK. Kikuchi disease mimicking malignant lymphoma on FDG PET/CT. *Clin Nucl Med* 2007;32:711-712.
11. Martinez-Vazquez C, Hughes G, Bordon J, Alonso-Alonso J, Anibarro-Garcia A, Redondo-Martinez E, Touza-Rey F. Histiocytic necrotizing lymphadenitis, Kikuchi-Fujimoto's disease, associated with systemic lupus erythematosus. *QJM* 1997;90:531-533.
12. Maek-a-nantawat W, Viriyavejakul P. Mycobacterium szulgai lymphadenitis mimicking Kikuchi's disease in Thailand. *Southeast Asian J Trop Med Public Health* 2001;32:537-540.
13. Hu S, Kuo TT, Hong HS. Lupus lymphadenitis simulating Kikuchi's lymphadenitis in patients with systemic lupus erythematosus: a clinicopathological analysis of six cases and review of the literature. *Pathol Int* 2003;53:221-226.
14. Facchetti F, Vermi W, Mason D, Colonna M. The plasmacytoid monocyte/interferon producing cells. *Virchows Arch* 2003;443:703-717.
15. Felgar RE, Furth EE, Wasik MA, Glucksman SJ, Salhany KE. Histiocytic necrotizing lymphadenitis (Kikuchi's disease): in situ end-labeling, immunohistochemical, and serologic evidence supporting cytotoxic lymphocyte-mediated apoptotic cell death. *Mod Pathol* 1997;10:231-241.
16. Mahajan VK, Sharma NL. Kikuchi-Fujimoto disease: immediate remission with ciprofloxacin. *Int J Dermatol* 2005;43:370-372.
17. Rezaei K, Kuchipudi S, Chundi V, Ariga R, Loew J, Sha BE. Kikuchi-Fujimoto disease: hydroxychloroquine as a treatment. *Clin Infect Dis* 2004;39:124-126.
18. Kikuchi M. Lymphadenitis showing focal reticulum cell hyperplasia with nuclear debris and phagocytosis. *Acta Hematol Jpn* 1972;35:379-380.
19. Hutchinson CB, Wang E. Kikuchi-Fujimoto disease. *Arch Pathol Lab Med* 2010;134:289-293.

20. Erhamamci S, Reyhan M, Kocer NE. Kikuchi-Fujimoto disease as a rare cause of benign lymphadenopathy and (18)F-FDG PET/CT findings. *Hell J Nucl Med* 2014;17:41-44.
21. Rosenbaum J, Basu S, Beckerman S, Werner T, Torigian DA, Alavi A. Evaluation of diagnostic performance of 18F-FDG-PET compared to CT in detecting potential causes of fever of unknown origin in an academic centre. *Hell J Nucl Med* 2011;14:255-259.
22. Meller J, Sahlmann C, Scheel AK. 18F-FDG PET and PET/CT in Fever of unknown origin. *J Nucl Med* 2007;48:35-45.
23. Liao AC, Chen YK. Cervical lymphadenopathy caused by Kikuchi disease: positron emission tomographic appearance. *Clin Nucl Med* 2003;28:320-321.
24. Ito K, Morooka M, Kubota K. Kikuchi disease: 18F-FDG positron emission tomography/computed tomography of lymph node uptake. *Jpn J Radiol* 2010;28:15-19.
25. Kim JE, Lee EK, Lee JM, Bae SH, Choi KH, Lee Y, Hah JO, Choi JH, Kong EJ, Cho IH. Kikuchi-Fujimoto disease mimicking malignant lymphoma with 2-[(18)F]fluoro-2-deoxy-D-glucose PET/CT in children. *Korean J Pediatr* 2014;57:226-231.
26. Kong E, Chun K, Hong Y, Hah J, Cho I. 18F-FDG PET/CT findings in patients with Kikuchi disease. *Nuklearmedizin* 2013;52:101-106.
27. Tsujikawa T, Tsuchida T, Imamura Y, Kobayashi M, Asahi S, Shimizu K, Tsuji K, Okazawa H, Kimura H. Kikuchi-Fujimoto disease: PET/CT assessment of a rare cause of cervical lymphadenopathy. *Clin Nucl Med* 2011;36:661-664.